

Winter 2015

Critical Shear Stress Estimates of Sunken Alberta Bitumen

Charles Bruno Richter Watkins
University of New Hampshire, Durham

Follow this and additional works at: <https://scholars.unh.edu/thesis>

Recommended Citation

Watkins, Charles Bruno Richter, "Critical Shear Stress Estimates of Sunken Alberta Bitumen" (2015). *Master's Theses and Capstones*. 1071.
<https://scholars.unh.edu/thesis/1071>

This Thesis is brought to you for free and open access by the Student Scholarship at University of New Hampshire Scholars' Repository. It has been accepted for inclusion in Master's Theses and Capstones by an authorized administrator of University of New Hampshire Scholars' Repository. For more information, please contact nicole.hentz@unh.edu.

CRITICAL SHEAR STRESS ESTIMATES OF SUNKEN ALBERTA BITUMEN

BY

CHARLES BRUNO RICHTER WATKINS

B.S. in Environmental Engineering, University of New Hampshire, 2012

THESIS

Submitted to the University of New Hampshire in Partial Fulfillment
of the Requirements for the Degree of

Master of Science

In

Civil Engineering

December 2015

This thesis has been examined and approved in partial fulfillment of the requirements for the degree of Master of Science in Civil Engineering by:

Thesis Director, Nancy E. Kinner, Professor of Civil and Environmental Engineering

Thomas P. Ballestero, Professor of Civil Engineering

Kenneth Baldwin, Professor of Ocean and Mechanical Engineering

On December 15th, 2015

Original approval signatures are on file with the university of New Hampshire Graduate School.

DEDICATION

I wish to express my gratefulness to my mother and grandmother, who have shown unwavering support throughout my academic and personal endeavors. I dedicate the completion of this degree to Doc and Modano.

ACKNOWLEDGMENTS

First and foremost I would like to thank my advisor Dr. Nancy Kinner. I will forever be grateful for this research opportunity and her continued support. I would also like to thank Dr. Thomas Ballesterro and Dr. Kenneth Baldwin for taking time to lend their expertise and insight on this project.

The work required to complete this project was the culmination of many people. Olivia Jobin, Jesse Ross, and Neil Thompson each made significant contributions.

Finally, I would like to thank the staff in the Environmental Engineering department. Your positive attitudes and willingness to help made it enjoyable to work in Gregg Hall.

Contents	Page
DEDICATION.....	iii
ACKNOWLEDGMENTS.....	iv
LIST OF TABLES.....	ix
LIST OF FIGURES.....	x
ABSTRACT.....	xii
CHAPTER 1 – INTRODUCTION.....	1
Risk of Nonfloating Oil Spills.....	1
Properties of Heavy Oil.....	2
Recovery of Nonfloating Oil.....	3
Research Objectives.....	5
CHAPTER 2 – LITERATURE REVIEW.....	6
Nonfloating Spill Models.....	6
BSS.....	8
Previous Laboratory Studies of Nonfloating oil.....	11
Oil Spreading.....	12
Thesis Research.....	12
CHAPTER 3 – MATERIALS and METHODS.....	14
Objectives.....	14
CRRC Facility.....	15
Annular Flume.....	15
Inner Flume.....	17

Flow Generation.....	19
Electric Motor.....	19
Flow Straighteners.....	19
Velocity Settings.....	20
Flow Field Measurements.....	21
ADV Profiler.....	21
ADV Calibration.....	22
ADV Positioning.....	23
Oil Observation.....	23
Digital Cameras.....	23
Displacement Grids.....	24
Oil Stranding.....	24
Video Analysis.....	25
Post Processing.....	26
Exporting VECTRINO Files.....	26
QA/QC.....	27
Calculation of CSS.....	27
Adhesion Determination.....	32
Environmental Health and Safety.....	32
CHAPTER 4 – RESULTS and DISCUSSION.....	34
Research Objectives.....	34
Flume BSS Estimates.....	34

Temperature Effect.....	37
Velocity Effect.....	39
Mass Effect.....	41
Oil Migration.....	43
Globule Size.....	47
CSS Estimates.....	50
Adhesion.....	54
Implications of Research.....	55
Recommended Response Protocol.....	57
CHAPTER 5 – CONCLUSIONS.....	60
CHAPTER 6 – RESEARCH RECOMMENDATIONS.....	62
REFERENCES.....	64
APPENDICIES:	
A: Case studies of nonfloating oil spills.....	66
B: Alberta bitumen MSDS.....	71
C: Density calculations for rock surrogate pretests.....	78
D: Annular flume background.....	79
E: Vectrino readout of ADV’s elevation during experiments.....	80
F: Bottom check test.....	81
G: MATLAB data structures.....	82
H: sample correlation of ADV velocity measurements.....	83

I: Raw and filtered ADV data.....	84
J: LP bed shear stress calculation code.....	85
K: TKE bed shear stress calculation code	87
L: Adhesion Procedure.....	89
M: Laboratory CSS estimates for grain sizes.....	90
N: Parameter test of LP and TKE BSS.....	91
O: Contingency analysis.....	92
P: Least squared profiler model.....	93
Q: Eroded oil globule size.....	94
R: Average oil migration patterns.....	96
S: Instantaneous CSS.....	97
T: Parameter test of LP and TKE CSS.....	98
U: Supplemental data.....	99
V: ADV Data of experimental runs.....	100

LIST OF TABLES

Table	Page
3.1 Durham, NH discharge limits and flume contaminant concentrations.....	33
4.1: Replicates of Bed Shear Stress Estimates Determined by TKE.....	36
4.2: Replicates of Bed Shear Stress Estimates Determined by LP.....	36
4.3: Tabular Results of Oil Experiments.....	53

LIST OF FIGURES

Figure	Page
1.1: Nonfloating oil.....	2
2.1: Relationship between water density and salinity.....	7
3.1: Side view of annular flume.....	16
3.2: Schematic of annular flume.....	17
3.3: Inner tank of annular flume.....	18
3.4: Schematic of inner flume.....	18
3.5: Trolling motor.....	19
3.6: Flow straighteners.....	20
3.7: Motor speed settings and corresponding current velocity.....	21
3.8: Vectrino profiler.....	22
3.9: Digital cameras.....	24
3.10: “Oil gun” used to strand bitumen on tank bottom.....	25
3.11: Schematic of trial synchronization.....	26
3.12: Schematic of vertical velocity profile.....	28
3.13: Schematic of velocity fluctuation.....	31
4.1: Estimation of bed shear stress using LP.....	35
4.2: Estimation of bed shear stress using TKE.....	35
4.3: Temperature as the driving variable of mass erosion.....	38
4.4: Nominal logistics plot for erosion as function of temperature.....	39

4.5: Erosion events per hour.....	40
4.6: Erosion events observed in experiments using 20g of bitumen.....	42
4.7: Erosion events observed in experiments using 5g of bitumen.....	42
4.8: Oil migration and Erosion.....	43
4.9: No oil spreading at 5.3 ± 0.4 °C.....	45
4.10: Oil advanced 176% at 18.5 ± 1.9 °C.....	45
4.11: Lengthening of oil on tank bottom.....	46
4.12: Mean eroding droplet size observed in experiments.....	48
4.13: Continuous erosion of oil globules.....	49
4.14: Comparison of CSS using TKE and LP methods.....	51
4.15: CSS increases with velocity and decreases with temperature.....	51
4.16: Adhesion number as a function of temperature.....	54

ABSTRACT

CRITICAL SHEAR STRESS ESTIMATES OF SUNKEN ALBERTA BITUMEN

by

Charles Bruno Richter Watkins

University of New Hampshire

December 2015

As observed in several recent spills (e.g., DBL-152, TX; Enbridge-Kalamazoo, MI), under certain circumstances, released oil can sink to the bottom of a water body. Once on the bottom, the oil can move or remobilize into the water column. The National Oceanic and Atmospheric Administration's (NOAA) Office of Response and Restoration (ORR) uses mathematical models to predict the trajectory of spilled oil. The critical shear stress (CSS) for an oil is used to predict the movement of sunken oil along and off the bottom. The CSS has only been measured for one oil (Hibernian crude). The Coastal Response Research Center (CRRC) at the University of New Hampshire (UNH) has an annular flume equipped with a velocity profiler that can be used to estimate CSS by measuring the instantaneous, three-dimensional water current velocities at which sunken oils undergo movement and erosion of visible oil droplets occur.

The CSS of sunken Alberta bitumen was determined by progressively increasing current velocities until deformation, movement and erosion of the stranded oil was observed. Tests were conducted in freshwater at water temperatures of 5, 15 and 25°C. At temperatures $\geq 18.5 \pm 1.9$ °C, mass erosion of visible droplets was observed in current velocities greater than 20 cm/s (0.39 knots.), corresponding to a CSS of 1.9 Pa. No erosion was observed at temperatures $< 18.5 \pm 1.9$ °C in current velocities up to 100 cm/s (2.25 knots).

Understanding the transport and fate of sunken oil is an important prerequisite for recovery of non-buoyant oils. Unfortunately, details regarding environmental conditions and physical properties of crude oil are limited. Spill trajectory modelers make a “best guess” of the expected conditions needed to erode and resuspend oil from the bottom. CSS data are needed for a range of oils. This thesis research estimated CSS for an Alberta bitumen, providing modelers information to predict the behavior of sunken Alberta bitumen.

Chapter 1: INTRODUCTION

Risk of Nonfloating Oil Spills

Spilled oil is one of the greatest threats to marine resources resulting in impacts to environments, and also to economies and societies. Modern oil exploration and transportation have increased the likelihood of maritime accidents resulting in oil spills. For most spills, less than 20% of the oil is ever recovered, while the rest weathers in the environment impacting ecosystems. Nearly one quarter of oil that is spilled in U.S national waters consists of a class known as Group V oil; heavy petroleum in which the specific gravity (Sp.G) is greater than 1 (NRC, 1999). Floating oil (i.e., Sp.G <1) may also become nonfloating, as lighter products weather and interact with sediment. Oils that sink to the bottom or remain suspended pose risks to certain resources that are not normally affected by floating oil. These resources include fish, shellfish, seagrasses, and other benthic and water-column biota. In addition, nonfloating oil is very difficult to monitor and new trajectory models need to be developed to accurately predict the behavior of heavy oil.

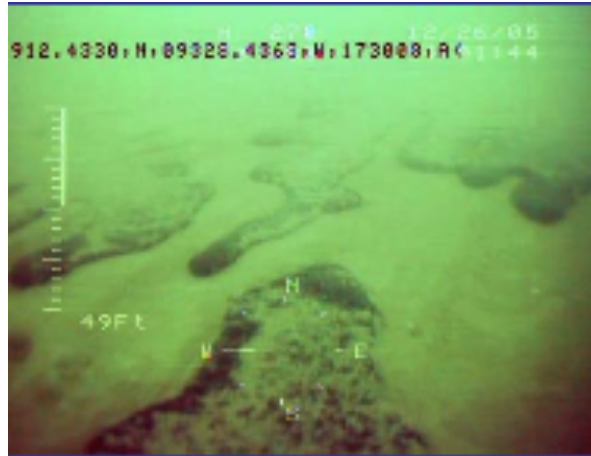


Figure 1.1: Sunken oil from T/B DBL-152 (orr.noaa.gov)

Properties of Heavy Oils

Federal rules governing oil spill contingency plans categorize petroleum cargoes according to their physical properties. Heavy oil is the term used by the response community to describe dense, viscous oils that have low volatility, lose very few constituents by evaporation, and have a viscous to semi-solid consistency (NRC, 1999). Heavy crudes include many of those from Venezuela and California. Heavy oil also refers to residual oils (No. 5 and No. 6 fuel oil, Bunker C, slurry oil), asphalt, coal tar, coke, carbon black, and pitch.

Oil is formed when biomass that collects on the land's surface or seafloor becomes covered by sediment and sinks into the earth's crust. Over millions of years in the anoxic zones of these sedimentary layers, microorganisms degrade the biomass into carbon-rich compounds that when subjected to heat and pressure form hydrocarbons. Microorganisms continue to feed on the oil, preferring to first devour the smaller hydrocarbons that make

up light crudes. Once the lighter fractions are gone, what is left is heavy crude that consists of larger aromatic compounds, which are more difficult for microorganisms to degrade.

Because heavy oils are typically located deeper underground, they tend to be exploited after lighter, shallower crudes have been recovered. For example, in the past, crudes recovered from the Norwegian continental shelf have been conventional or light (low density, easy flowing). Those fields have matured and their quality and quantity have reduced. Currently, the Norwegian oil company, Statoil, has two heavy oil fields in operation (Zuata: 8.5 API, Venezuela and Alba: 19 API, UK), while three are in early development (Linerle: 16 API, Norway, Falk: 18 API, Norway, and Bressay: 10.8 API, UK).

Recovery of Nonfloating Oil

Oil spilled into water can float, be neutrally buoyant, or sink depending on: the density of the water, the specific properties of the oil, and interactions with suspended material (e.g., sediments, marine snow). Oil that sinks to the bottom (i.e., sunken oil) pose great challenges during an emergency response. Most oil spill cleanup technologies, developed for floating oils, are not very effective for nonfloating oil. Because it sinks, it is impossible to locate and track the oil visually. Furthermore, sunken oil is especially difficult to track if it mobilizes along the bottom or re-suspends into the water column.

Remobilization of sunken oil was observed at several spills under various wave and bottom current conditions (e.g., DBL-152, TX; Enbridge-Kalamazoo, MI). Knowing or having the ability to estimate the bed shear stress (BSS) water exerts on sunken oil during a spill and comparing it to the estimated critical shear stress (CSS) of the oil gives responders an indication as to whether the material will become mobile, posing risks to resources such as power plant cooling water intakes or critical biota. Data on the velocity and CSS needed to mobilize and erode sunken oils from a sea or riverbed is lacking. Cloutier et al. (2002) has provided the only published data. Their laboratory experiments, using an annular flume (Ames et al; 1992), determined the CSS necessary to resuspend a Hibernian crude (Sp.G. = 0.86) from the bottom (See chapter 2). While existing models for erosion of sunken oil are empirically based, further research could develop theoretical relationships.

While the U.S Coast Guard (USCG) has had recent success with new detection methods for sunken oil, many issues associated with predicting its behavior, fate, and transport remain unresolved. Furthermore, recovery of sunken oil and protection of benthic natural resources is dependent on understanding and predicting its *in situ* transport. Details regarding the environmental conditions and physical properties of sunken oils are often unknown or extremely limited, which makes predicting their fate and behavior very difficult. Oil spill trajectory modelers attempt to make a “best guess” of a sunken oil’s behavior by making certain assumptions and using the limited CSS data available.

Research Objectives

Presently, a spill modeler's only option to predict the remobilization of sunken oil is to use the CSS of the Hibernian crude (Simecek-Beatty, 2007). Group V oils with low API gravities (<22) have greater density and viscosity than the Hibernian and hence, will require higher BSS to mobilize or erode because they have a greater resistance to deformation. Therefore, experiments are needed to estimate the CSS for a range of oils, particularly those with low API gravities that may readily sink, and are becoming increasingly more common in certain regions. Laboratory, real-time measurements on sunken oil can generate CSS estimates to be incorporated into existing three-dimensional trajectory models used for predicting the transport of sunken oil.

This thesis discusses the first nonfloating oil study conducted by the CRRC using the annular flume facility. The project scope included: the observation of sunken oil, definition of the environmental conditions likely to cause mobilization of oil on the seabed, and calculation of the CSS necessary to resuspend the oil into the water column (See chapter 4). Velocity measurements and calculations were documented using sunken Alberta bitumen in freshwater ranging from 5 to 25°C at current speeds up to 100 cm/s (>2 kn). The study was designed using guidance from ORR oil spill modelers, who can use the information generated in their trajectory models.

Chapter 2: LITERATURE REVIEW

Spill modeling is well developed, but is not commonly used in response to nonfloating oil spills because of limited environmental data and observations of oil suspended in water or deposited on the seabed. However, based on an understanding of the physical and chemical properties of heavy oils, simple qualitative predications can be made of how it may behave. Several case studies (Appendix A) were identified and demonstrate the challenge of responding to sunken oil spills and the need for CSS estimates.

A literature review was conducted for laboratory and field measurements of the CSS needed to erode and resuspend oil from the bottom. This is a highly specialized topic and only one paper, Cloutier et al. (2002) has been published with this type of data. However, there is an abundance of literature available describing methods for calculating BSS (e.g., Soulsby, 1997; Kim et al., 2000; Biron et al., 2004). Oil sediment interaction models may allow for relationships between oil erosion and sediment transport to be developed.

Nonfloating Spill Models

Behavioral models of nonfloating oils have been developed from observations of past spills. These models are descriptive, qualitative predictions of how a petroleum

product with a given density will behave when spilled into a receiving water. The key factors that determine the behavior of spilled nonfloating oils are: water density, current speed, and sediment interaction (NRC, 1999).

If the ratio of the density of oil to that of the receiving water is greater than 1.0, the oil will not float. However, a small volume release and strong surface tension could allow droplets to float. If an oil's specific gravity is very close to 1.0 (a few percent above or below), its fate is subject to wave action and it is likely to become submerged. There is a linear relationship between the density of water (g/cm^3) and salinity of the water at any given temperature (Figure 2.1 shows example at 15°C). The density of oil is shown as horizontal lines in units of API (American Petroleum Institute) gravity. Oils with higher densities (and therefore lower API numbers) than the receiving water (above line) will sink; oils with lower densities than the receiving water (below line) will initially float, but may ultimately sink.

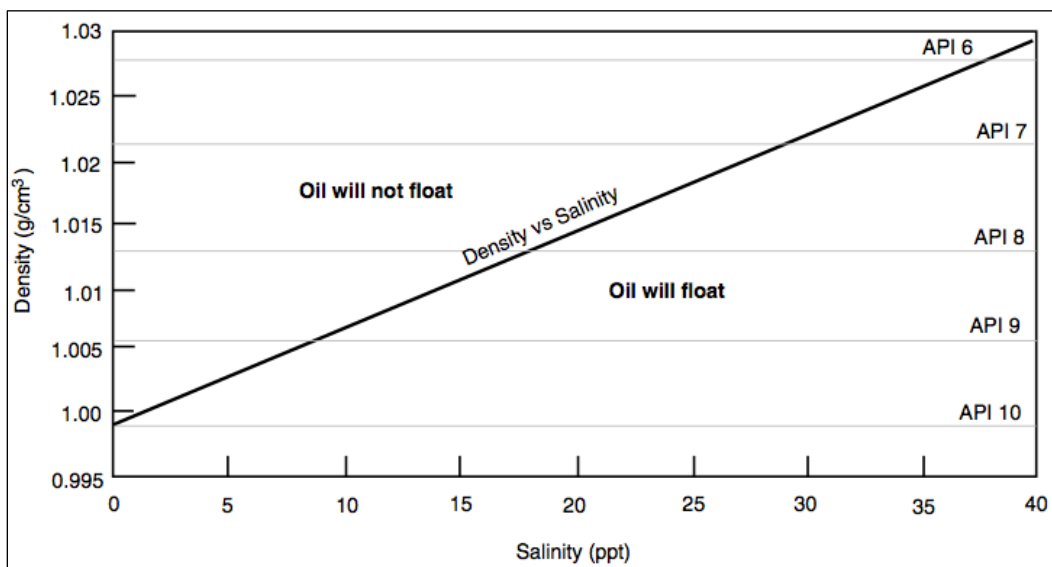


Figure 2.1: Relationship between water density and salinity at 15°C (NRC, 1999)

If current speeds are greater than 10 cm/s, non-floating oil will initially be suspended in the water column before settling. If there is little to no current, oils heavier than the receiving water will immediately sink to the bottom.

The percentage of sediment is a major consideration when predicting an oil's behavior. When lighter, normally floating oil is mixed with as little as 2 to 3 % sand, it becomes heavier than water and sinks. The density of sand (Sp.G=2.03) grains is higher than the density of silt (Sp.G=1.6) or clay particles (Sp.G=1.26); therefore more concentrated cohesive mixtures of the latter are required for submergence.

BSS

Water flowing over the seabed creates a frictional drag force between the water and the bottom that extends upwards towards the surface. At the bottom, the velocity is considered zero where the thin layer of water is in direct contact with the boundary (i.e., no slip condition). Each successive water layer above the bottom increases in velocity and shears the layer beneath until the maximum ambient velocity is reached (i.e., free stream). The most rapid increase in velocity shear occurs nearest the bottom. Sunken oil erodes into the water column from the bottom when the magnitude of the total BSS exceeds the CSS (threshold for erosion), overcoming the forces holding the oil to the bed. This might also explain how large masses of oil can move and be torn apart.

Techniques to calculate BSS due to currents (e.g., tides, winds, river outflow, density differences) include velocity profile (VP), depth-averaged, Reynolds, and turbulent kinetic energy (TKE) (See chapter 3). In addition to currents, waves may play an important role in eroding oil in shallow water conditions. Given limitations during an emergency response, it is unclear what field instrumentation and methods would be used to calculate BSS. The best method will likely depend on the logistics of deploying field equipment, instrument availability and technical support.

The VP method fits measured current velocity above the bottom to the von Karman-Prandtl equation (see chapter 3). In general, a minimum of three current velocity measurements is needed at small depths above bottom within the boundary layer. The boundary layer has been defined as that part of the water column in which the velocity profile is strongly influenced by the presence of the river bottom, where the flow velocity decreases to zero. Biron et al. (1998) suggest that the boundary layer does not reliably extend above 20% of the flow depth. Ideally, the velocity is expected to increase with height logarithmically. For a variety of reasons (e.g., tidal currents, wind effects, density stratification, wave action) the VP may not be logarithmic and the BSS can be over or under-estimated

Wilcock (1996) suggests the VP is the most restrictive method because it is limited to flows with finite log layers. The method loses accuracy in flow structures that vary rapidly in space or time. Kim et al. (2000) found the VP method generally gave the

largest estimates of BSS, a tendency that is consistent with the effects of sediment-induced stratification, which increases in intensity towards the bed.

The TKE method superimposes the turbulent fluctuations on the average current flow. Simple linear relationships between turbulent energy and BSS have been formulated in turbulence models (Galperin et al., 1988). Kim et al. (2000) have used the absolute intensities of velocity fluctuations to infer BSS through TKE (Equations are shown in chapter 3).

Methods of single-point measurements require appropriate flows only near the bed, so it may be applied under a wider range of flow conditions, including spatially variable flow. Biron et al. (2004) compared the BSS using several methods and determined the TKE method provided the best estimate of BSS.

The methods used to estimate BSS were evaluated by Simecek-Betty (2007) who wanted to propose a practical method for modeling the resuspension of sunken oil using real-time laboratory measurements of bottom currents. She emphasized the need for spill modelers to have data on the CSS for a range of heavy oils and highlighted one paper, Cloutier et al. (2002), which described a series of oil erosion experiments in an annular flume, as one method for collecting such data.

Previous Laboratory Studies of Nonfloating Oil

Cloutier et al. (2002) performed laboratory experiments in an annular flume using Hibernian crude oil ($\rho=0.875$, $\nu=400$ cSt at 15°C) to determine the CSS necessary to move stranded oil from the bottom of the tank. Their flume consisted of an acrylic annular trough 2 m in diameter, 0.15 m wide, and 0.45 m deep. The water depth was held constant at 30 cm which gave a volume of 0.3 m^3 . They stranded 200g of crude, which formed a 2 mm thick oil slick to a section of the flume base (1.20 m x 0.15 m). After introducing seawater, they progressively increased current velocities in small step increments until erosion was observed.

Two types of erosion were evident: dissolution and erosion of soluble aromatics, and mass erosion of visible globules. They observed mass erosion of visible globules under a BSS of 5.0 Pa or equivalent to a mean current velocity of 55 cm/s in seawater (35 ppt) at 13°C . At 4°C , under a bed stress of 8 Pa in 75 cm/s current, there was no mass erosion of visible globules. The abrupt onset of visible oil erosion indicated threshold conditions. Cloutier et al. (2002) found that once the critical velocity is surpassed, erosion increases with increasing current velocities.

A temperature effect was demonstrated on the threshold and rate of oil erosion: the colder the temperature, the higher the BSS required for erosion. This is attributed to the increase in oil density and viscosity in cold water. The viscosity of crude oils and oil

products is dependent on the oil type, but also on the temperature and degree of weathering.

Oil Spreading

Oil spreading on the sea surface has been studied extensively, but little information is available about spilled oil spreading on the bottom. Spreading of sunken oil is likely far more complicated than surface spreading. BSS from waves and currents may induce/enhance spreading. Oil adhering to the underlying sediments may inhibit oil spreading and is a function of the oil adhesion characteristics and sediment matrix.

Thesis Research

Cloutier et al. (2002) published the results of laboratory experiments used to determine the CSS needed to erode an Hibernian crude from the bottom of an annular flume. Hibernian crude has a high API gravity. Therefore, it is unlikely to become submerged without weathering and sediment entrainment. There is a data gap for oils with medium API gravities (API of 22-31) that are neutrally buoyant and for low API gravities (API of <22) that are denser than seawater, which would most likely become submerged or sunken.

If spill modelers knew the approximate conditions in which sunken oil mobilizes from the bottom, they could predict with some accuracy when and where it would travel, allowing time to protect shorelines, sensitive marine areas and intakes. Also, first

responders could be more prepared by knowing whether the oil will remain entrained on the bottom, be resuspended, transported away from the release site, and/or re-sink.

The literature revealed a lack of quantitative models for predicting the behavior of heavy oils. This makes response to spills involving sunken oil very difficult and limits protection of sensitive resources. The importance of knowing the bottom stress needed to erode oil from the sea bottom was highlighted in the case studies. Clearly, there is need for more work in this area for a variety of oils. This thesis research aimed to achieve this by exploring the relationship between oil density, viscosity and CSS for a low API oil Alberta Bitumen.

Chapter 3: MATERIALS and METHODS

Objectives

The main objectives of the sunken oil erosion experiments were to determine the CSS, erosion frequency, and spreading rate of the bitumen along bottom. The behavior of the bitumen was observed as a function of temperature, its original mass and current velocity. The CSS is the minimum force applied to the oil on the flume bed that causes it to spread and move into the water column. The water velocity above the bed created this adjacent force. The erosion frequency was defined as the number of erosion events observed during an experiment. The spreading rate was the distance the oil migrated in horizontal (longitudinal direction) (x) and lateral (cross-tank sectional direction) (y) per unit time. Digital cameras, that recorded the oil's behavior during each experiment, were used to collect these data.

The oil erosion experiments were conducted using an Alberta bitumen (Appendix B), a heavy product from the oil sands in Canada (~8° API). This thesis research represents the first laboratory experiments to estimate the conditions in which bitumen erodes off a flume bed. The Alberta bitumen was obtained from a Canadian producer and serves as a data point for heavy crudes and bitumen of similar characteristics (e.g., API gravity, density, viscosity, adhesion).

Oil erosion experiments were conducted varying three primary variables: water temperature, current velocity, and oil mass. To establish run protocols, trials were performed using bitumen surrogates: molasses, chocolate pudding, and coral (Appendix C) all with specific gravities similar to those of the bitumen. The velocities chosen (~20, ~50, ~80 cm/s) were based on those observed in possible spill scenarios (e.g., tidal zones, ocean and river systems). The oil mass aliquots (5 and 20 g) were similar, on a density-normalized basis, to those used by Cloutier et al. (2002) in previous oil erosion experiments with a Hibernian crude (API 35°). Temperatures (5, 15, 25 °C) covered a range based on case studies and normal marine transportation routes.

CRRC Facility

The sunken oil erosion experiments were conducted in an annular flume (Appendix D) owned and operated by the CRRC. The facility is located in a high bay in Gregg Hall (Room 137) (Figure 3.1). It was constructed in 2012 as part of a senior capstone project with the intention of conducting a wide application of oil spill response studies, but most specifically for investigating sunken oil.

Annular Flume

The flume has a 4000-L capacity with a 9 m and 0.8 m channel length and width, respectively (Figures 3.1 and 3.2). The circular shape allows for continuous flow, which is advantageous as it allows longer observational periods and better simulates seabed conditions in the field. The outer and inner flume walls are ¾” clear Lexan® allowing

real-time bottom visual observation and monitoring by cameras. The inside of the flume is lined with a 20-mil opti-clear PVC liner (Specialty Plastic Fabrics; Monkona, IL), which acts as secondary containment. The flume sits on a subfloor constructed of plywood. A lined berm surrounds the subfloor for containment redundancy in the event the PVC liner or the Lexan are breached. The tank is filled with 2.5 m^3 ($h = \sim 43 \text{ cm}$) of fresh water using the potable water source located in the high bay

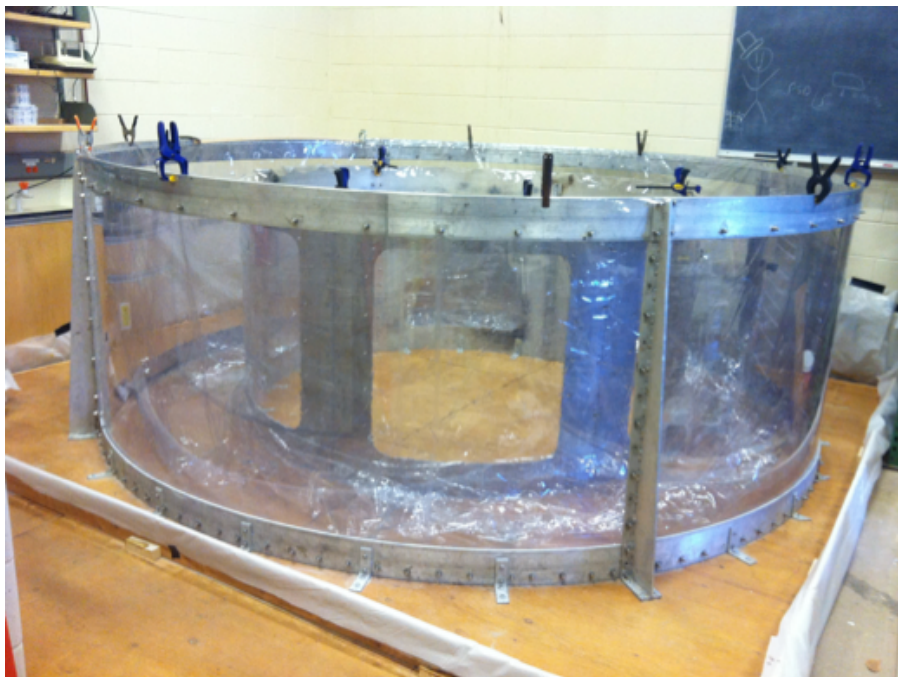


Figure 3.1: Side view of annular flume.

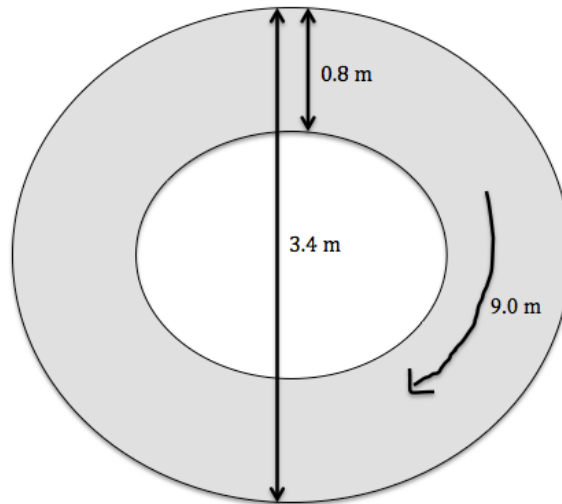


Figure 3.2: Schematic of annular flume

Inner Flume

While the flume's circular shape has advantages, one disadvantage that limits its use for highly sensitive boundary layer studies is the excessive cross shears, which yield highly turbulent currents that, are difficult to measure. This was resolved by the use of an inner rectangular tank (i.e., a flume within a flume). This inner tank contains the test area and consists of clear Lexan® 1.2 m long with a 0.2 m width and 0.9 m height (Figures 3.3 and 3.4). The test section has inlet and outlet structures conforming to each side of the tank to promote unidirectional flow so that increases in velocity do not lead to turbulence associated with curvilinear walls.

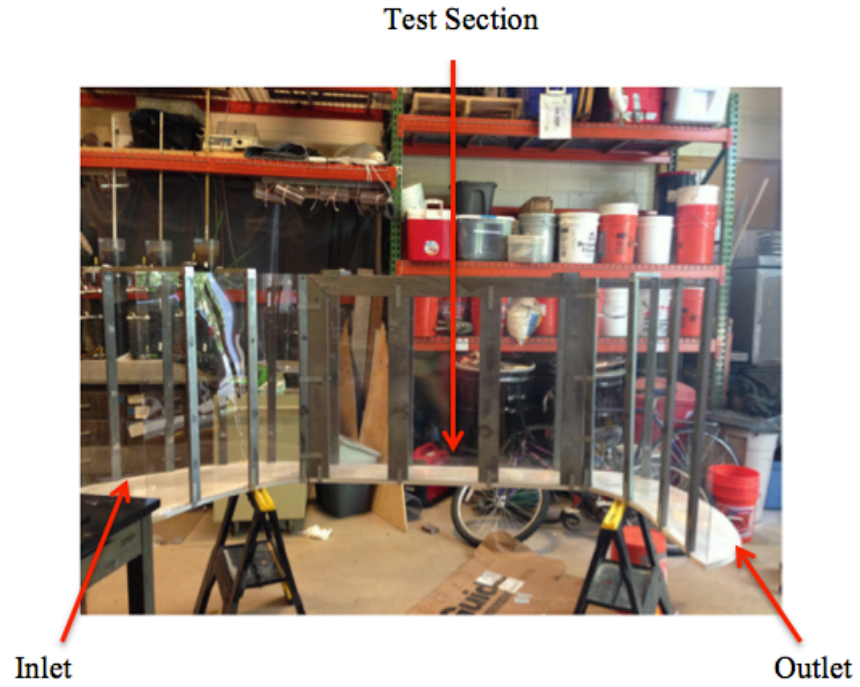


Figure 3.3: Inner flume

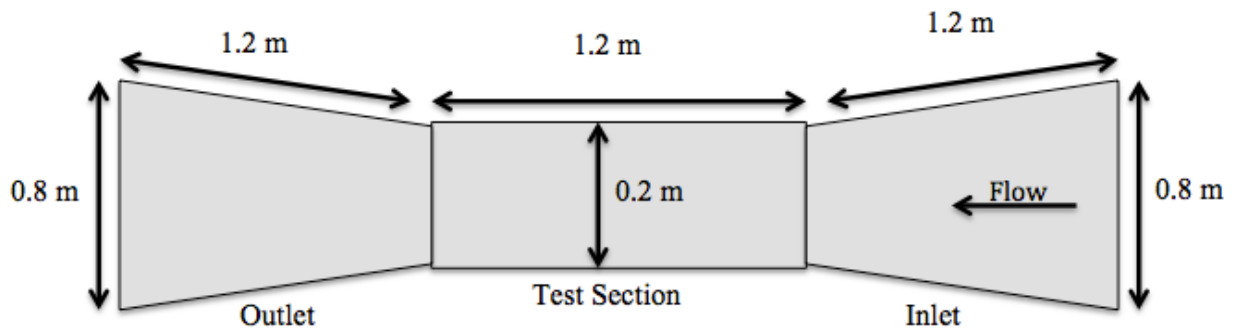


Figure 3.4: Schematic of inner flume

Flow Generation

Electric Motor

The water current is generated using a transom-mount trolling motor (Figure 3.5) with a thrust rating of 50 kgs (Motor Guide; Tulsa, OK). The motor is powered by three 12V marine grade batteries and charged by continuous smart-chargers to allow consistent output by the batteries during long experimental runs (~60 min.). Sturdy (2x4) wooden mounts hold the trolling motor. The motor mount is bolted to the floor outside the tank to resist the force exerted by the motor. A vortex dampener prevents the formation of cavitation in the area of the motor reducing turbulence and increasing efficiency of the motor output.

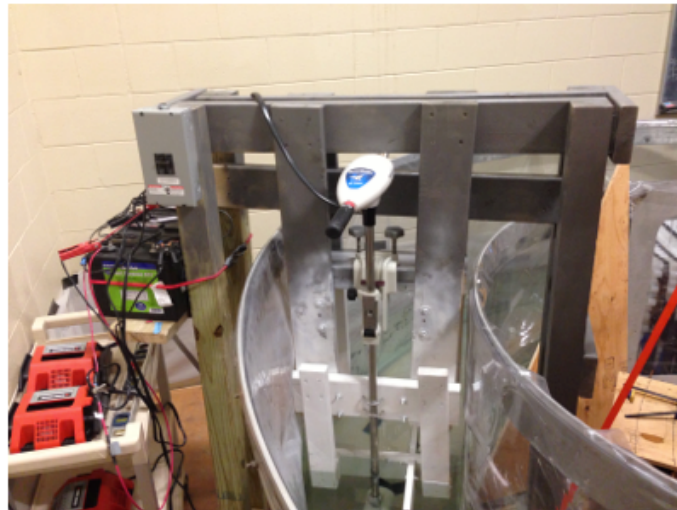


Figure 3.5: Trolling motor

Flow Straighteners

The flume has two upstream flow straighteners to reduce motor turbulence (Figure 3.6). The first is a series of 3.8 cm diameter PVC pipes (L=12-18 in) heat-molded to a

13-degree angle to conform to the circular radius of the flume. The second is directly inside the test area and is made from 3.8 cm diameter PVC piping (L=4 in). This piping is straight and allows for enhanced uniformity of the water current within the “flume within a flume” straight test section.



Figure 3.6: Curved and straight flow uniformity piping

Velocity Settings

The motor is capable of generating a range of velocities to achieve the desired conditions (Figure 3.7). Experimental runs lasted 60 min and were conducted at speed settings 3, 5 and 7. Constant velocity was maintained, as it was best for interpreting relationships (e.g., velocity vs. spreading, spreading vs. erosion). Depending on the speed setting, approximately one minute was necessary to establish a fully developed, steady flow regime, once the motor was started, as determined by the Vectrino (See ADV profiler).

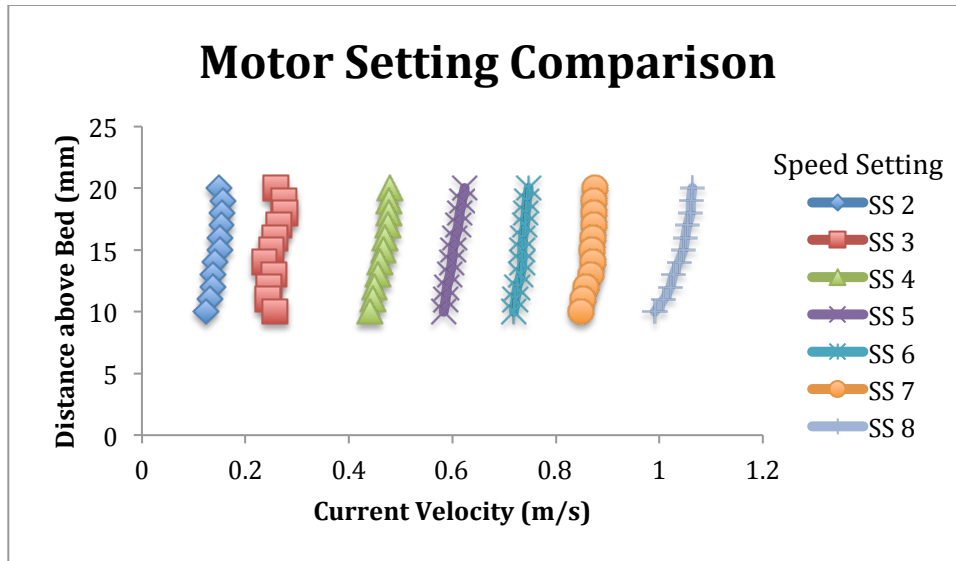


Figure 3.7: Motor speed settings and corresponding current velocity

Flow Field Measurements

ADV Profiler

The current velocity was measured using a Nortek Vectrino II (Vangkroken, Norway) (Figure 3.8). The Vectrino II is a profiling velocimeter that measures 3D water velocities using coherent Doppler processing. Doppler velocity measurements observe the changing distance of particles in the water by transmitting pulses of sound and comparing the echoes. The acoustic Doppler velocimeter (ADV) provides high-resolution velocity measurements with 1 mm readings over a vertical profile of 3 cm, at sampling rates up to 100 Hz. Simultaneously, it can measure bottom distance at 10 Hz. The Vectrino is secured to a wooden mount to avoid artificial acceleration, which can skew its recordings.



Figure 3.8: Vectrino Profiler

ADV Calibration

The Vectrino is an acoustic instrument; therefore it does not require any user calibration. During production, the probe head geometry is determined via a tow tank calibration, but unless there is damage to the probe head this will remain fixed. However, the manufacturer does recommend routine verification to ensure the instrument is functioning properly. Performing the transducer and probe checks detailed in the owner's manual does this. To verify they are working as expected, all four beams should show roughly the same profile shape with amplitude peaks at the manufactures "sweet spot" and bottom reading.

ADV Positioning

The ADV mount has lockable wheels so the Vectrino can be moved forward and backward in the test section. A track can move the probe from side to side within the flume and an extension allows it to be lowered and raised within the water column. The ADV was placed 6 to 7 cm above bottom to profile the boundary layer (Appendix E). A test comparing bottom measurements of Lexan® and oiled surfaces validated the use of the ADV's bottom check to reference the distance to oil (Appendix F). Slight variations in ADV positioning would not have affected the comparison between runs as long as the sampling volume included the bottom.

Oil Observation

Digital Cameras

GoPro Hero 3 cameras (San Mateo, CA) are used to monitor each trial run in the tank (Figure 3.9). The cameras record data at rates up to 100 frames per second, allowing for precise time-correlated measurements of how the oil moves. One camera is placed above the tank bottom facing downward, while a second is placed inside a watertight box on the outside of the test section looking inward. The cameras can be operated by smartphone or tablet using a WiFi connection.

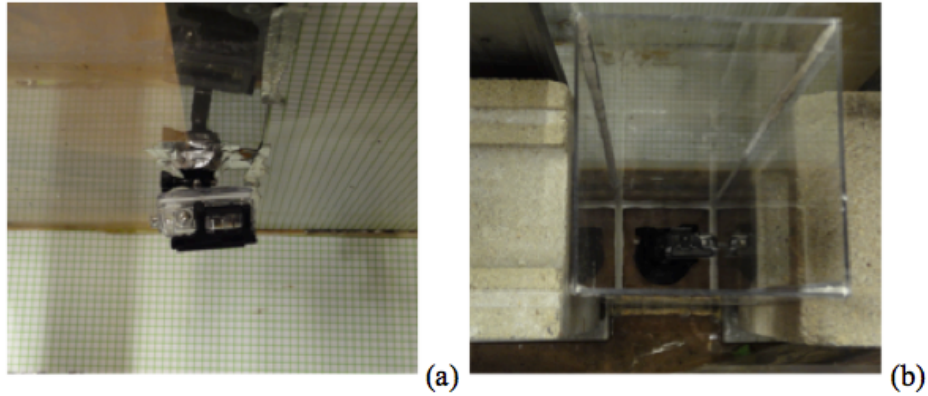


Figure 3.9: GoPro cameras in annular flume (a) downward-facing camera and (b) view of the watertight box that holds inward-facing camera

Displacement Grids

Displacements grids are attached to the bottom and side of the test section allowing the operator to measure the displacement of material along the bottom. The 1-cm grids were procured online and printed on large poster paper. They were cut into 91 cm x 19 cm pieces and then laminated at UNH Printing so they would not deteriorate underwater.

Oil Stranding

The desired aliquot size (measured by mass balance) was deposited on the displacement grids using a hand suction pump then placed in the test section of the inner flume (Figure 3.10).



Figure 3.10: Stranding of bitumen on tank grid

Video Analysis

The memory card files were uploaded to the CRRC computer using Windows movie player or the GoPro video application. Both software packages allow quick viewing at rates (10 frames per second) sufficient to classify oil erosion events. However, in order to view the videos with maximum resolution (100 frames per second), they were uploaded to iMovie or Final Cut Pro at the UNH Parker Media Laboratory. Experiments were synchronized, so time stamps on the digital cameras recording the events matched, as closely as possible, to those of the Vectrino. To ensure this, the cameras and vectrino were activated at the same time followed by the motor (Figure 3.11). The cameras also took still photographs of the oil before and after each experiment in addition to video footage. Colored plastic beads (5-10 mm) (Jo-Ann Fabric and Craft; Newington, NH) suspended in the water column were used to reference current velocities through the test

section. JMP statistical software (Cary, NC) was used to identify relationships and trends of the major variables (i.e., oil, mass, water temperature, current speed) and how they impacted critical oil erosion, erosion frequency, and migration using regression analysis.

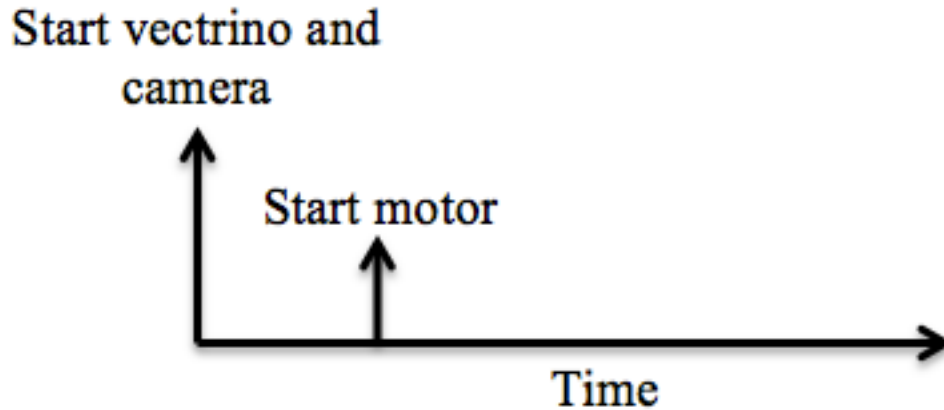


Figure 3.11: Schematic of trial synchronization

Post Processing

Exporting Vectrino Files

Once the data were collected, they were exported into Matlab from the Vectrino application page. Matlab offered advantages over Excel in processing because codes could be written to streamline analysis. In Matlab, the data can be easily accessed in tabular form (Appendix G). Two structure arrays were created to group related information using data containers called fields. The “Data” structure saved all recorded measurements using separate fields (e.g., Profiles_Vel contained current velocity data). The “configuration” structure contained fields related to the pre-specified arrangement of the Vectrino’s functional variables (e.g., Config.SampleRate contained the specified sample rate in Hz).

The ADV's four probes provide velocity measurements in 3 directions plus an additional vertical velocity (i.e., Z1 & Z2). The probes are co-located, so the estimates should be the same. This is redundant information, but can be used in post-processing. One Z variable was created as an average of Z1 and Z2.

Quality Assurance and Control

There must be a “reasonable” amount of suspended particles in the water for the successful operation of the Profiler (Nortek Vectrino II, 2013). Quality assurance (QA) procedures recommended by the manufacturer include using synthetic particles (e.g., Nortek seed, baby powder) to generate a sufficient number of suspended materials to facilitate adequate measurement of the Doppler shift. Quality control (QC), as suggested by manufacturer included processing of the collected data to exclude points with correlation and signal-to-noise ration (SNR) of less than 40% and 15 dB, respectively. In this thesis research, the mean correlations of all data sets were ~ 90% (Appendix H). A 3-standard deviation filter was used to remove velocity data that was statistically different than expectations (Appendix I).

Calculation of CSS

Sunken oil erodes into the water column from the bottom when the magnitude of the BSS exceeds the CSS. The CSS condition was created by progressively increasing current velocities until the cameras observed deformation, movement and erosion of the bitumen. The BSS, τ_0 , was determined from:

$$\tau_0 = \rho_w U_*^2 \quad [\text{eq. 1}]$$

Where: ρ_w is water density (kg/m^3) and U_* is shear velocity (cm/s) (i.e., a velocity that relates shear between layers of flow).

VP Method

Shear velocity was calculated by fitting the measured current velocity above the bottom to the von Karman-Prandtl equation (Appendix J):

$$U_{(z)} = \frac{U_*}{K} \ln\left(\frac{z}{z_0}\right) \quad [\text{eq. 2}]$$

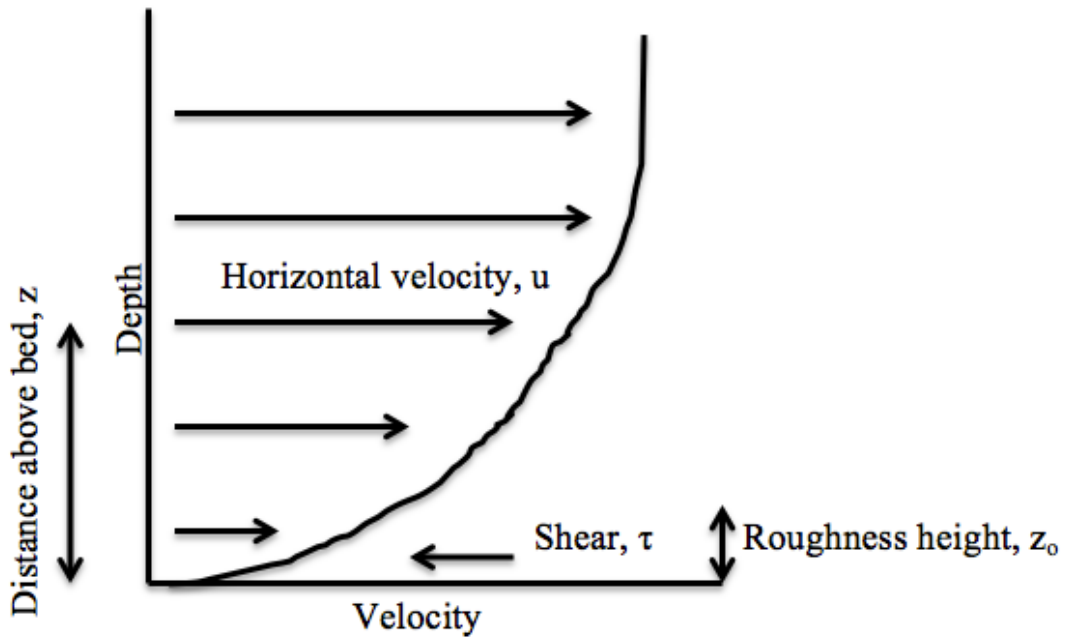


Figure 3.12: Schematic of vertical velocity profile with labeled parameters of Karman-Prandtl equation

Where $U_{(z)}$ is the mean flow velocity at a height z , K is the von Karman constant (~ 0.40), U_* is the shear velocity, and z_0 is the roughness height (i.e., elevation at which water velocity theoretically becomes zero).

The equation describes the variation of water velocity from zero at the bed to maximum velocity at the surface of the boundary layer and can be rewritten as:

$$U_{(z)} = \frac{U_*}{K} \ln(z) - \frac{U_*}{K} \ln(z_0) \quad [\text{eq. 3}]$$

with z and $U_{(z)}$ being measured by the Vectrino and its setting

Where:

$$m = \frac{U_*}{K} \quad [\text{eq. 4}]$$

$$b = -\frac{U_*}{K} \ln(z_0) \quad [\text{eq. 5}]$$

Regressing the values of $U_{(z)}$ against the logarithms of z yields estimates of the slope (m) and y-intercept (b). Shear velocity (cm/s) and roughness height can be calculated from the relationships:

$$U_* = Km z_0 = e^{-b/m} \quad [\text{eq. 6}]$$

$$z_0 = e^{-b/m} \quad [\text{eq. 7}]$$

The BSS, τ_0 , is then calculated using eq.1.

The specific calculation interval for estimating LP BSS was different for each experiment (i.e., 0.5-2.0 cm). The selected range was within the boundary layer, which extended 5-10% of the flow depth.

TKE Method

CSS was also calculated using the TKE method (Appendix K):

$$TKE = \left[\frac{1}{2} \right] \rho_w (u'^2 + v'^2 + w'^2) \quad [\text{eq. 7}]$$

Where: u', v', w' are the velocity fluctuations in the x, y, and z-axis (Figure 3.13).

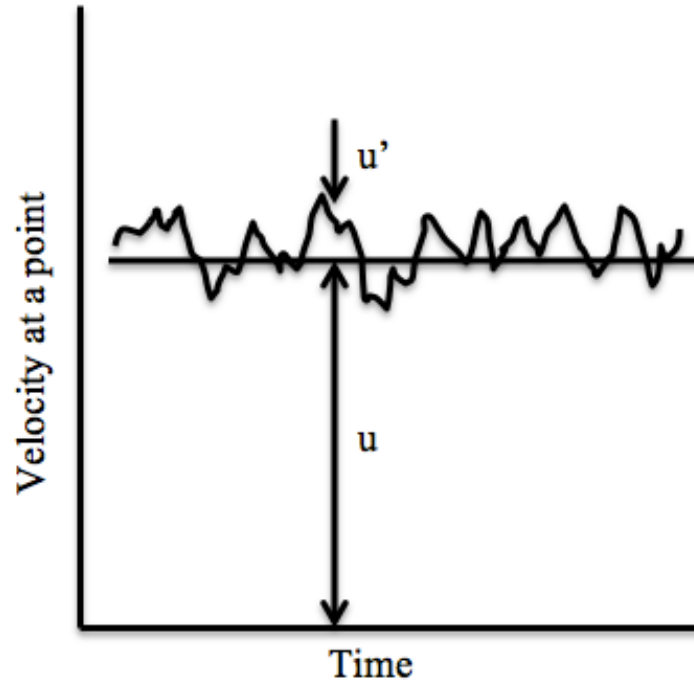


Figure 3.13: Schematic of velocity fluctuation (u')

From the turbulent kinetic energy, BSS can be estimated as:

$$\tau_o = C \cdot TKE \quad [\text{eq. 8}]$$

Where C is a proportionality constant, typically 0.19 (Stapleton and Huntley, 1995) and was used in this research.

The average of the variance terms (i.e., highest 10% of velocity fluctuations) for x , y , and z was calculated within a 0.5 cm interval, 0.5 cm off bottom. These terms were used to calculate the turbulent energy (eq. 7). The location was chosen to eliminate data

contamination from influence of the bedform and the interval smoothed spikes from depth bands closest to the oil-water interface.

Adhesion Determination

Oil adhesion characteristics were measured in the laboratory using a penetrometer (Model G-118-H-1200, Hoskin Scientific LTD.; Burnaby, BC) as described by the ASTM D5 method (Appendix L). The temperatures at which the adhesion of bitumen was measured were similar to those in the oil erosion experiments (i.e., 5, 20, 27°C).

Environment Health and Safety

Following each experiment, surface oil sheens were removed using absorbent pads and the oil stranded on the bottom was recovered simply by removing the oiled grid in the test section. A sump pump removed the water from the flume at the end of an experiment. The water was stored in aerated tanks then discharged to the Durham, NH sewer collection sewer. The ADV probe was washed with a mild detergent using a microfiber cloth and rinsed with water, as recommended by the manufacturer.

A lab study was performed to determine the toxicity of the oil-contaminated water. The amount of oil used in the experiment (5 and 20g) resulted in concentrations for benzene, toluene, ethyl benzene, and the xylenes that were below the direct discharge permits (Table 4.1). The tank liner was cleaned with mild detergent, if visibility was impaired, and vacuumed to remove any debris.

Table 3.1 Durham, NH discharge limits as compared to measured tank water contaminant concentrations

Industrial User Discharge Permit		
Compound	Regulatory Limit (mg/L)	Tank Water (mg/L)
Benzene	0.13	ND
Toluene	1.35	ND
Ethylbenzene	1.59	ND
Xylene	0.4	ND
TPH	25	1.3

Where ND = non detect

Chapter 4: RESULTS and DISCUSSION

Research Objectives

The primary objective of this thesis research was to determine the BSS at which an Alberta bitumen resuspends into the water column (i.e., CSS). Secondary outcomes included defining the environmental conditions (e.g., water temperature, current velocity) likely to cause mobilization of bitumen on a flat seabed and characterize its erosion behavior (e.g., frequency, size).

Flume BSS Estimates

Minimum and maximum current velocities measured in the flume test section during the bitumen experiments were 16 and 106 cm/s (See Table 4.3 for all test values). This corresponds to 0.3 to 2.1 knots, which is comparable to current velocities found in river systems and marine/estuarine environments. The minimum and maximum BSS were 0.6 and 1.9 Pa and 9.6 and 17.3 Pa as calculated by the VP and TKE methods, respectively (Figures 4.1 and 4.2). This is comparable to the BSS generated by natural currents (Appendix M), but higher than those of Cloutier et al., 2002 due to flume limitations.

LP

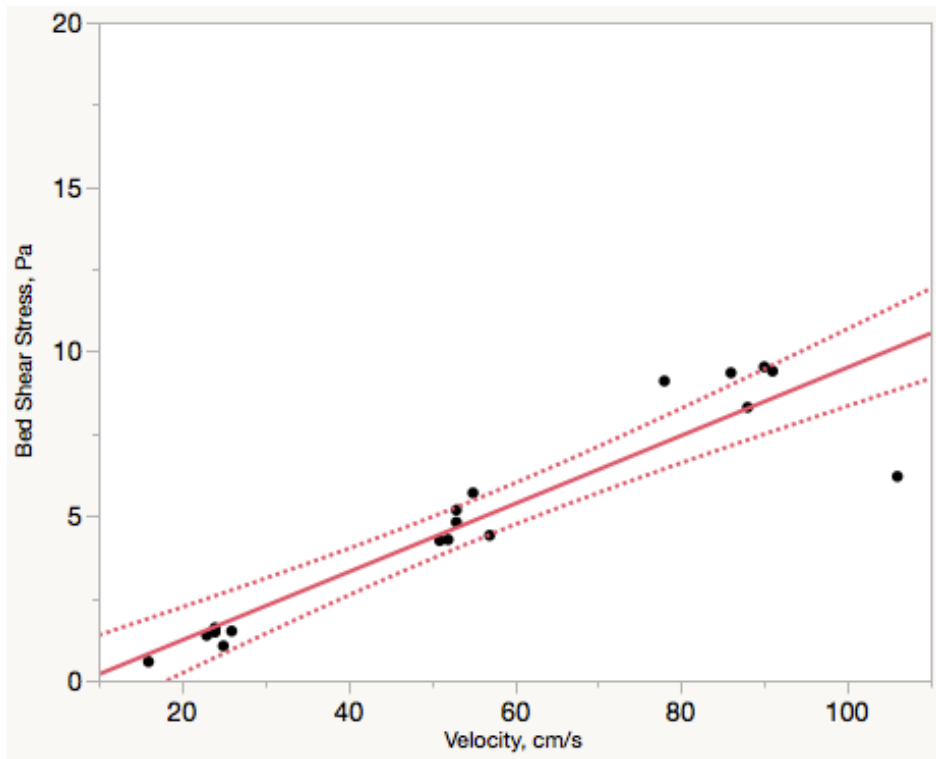


Figure 4.1: Estimation of BSS using LP with 95% CI, $y=0.1x-0.85$, $R^2=0.86$

TKE

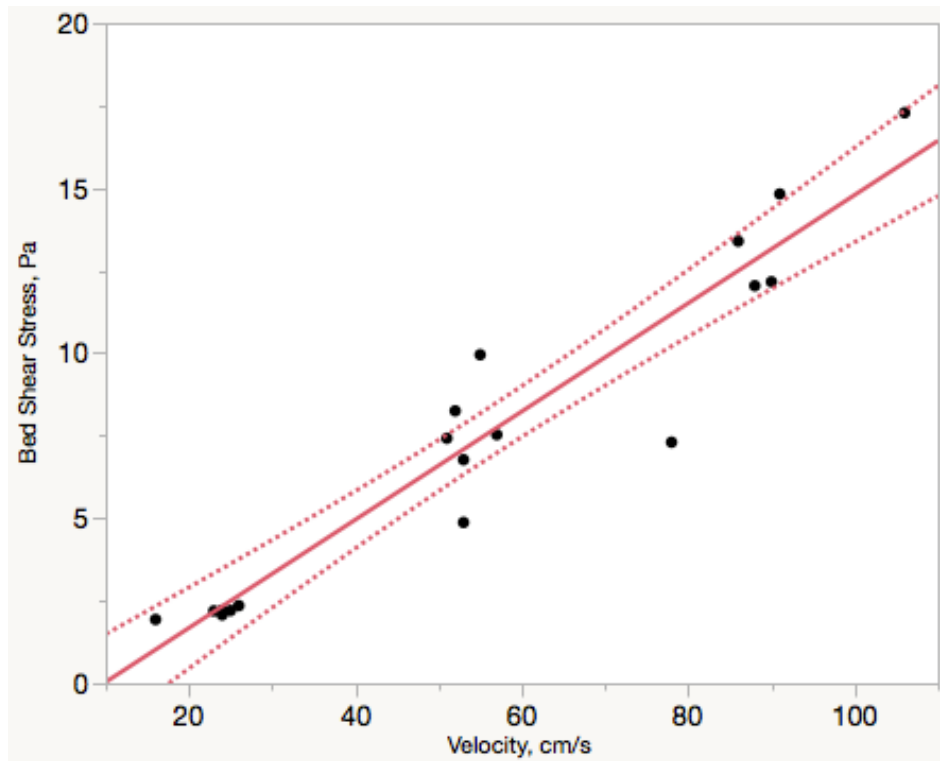


Figure 4.2: Estimation of BSS using TKE with 95% CI, $y=0.16x-1.6$, $R^2=0.91$

Linear relationships were observed between flow velocity and BSS with the LP and TKE methods yielding R^2 values of 0.85 and 0.91, respectively (Figures 5.1 and 5.2). Thompson et al. (2003) found a similar relationship, but developing a standard relation would be difficult since BSS varies between flume systems with different flow conditions and bed structures. A custom parameter test indicates the fits of LP and TKE were not significantly different (Appendix N).

Current velocity was binned into three categories. Six replicate datasets were collected for each velocity category. The intent of acquiring replicate datasets was to determine the reproducibility of desired BSS loads. (Tables 4.1 and 4.2).

Table 4.1: Replicates of BSS estimates determined by TKE

Comparison of repeatability of BSS TKE in Pa					
Current Velocity	Count	Mean	Min	Max	%RSD
24.6 ± 1.3	6	2.16	1.93	2.35	6.6
52.7 ± 1.3	6	7.46	4.87	9.95	22.4
89.8 ± 9.2	6	12.83	7.30	17.28	26.0

Table 4.2: Replicates of BSS estimates determined by LP

Comparison of repeatability of BSS LP in Pa					
Current Velocity	Count	Mean	Min	Max	%RSD
24.6 ± 1.3	6	1.26	0.57	1.47	30.6
52.7 ± 1.3	6	4.77	4.25	5.7	12.1
89.8 ± 9.2	6	8.65	6.2	9.53	14.8

The RSD of replicates generally increased with flow velocity. This suggests the system was more difficult to control at higher velocities due to higher variance in the flow field, possibly caused by flume geometries and motor induced turbulence. However,

velocities generated at the lowest speed settings were the most sensitive to motor adjustments. The highest RSD (i.e., LP = 30.6%) was observed at the lowest velocity due to this sensitivity. TKE generally had higher RSD than VP because of the uncertainty associated with single-point observations.

In addition, triplicate calculations were made within each dataset to measure instantaneous BSS over an averaged 1-minute period. The intent of calculating BSS at various points within the dataset was to determine the precision of any given estimate in the time series. The estimate of BSS by the TKE method had a mean relative percent difference of 19%. Estimates of BSS made using the LP method had a mean relative percent difference of 10%. The precision of estimates suggests instantaneous BSS did not deviate far from the mean BSS. While this discussion assumes the mean velocity for each experiment, the instantaneous values are also reported as the electric motor failed to maintain constant flow in 3 experiments (e.g., yr.day 14.041). This only occurred when performing multiple runs in a single day.

Temperature Effect

Oil erosion experiments were conducted at 5.3 ± 0.4 , 18.5 ± 1.9 , and $26.5 \pm 1.0^\circ\text{C}$. CSS (reported as TKE values) of bitumen is a function of temperature. No erosion was observed at $<17.5^\circ\text{C}$ in current velocities up to the facility maximum (106 cm/s, 2.06 kn) and under BSS conditions of 17.3 Pa. At $18.5 \pm 1.9^\circ\text{C}$, mass erosion of visible oil globules was observed in current velocities of 24.6 ± 1.3 cm/s (0.5 kn), corresponding to

a CSS of 2.2 Pa. At 26.5 ± 1.0 °C, the CSS was 1.9 Pa at 24.6 ± 1.3 cm/s (0.5 kn) current. Mass erosion was driven by temperature, where a lower threshold existed, under which, no erosion was observed (Figures 4.3 and 4.4).

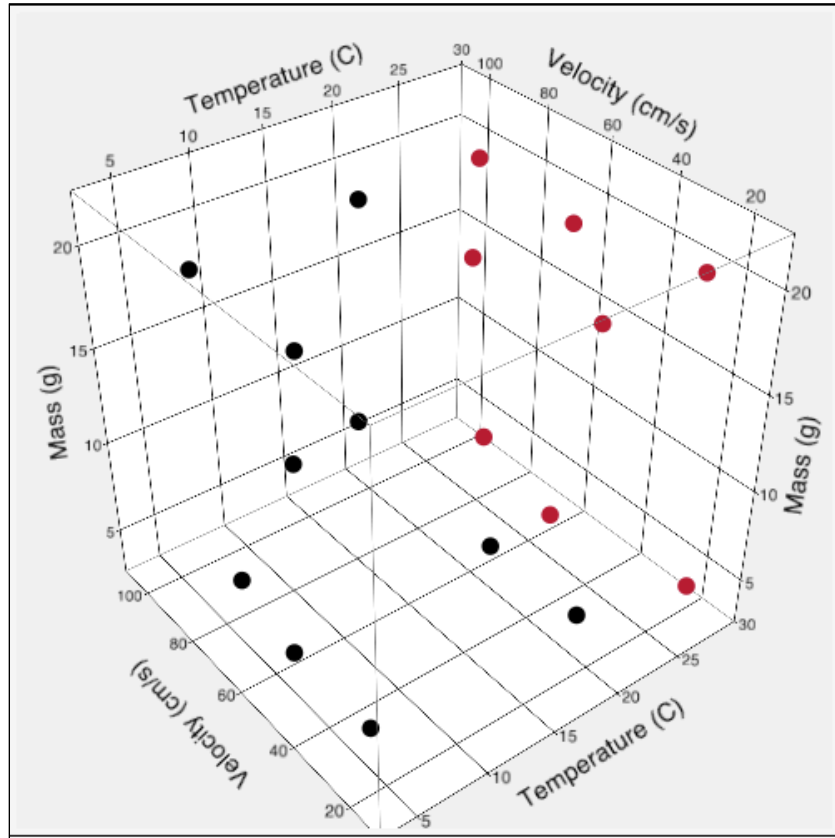


Figure 4.3: Temperature as the driving variable of mass erosion (red dots = experiment with erosion & black dot = experiment without erosion)

A nominal logistics regression (Baldi and Moore, 2009) for erosion was created using water temperature, current velocity and oil mass (Figure 4.4). Water temperature demonstrated the highest statistical significance ($p < 0.0001$). The potential for visual erosion exists above the threshold of 15°C. At 25°C, erosion is certain. The likelihood increases sharply from 17.5 to 22.5°C.

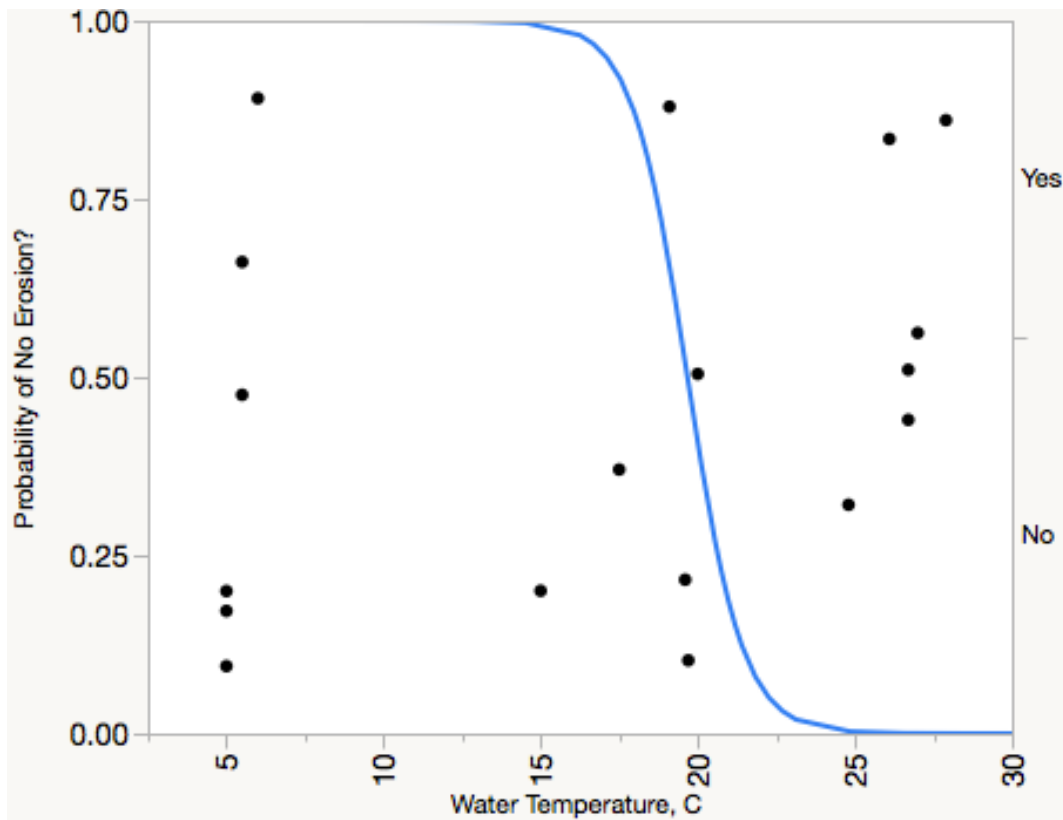


Figure 4.4: Nominal logistics plot for erosion as a function of water temperature (right side of line = erosion and left side of line = no erosion)

The model was validated using a contingency analysis (Appendix O) of observed data from the experiments in binary form. Of the ten conditions in which the model predicted no erosion, nine were verified by the data. Of the eight conditions in which the model predicted erosion, seven were verified. The model proved to be ~90% accurate with only two false predictions occurring in the simulated conditions (n=18).

Velocity Effect

Oil erosion experiments were conducted with fairly constant velocities of 24.6 ± 1.3 , 52.7 ± 1.3 , and 89.8 ± 9.2 cm/s. An inverse relationship between the occurrence of

mass erosion and current velocity was observed at all temperatures (Figure 4.5). The highest erosion frequencies were observed under the lowest velocity setting. Further, the highest erosion (i.e., 67) was associated with a velocity of 24 cm/s and the highest temperature (27.9°C) and largest initial oil mass (20g).

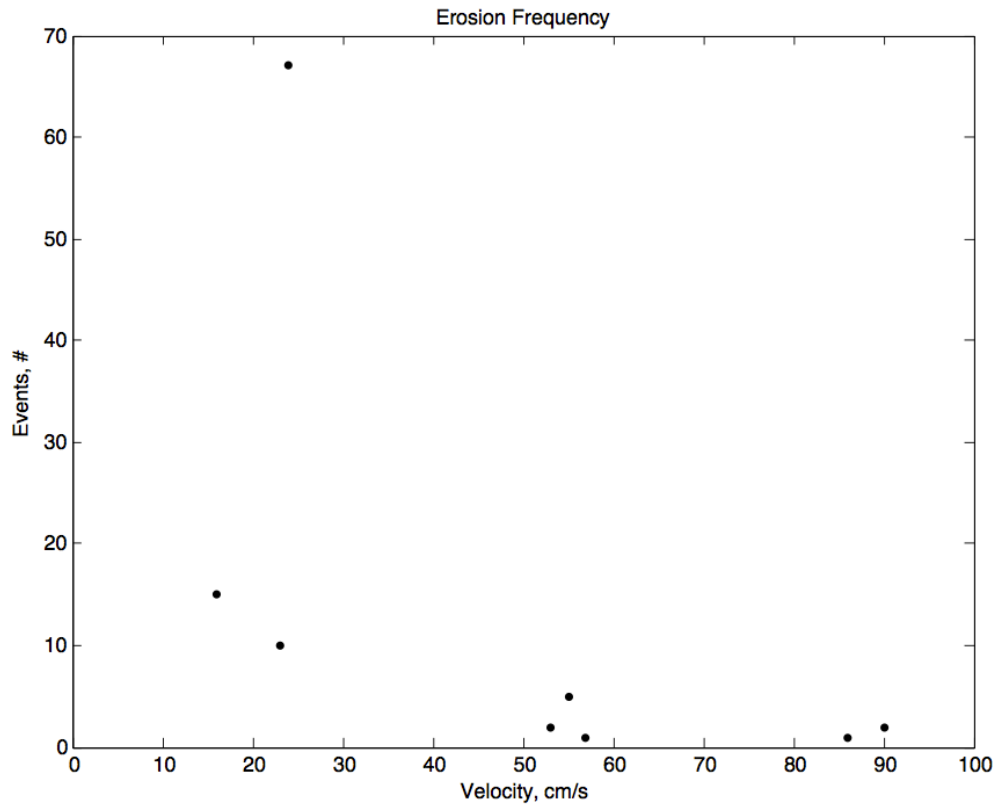


Figure 4.5: Erosion events per hour as a function of current velocity

A literature review on the rheology of bituminous materials explains the observed response. Viscoelasticity is the property of a material that exhibits both viscous (fluid's resistance to flow) and elastic (solid's tendency to return to its original form) characteristics (Roberson and Crowe, 1997). Bitumen is a viscoelastic material (Abivin et al., 2012) and exhibits shear-thickening behavior where, as the shear rate is increased, its

viscosity also increases. The bitumen will act stiffer (deform less) under faster rates of loading (i.e., higher flume current velocity).

This was observed in the experiments as the sunken bitumen eroded less with greater shear as current velocity increased (Figure 4.5). A light crude, such as Alaskan North Slope (API 31.4), does not have strong viscoelastic properties and will more closely resemble Newtonian flow (Ronningsen, 2012). The oil will behave similarly to Hibernian crude (API gravity of 35.1) observed by Cloutier et al. (2002) and erode more frequently under faster currents. Sediment interaction may result in a deviation from Newtonian flow if concentrations are high enough.

Viscoelastic effects are significant for all petroleum products consisting of high molecular weight compounds and large amounts of wax (paraffins) (Wardhaugh and Boger, 1991). These crudes (e.g., Californian Kern River Crude, other heavy oils) are likely to become submerged when released into the environment (Abivin et al., 2012). Hence, similar viscoelastic behavior can be expected for these types of sunken crudes making the data on Alberta bitumen even more helpful in predicting their fate during a spill in freshwater (e.g., rivers).

Mass Effect

Oil erosion experiments were conducted by stranding two different oil masses (20.1 ± 0.4 and 5.7 ± 0.5 g) on the tank bottom. Erosion was observed to be greater in

experiments using the larger mass of bitumen (Figures 4.6 and 4.7). In experiments using larger oil masses, erosion was also observed at lower temperatures.

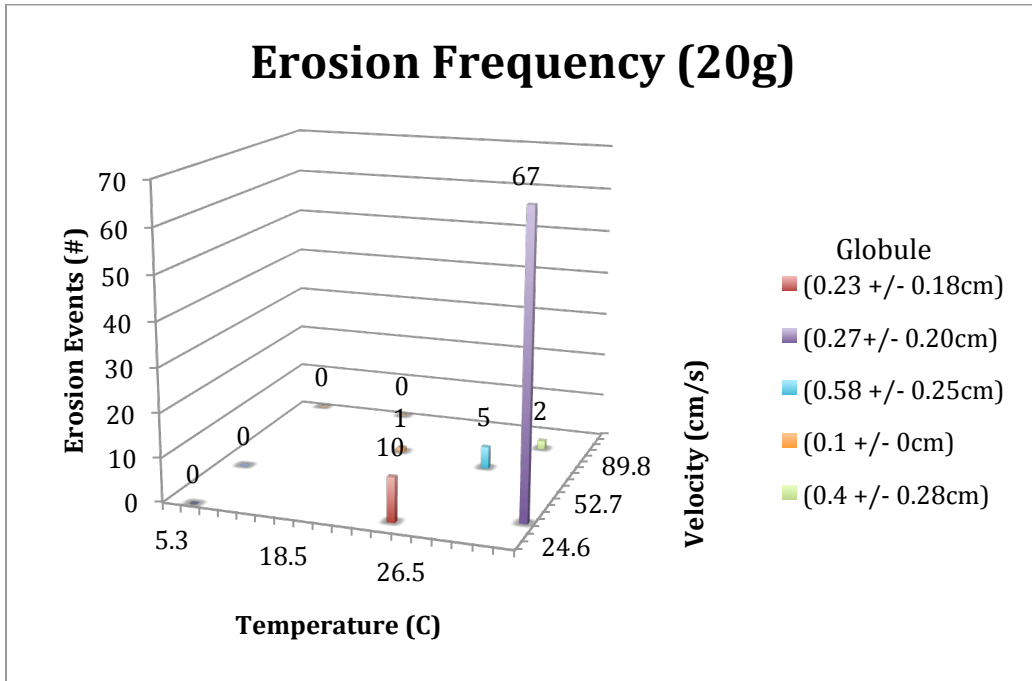


Figure 4.6: Erosion events observed in experiments using 20.1 ± 0.4 g of bitumen (digits above bars are number of erosions observed)

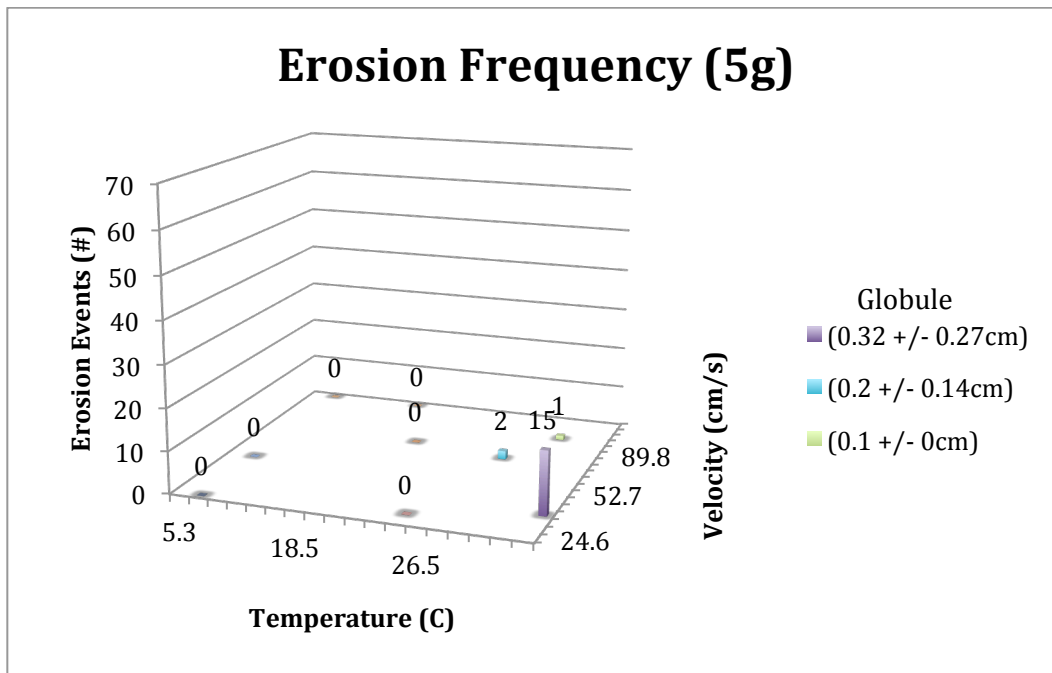


Figure 4.7: Erosion events observed in experiments using 5.7 ± 0.5 g of bitumen (digits above bars are number of erosions observed)

It is difficult to model erosion frequency because it resembles a one-point model (Baldi and Moore, 2009) where the experiment with 67 erosion events is extremely large relative to other experiments and dictates the model. Excluding the event to perform the analysis alters the model. This is also true when distinguishing between aliquot masses. While conclusions about erosion frequency can be made, it cannot be modeled without a more normally distributed dataset (i.e., more intermediate values). A greater number of experiments with replicates could allow future modeling.

Oil Migration

Disturbance of the stranded oil's surface and ripple formation was observed in all experiments. Migration of ripples along the surface of the oil slick was observed at temperatures $>15^{\circ}\text{C}$ and mass erosion of globules occurred into the water column at temperatures $>17.5^{\circ}\text{C}$ (Figure 4.8). Initially, ripples were 1 cm or larger in height and then diminished to a few millimeters over time, a possible mass limiting effect.

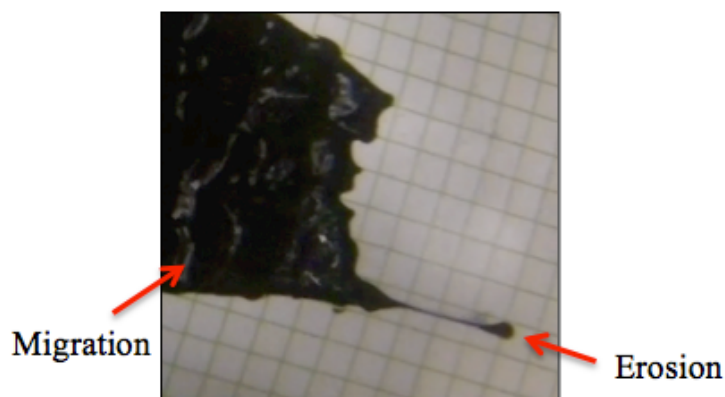


Figure 4.8: Oil migration showing ripple formation and globule erosion

As anticipated, the temperature had the greatest effect on rate of spreading along bottom. At 5.3 ± 0.4 °C, in 24.6 ± 1.3 cm/s current, the oil “pancake” did not appear to move (Figure 4.9). At 18.5 ± 1.9 °C, the lengthening was 176% in 89.8 ± 9.2 cm/s current (Figure 4.10). The “pancake” moved the greatest along bottom at 26.5 ± 1.0 °C in 89.8 ± 9.2 cm/s current, lengthening 350%.

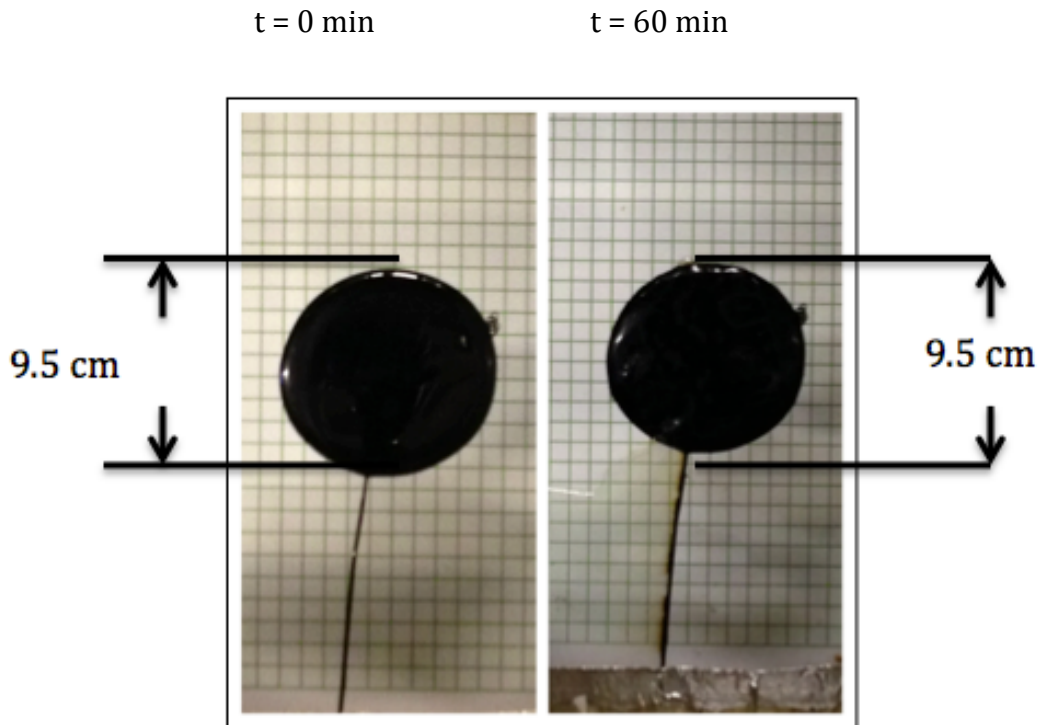


Figure 4.9: No oil spreading at $5.3 \pm 0.4 \text{ }^\circ\text{C}$

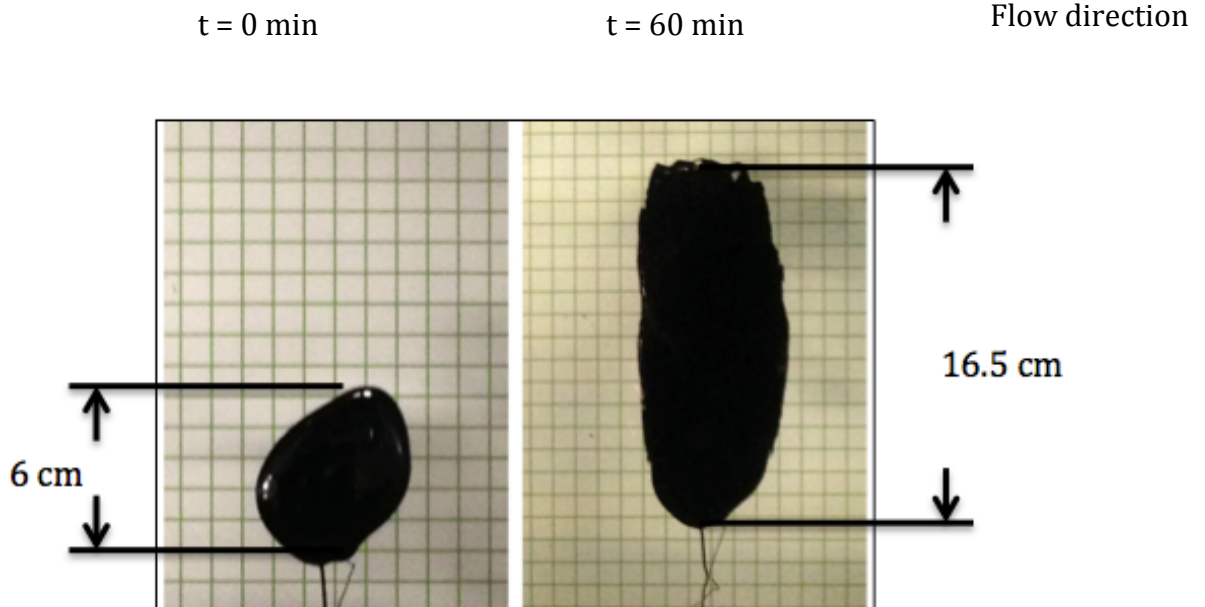


Figure 4.10: Oil advanced (i.e., component of migration) 176% at $18.5 \pm 1.9 \text{ }^\circ\text{C}$

Rise in temperature greatly increased the rate of oil migration (i.e., longitudinal lengthening) along bottom as the bitumen's viscosity decreased in warmer water (Figure 4.11). The amount of oil mass stranded on bottom had little effect on magnitude of spreading.

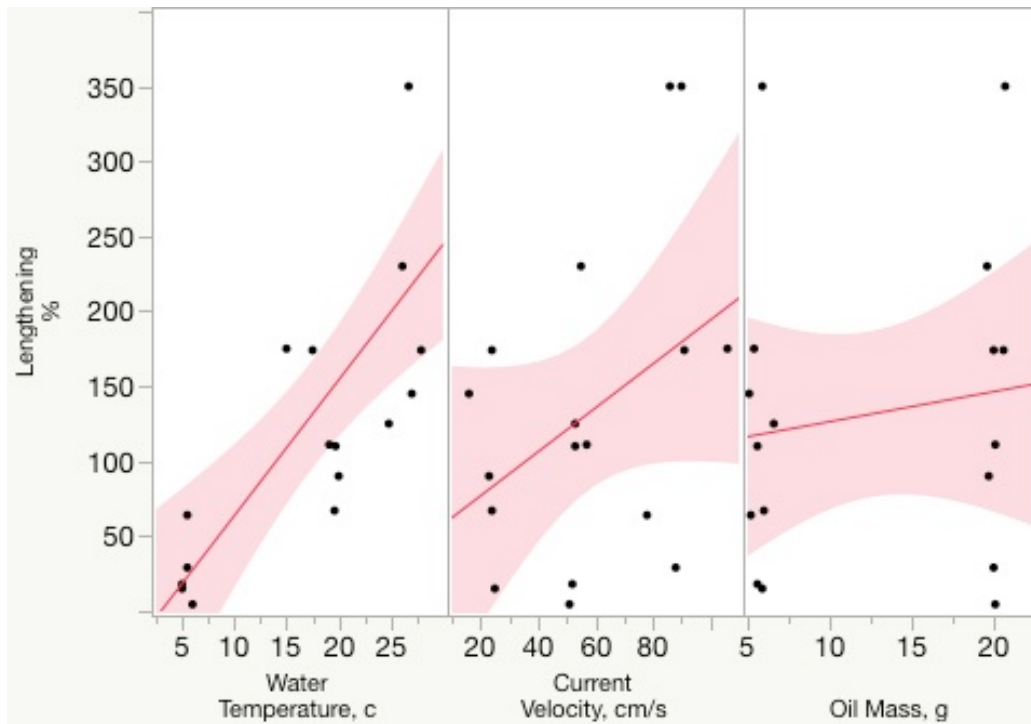


Figure 4.11: Lengthening of oil as function of water temperature, velocity and mass.

Performing a least squared analysis (Appendix P) of oil lengthening on bottom allowed a determination to be made on variable importance (e.g., total effect (TE) is an index that reflects the relative contribution of that factor alone and in combination with other factors). Temperature had the largest effect (TE = 0.78) on the magnitude of oil spreading by a significant margin. Current velocity had a modest effect (TE = 0.27), while oil mass was nearly negligible. A generalized regression analysis was also

performed for comparison and yielded similar results with temperature and velocity having total effects of 0.81 and 0.25, respectively.

The coefficient of multiple determination (i.e., proportion of variation in the response that can be attributed to the model rather than random error) of the lengthening profile was 0.96 suggesting the model is an excellent predictor of response. The response from water temperature and current velocity may be applied in the field during an emergency response in freshwater because of the large dynamic range investigated in the experiments. However, because the oil aliquot sizes were so small relative what would be released in a spill, extrapolating the response from initial oil mass is not recommended because the dynamics above that range are unknown (e.g., with thicker or broader oil masses on different substrates).

Globule Size

The oil globule size (in length, as long globules were observed) was measured using video camera footage and the test section grid. Erosion globule size (Appendix Q) was greater with an increase in water temperature (Figure 4.12). Water velocity and oil mass appeared to have little effect on sizes of eroding globules.

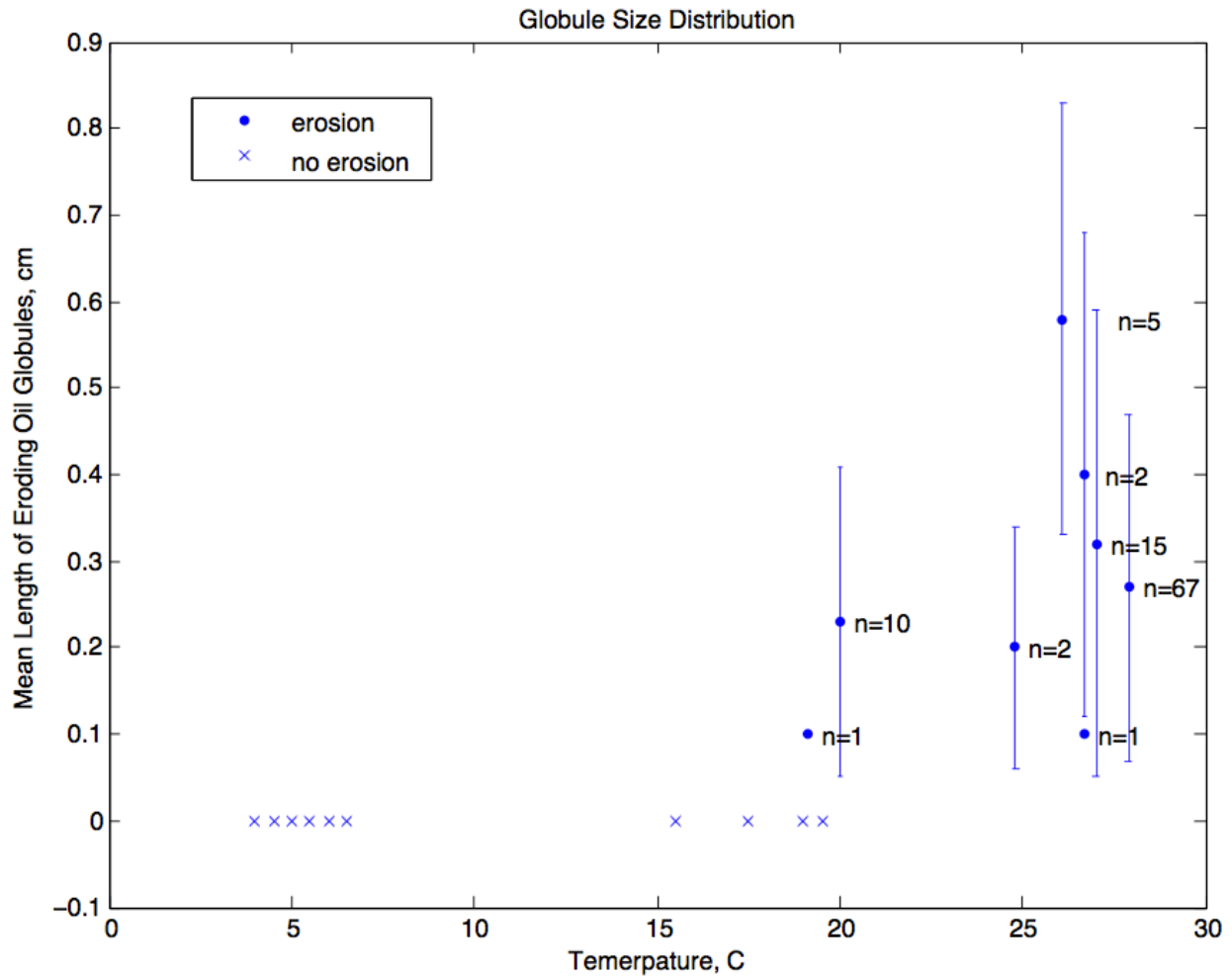


Figure 4.12: Mean eroding globule size observed in experiments

With sufficient BSS, globules of varying sizes were sheared off the oil film (~2mm thick) on bottom. NRC (1999) suggests for oil heavier than water under low currents, the oil will form small (mm) globules. However, until now, no laboratory measurements of eroding oil sizes have been made to substantiate this claim. While measuring globule size is subjective, the use of displacement grids provided a visual reference for estimates. Globule sizes of eroding bitumen ranged from several millimeters to centimeters, which is larger than the field observation made by NRC (1999). It is

difficult to model globule size because of subjectivity and is limited to a few data points, but trends suggest the size distribution may be a function of the oil's physical properties (e.g., viscosity due to temperature) and not water turbulence.

The manner in which the globules eroded from tank bottom provides insight into the expected behavior of sunken oil in the field. The globules tended to be elliptical with long tails and pulled off the oil mass in a “taffy-like” motion (Figure 4.8). At 26.5 ± 1.0 °C, steady erosion of globules were observed from all areas of the oil slick (Figure 4.13). At 18.5 ± 1.9 °C, globules eroded in “bursts” from the anterior of the oil slick, often following the “surge” of a large ripple (i.e., spike in migration rate (Appendix R)).

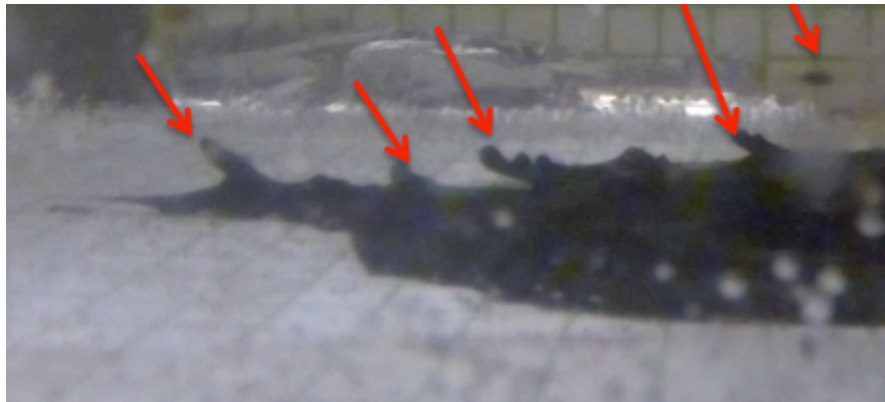


Figure 4.13: Continuous erosion of oil globules observed at 26.5 ± 1.0 °C (black arrow = direction of flow and red arrows = eroding globules)

←
Direction of flow

CSS Estimates

The CSS was defined as the minimum mean BSS to cause deformation of oil slick and resuspend bitumen into the water column (Figure 4.14). Oil erosion was observed in experiments where the mean BSS was 1.93, 2.07, 2.19, 6.77, 7.53, 9.95, 12.16, and 13.39 Pa based on TKE calculations (Table 4.3). Those same conditions as calculated by LP were 0.57, 1.37, 1.6, 4.41, 5.18, 5.7, 9.34, and 9.53 Pa. The conditions where erosion was observed were 18.5 ± 1.9 °C or 26.5 ± 1.0 °C and the majority were using the larger oil mass (20.1 ± 0.4 g). These estimates of the CSS are the first to quantify conditions in which Alberta bitumen on a smooth surface will undergo mass erosion (Appendix S). The relationship between bitumen erosion and environmental conditions (i.e., temperature and velocity) is shown in Figure 4.15.

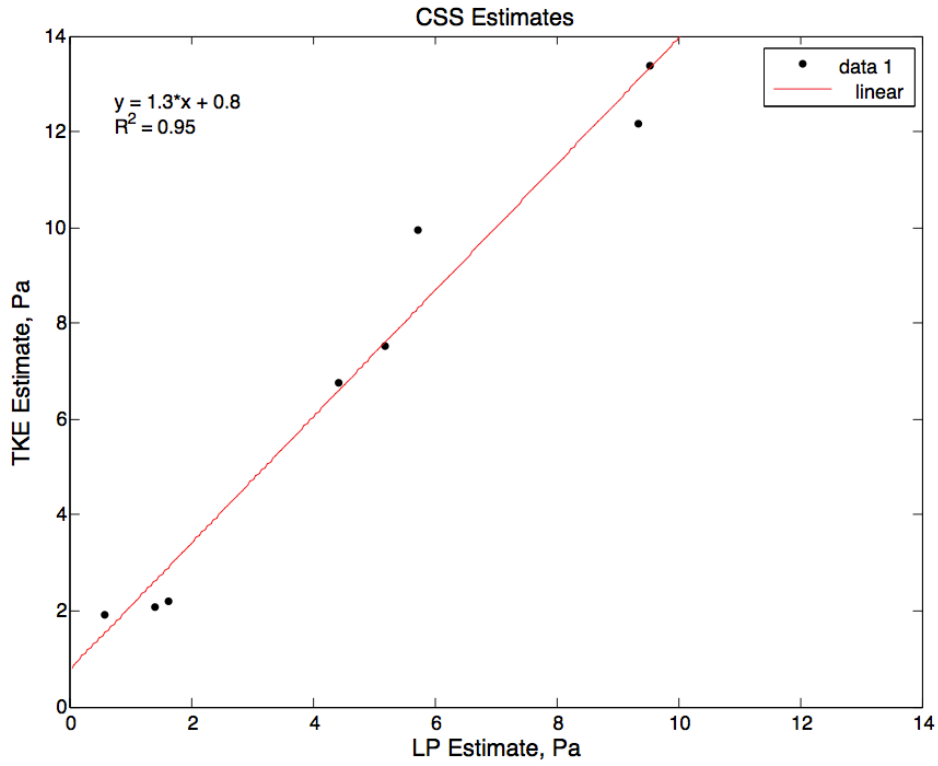


Figure 4.14: Comparison of CSS using TKE and LP methods

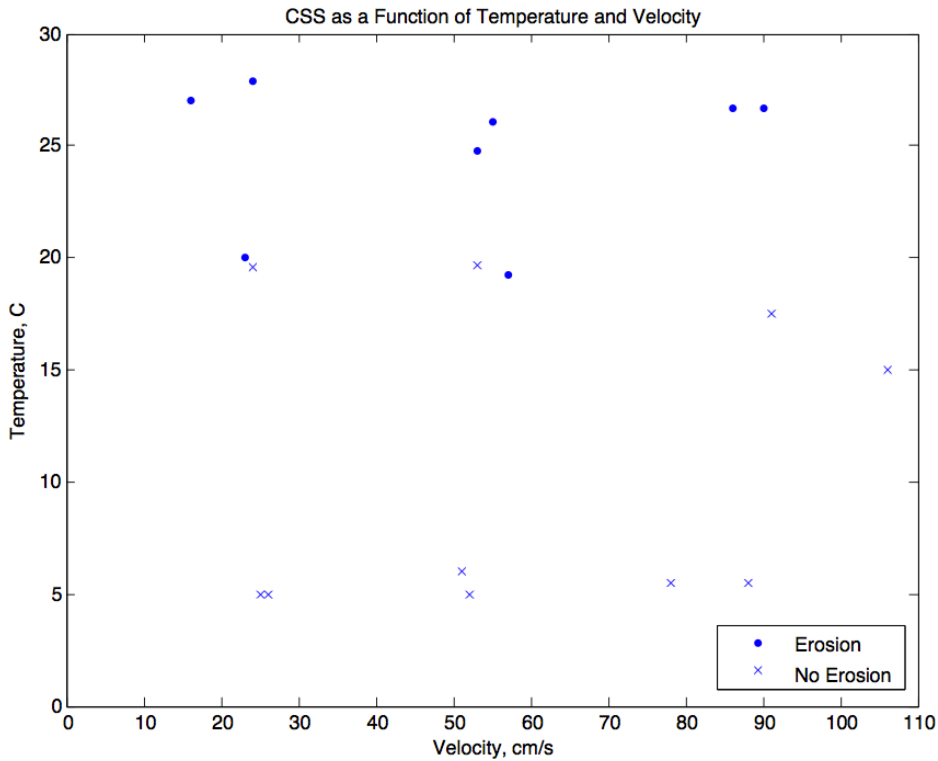


Figure 4.15: CSS increases with velocity and decreases with temperature

The LP and TKE values were statistically significant ($p=0.002$) as determined by a custom parameter test (Appendix T). However, this is likely a type II error because the change in significance is the result of a reduced sample size (i.e., $n=8$ vs. $n=18$). The earlier analysis (Appendix N) had more statistical power and determined the two methods were not statistically significant.

Literature suggests the TKE method is the best estimate of BSS (Biron et. a., 2009). The TKE method exhibited the most consistency in the experiments (i.e., required assumptions were never violated) and has fewer limitations (e.g., appropriate for non-steady state conditions) than the LP method when applied to the field. Therefore, this thesis reported the CSS using TKE. At $\geq 18.5 \pm 1.9$ °C, the CSS of Alberta bitumen was ~ 2 Pa. The CSS of Alberta bitumen was not reached up to ~ 18 Pa at temperatures $< 18.5 \pm 1.9$ °C.

The experiments in which the CSS of bitumen was determined were conducted using freshwater. If the water were more saline (i.e., estuarine, oceanic), the BSS would be slightly higher due to increased density ($\rho_{\text{H}_2\text{O}}=998\text{kg/m}^3$ vs. $\rho_{\text{NaCl}\cdot\text{H}_2\text{O}}=1025\text{ kg/m}^3$) of the saturated fluid ($\tau_0 = \rho_w U_*^2$), but the CSS of bitumen would remain the same even if the velocity profile was affected because it is a physical property of the bitumen. Hence, this thesis research can be applied to a variety of environments.

Table 4.3: Summary of all experimental results

Temp, C	Velocity, cm/s	Mass, g	Erosions, #/hr	Lengthening %/hr	τ, Pa (TKE)	τ, Pa (LP)	Mean Globule Size (cm)
17.5	91	20.6	0	174	14.82	9.40	-
5.5	88	20	0	29	12.04	8.30	-
5.5	78	5.2	0	64	7.30	9.10	-
15.0	106	5.4	0	175	17.28	6.20	-
5.0	26	20.1	0	0	2.35	1.50	-
26.1	55	19.6	5	230	9.95	5.70	0.58
24.8	53	6.6	2	125	6.77	5.18	0.20
6.0	51	20.1	0	4.5	7.42	4.25	-
27.9	24	20	67	174	2.07	1.60	0.27
27.0	16	5.1	15	145	1.93	0.57	0.32
5.0	52	5.6	0	18	8.25	4.28	-
5.0	25	5.9	0	15	2.20	1.05	-
26.7	86	5.9	1	350	13.39	9.35	0.10
26.7	90	20.7	2	350	12.16	9.53	0.40
19.7	53	5.6	0	110	4.87	4.81	-
19.1	57	20.1	1	111	7.53	4.41	0.10
19.6	24	6	0	67	2.21	1.47	-
20.0	23	19.7	10	90	2.19	1.37	0.23

*0 and - no erosion observed; hence no globule size. Supplemental data can be found in Appendix U.

Adhesion

The adhesion numbers of the bitumen were 3150, 531, and 376 g/m² at 5, 20, and 27 °C, respectively (Figure 4.16).

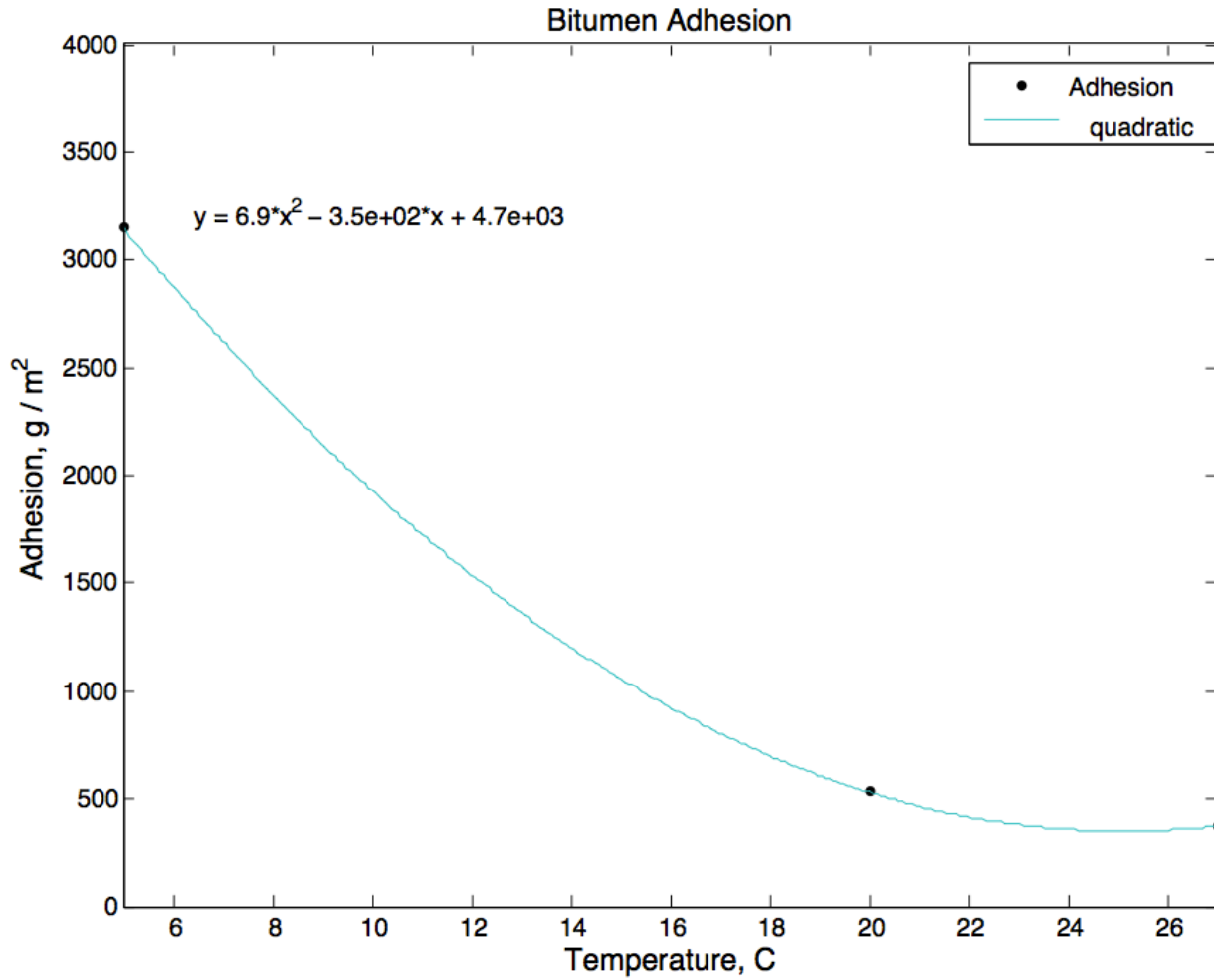


Figure 4.16: Adhesion number as a function of temperature

The adhesion characteristic is informative in an emergency response as it helps predict the “stickiness” of oil. The penetrometer test determined that Alberta bitumen has a strong affinity to adhere to a substrate and to have particles stick to its surface.

Broje and Keller (2006) measured interfacial interactions between hydrocarbons and various surfaces for oil recovery purposes. A dynamic contact angle (DCA) analyzer (Cahn Radian 315, Thermo Electron Corporation) was used to measure adhesion-related parameters. Oil recovery was measured as the weight of adhered oil per unit surface area. The adhesion of Cooks Inlet, AK ($\rho=886 \text{ kg/m}^3$, $\nu=9.6 \text{ mPas}$) and marine fuel IFO-120 ($\rho=965 \text{ kg/m}^3$, $\nu=1540 \text{ mPas}$) on a steel surface at $15 \text{ }^\circ\text{C}$ was 10 and 30 g/m^2 , respectively.

The DCA analyzer automates the adhesion method and achieves more consistent and reliable results than the penetrometer. However, because of the similarities in methods, a comparison between the test oils can be made. The adhesion of Alberta Bitumen ($\rho=1,100 \text{ kg/m}^3$, $\nu=29,116 \text{ mPas}$) to a similar surface was significantly greater at all temperatures than the oils investigated by Broje and Keller. This suggests that during a spill, the Alberta bitumen is more likely to foul structures and settle to the bottom of a water body.

Implications of Research

The containment and recovery of sunken oil has proven to be very difficult. The shearing off or movement of sunken oil is especially bad (e.g., shuts down cooling water intakes, raw intakes for potable water, sensitive species impacts, reduces amount of recoverable oil). Spill modelers can use the data generated by this research to help predict the fate and transport of sunken oil. In the experiments, temperature was found to be the

most important variable affecting the CSS of bitumen with no erosion observed at temperatures $< 18.5 \pm 1.9^{\circ}\text{C}$. Therefore, sunken bitumen resulting from spills occurring in cold or temperate climates would likely remain stranded on bottom once it settled. This also applies to deeper ocean spills where there is a steep cooling temperature gradient to 4°C . In the experiments, all visual erosion of bitumen was observed at temperatures $> 18.5 \pm 1.9^{\circ}\text{C}$. Hence, potential for erosion of bitumen is greater in tropical or subtropical climates where water temperatures can reach 20°C (68°F) or higher (e.g., T/B Morris J. Berman Spill (API gravity of 9.5) in San Juan, Puerto Rico, 1994).

While heavy petroleum products such as bitumen may initially suspend in the water column, once stranded on bottom even the strongest tidal systems (e.g., Piscataqua River, NH = 200 cm/s , 4 kn) would probably not cause erosion of sunken bitumen unless the ambient water temperatures met the thresholds for erosion observed in these experiments. Observations from a recent Mississippi River spill of slurry oil (API gravity < 13) in summer 2015 verified this laboratory model. Changes in side-scan sonar images over a few days showed minimal mobilization of the oil along the riverbank suggesting no erosion at $\sim 14^{\circ}\text{C}$. The recovery of sunken oil was accomplished using an environmental clamshell bucket.

Recommended Response Protocol

Model development of submerged oil has rarely been studied and establishing a methodology to compute resuspension of sunken oil is needed. In the event heavy oil is spilled, the following is recommended to determine its fate.

1. Determine what class of oil is released into the environment: Check manifest and MSDS for description of oil. The oil's API gravity and initial visual observations can be used to determine likelihood of it floating, submerging or sinking to the bottom.
2. Determine if submerged oil will likely remain suspended in the water column or sink to bottom: Conduct oil-to-water contact experiments (e.g., introduce small samples of collected spill oil into jars of ambient water) to determine potential oil behavior. Confirm the oil is on the seabed/riverbank using side-scan sonar and/or divers.
3. Determine physical properties of the oil: Obtain viscosity and specific gravity estimates from MSDS and send samples of "neat" oil and "weathered oil" to a lab (e.g., Environment Canada) for physical characterization (i.e., density, viscosity) at various temperatures (e.g., temperature profile as a function of water depth) specific to ambient conditions at spill site.

4. Determine coastal processes and measure physical conditions at the spill site: Few if any real-time measurements of currents have been made during recent spills (e.g., Delaware River, 2004; Mississippi River, 2015), but current estimates with depth are necessary in a response to potentially predict the movement of the sunken oil. Request an Oil Spill Response Vessel take physical measurements (i.e., water temperature, salinity, bathymetry). For some incidents, there may be automated oceanographic buoy systems nearby equipped with instrumentation capable of measuring these characteristics in mid-water column and near-bottom.

5. Obtain measurements needed to calculate BSS: Depending on equipment availability, measure single-point 3D current velocity (u, v, w). Measurements should be taken close to the boundary layer, preferably within 20% of flow depth (e.g., if water depth is 10 ft., take measurements at ≤ 8 ft.). If this is not possible, free stream velocity measurements can be used. If deployment of a velocimeter is not possible, then a determination of bed stress can be made as a function of pressure using $\tau_o = \gamma RS$ where γ is the specific gravity of water, R is the hydraulic radius (approximately the depth of water for a wide channel), and S is slope of channel.

6. Calculate BSS: Plot average current flow and superimpose velocity fluctuations to obtain the three velocity components, u', v', w' used to calculate turbulent energy.

7. Predict potential movement of sunken oil: Compare ambient BSS to available CSS estimate for the spilled oil or a similar oil under same conditions. If BSS is significantly less than the CSS, oil will remain stranded on bottom. If BSS is above critical values, then oil will mobilize and resuspend. At a minimum, spill modelers can approximate the conditions under which the oil globules will shear off oil adhered to the bottom. While digital cameras may allow for quick on-site observations, it is often very difficult to videotape because of turbidity and depth of water.

Chapter 5: CONCLUSIONS

Simecek-Beatty (2007) proposed a method for modeling the resuspension of submerged oil using laboratory and real time measurements of bottom currents, but its abilities are limited if the CSS of the oil is not known. The UNH CRRC flume facility is capable of conducting experiments to determine the CSS of specific oils. Only one study, Cloutier et al. (2002) has been published showing data estimating the conditions under which a sunken oil will erode off bottom. They determined mass erosion of Hibernian crude (API 35) will occur at CSS of >5 Pa in seawater at 13 °C. At 4 °C, they determined the Hibernian will not erode under bed loads <7 Pa.

Unfortunately, the oil Cloutier et al. used was a high API gravity and will not readily sink in the event of a spill. Spill modelers need the CSS values of heavier oils to more accurately predict the fate of sunken oil. This thesis research provides such data on Alberta bitumen, a low API gravity petroleum product ($\sim 8.5^\circ$). Mass erosion of bitumen will occur at ~ 2 Pa. in freshwater $\geq 18.5 \pm 1.9$ °C and will not erode under BSS up to ~ 18 Pa between 5.3 ± 0.4 and 18.5 ± 1.9 °C. The estimated CSS can be used in spills of similar products (Group V oils), as it is common practice to use one group V oil's characteristics to represent the likely behavior of another. This gives modelers the option to apply the expected behavior of Alberta bitumen during an emergency response and

would be a more realistic assumption for heavy oil spills than currently available based on the Hibernian crude.

Chapter 6: RESEARCH RECOMMENDATIONS

- Research is needed to determine the CSS of more oils with varying API gravities. This research investigated an oil of low API gravity (Alberta bitumen, 8.5° API). Oils of medium API gravities (California Kern River Crude, 15° API) need to be studied, as well as lighter oils (Alaskan crude, 32° API) mixed with sediment to make them sink. Experiments also need to be conducted using oil stranded on various bottom types (e.g., sand, mud). This research examined stranded oil on a smooth, flat artificial (Plexiglas) surface, which best resembles a flat bedrock bottom. It is also possible that the CSS of the bed substrate (e.g., silt) could be less than that of the oil, which lowers its velocity threshold for erosion.
- Improved estimation of BSS is essential to improving predictions of the conditions under which erosion of sunken oil will occur. While oil spill modelers suggested the methods used in the study, a thorough investigation of other possible BSS calculation methods such as Reynolds stress and the Shields approach are recommended. Each estimation method is subject to different types of errors (e.g., instrument noise, selection of sample volume for turbulence analysis). So, in future experiments, multiple methods appropriate for the local flow environment should be used for estimation.

- The velocity profiles (Appendix V) revealed some inconsistencies that may have affected the accuracy of BSS estimates. The velocity profile method requires that the flow conform to a logarithmic profile. In some experiments, the velocity departed from this assumption. The flow straightener inside the test section was the likely source of error. Moving the test section further downstream may reduce artificial turbulence and achieve more consistency among the experiments. A comparison of BSS estimates using the free stream velocity is recommended when certain boundary layer assumptions are violated.
- Acoustic interference (i.e., echoes from past pings affecting present measurements) is a concern when using coherent Doppler instruments, but often resolved by moving the instruments position or changing sampling parameters (e.g., pulse length). However, when profiling near the boundary a reflection is difficult to avoid. Despite the hard tank bottom, the signal-to-noise ratios in this research (Appendix V) suggest minimal acoustic reflection within sampling volume. In the future, acoustic interferences could be avoided using soft and more acoustically absorbent materials (e.g., wood, rubber, foam, natural substrate).

REFERENCES

- Abivin, P., Taylor, S., & Freed, D. (2012). Thermal behavior and viscoelasticity of heavy oils. *Energy & Fuels*, 26(6), 3448-3461.
- Amos, C., Grant, J., Daborn, G., & Black, K. (1992). Sea Carousel—A benthic, annular flume. *Estuarine, Coastal and Shelf Science*, 34(6), 557-577.
- Biron, P., Lane, S., Roy, A., Bradbrook, K., & Richards, K. (1998). Sensitivity of bed shear stress estimated from vertical velocity profiles: The problem of sampling resolution. *Earth Surface Processes and Landforms*, 23, 133-139.
- Biron, P., Robson, C., Lapointe, M., & Gaskin, S. (2004). Comparing different methods of bed shear stress estimates in simple and complex flow fields. *Earth Surface Processes and Landforms*, 29, 1403-1415.
- Broje, V., & Keller, A. (2007). Interfacial interactions between hydrocarbon liquids and solid surfaces used in mechanical oil spill recovery. *Journal of Colloid and Interface Science*, 305(2), 286-292.
- Cloutier, D., Amos, C., Hill, P., & Lee, K. (2002). Oil Erosion in an Annular Flume by Seawater of Varying Turbidities: A Critical Bed Shear Stress Approach. *Spill Science & Technology Bulletin*, 83-93.
- Hamilton, E. (1970). Reflection Coefficients And Bottom Losses At Normal Incidence Computed From Pacific Sediment Properties. *Geophysics*, 35(6), 995-1004.
- Hassid, S., & Galperin, B. (1988). A turbulent energy model for geophysical flows. *Boundary-Layer Meteorol Boundary-Layer Meteorology*, 397-412.
- Kim, S., Friedrichs, C., Maa, J., & Wright, L. (2000). Estimating bottom stress in tidal boundary layer from acoustic Doppler velocimeter data. *Journal of Hydraulic Engineering*, 126(6), 399-406.
- Rønningsen, H. (2012). Rheological properties of water-in-oil emulsions with some waxy North Sea crude oils. *Theoretical and Applied Rheology*, 20, 687-687.
- Simecek-Beatty, D. (2007). A proposed method for computing re-suspension of submerged oil. Paper in: Proceedings of the 30th Arctic and marine oil spill program (AMOP) technical seminar.
- Soulsby, R. (1983). Chapter 5 The Bottom Boundary Layer of Shelf Seas. *Physical Oceanography of Coastal and Shelf Seas Elsevier Oceanography Series*, 189-266.

- National Research Counsel. *Spills of nonfloating oils risk and response*. (1999). Washington, D.C.: National Academy Press.
- Stapleton, K., & Huntley, D. (1995). Seabed stress determinations using the inertial dissipation method and the turbulent kinetic energy method. *Earth Surf. Process. Landforms Earth Surface Processes and Landforms*, 20, 807-815.
- Thompson, C., Amos, C., Jones, T., & Chaplin, J. (1993). The manifestation of fluid-transmitted bed shear stress in a smooth annular flume – A comparison of methods. *Journal of Coastal Research*. 19(4), 1094-1103.
- Voulgaris, G., & Trowbridge, J. (1998). Evaluation of the acoustic Doppler velocimeter (ADV) for turbulence measurements. *Journal of Atmospheric and Oceanic Technology*, 15, 272-289.
- Wardhaugh, L., & Boger, D. (1991). Flow characteristics of waxy crude oils: Application to pipeline design. *AIChE Journal*. 37(6), 871-885.
- Wilcock, P. (1996). Estimating Local Bed Shear Stress from Velocity Observations. *Water Resources Research*, 32(11), 3361-3366.
- Baldi, B., & Moore, D. (2009). *The Practice of statistics in the life sciences*. New York: W.H. Freeman and Co.
- Roberson, J., & Crowe, C. (1997). *Engineering fluid mechanics* (6th ed.). New York: J. Wiley & Sons.
- Bendat, J., & Piersol, A. (2010). *Random data analysis and measurement procedures* (4th ed.). Hoboken, N.J.: Wiley.

Appendix A: Case Studies of Nonfloating Oil Spills

T/B DBL-152

In 2005, the Tanker Barge DBL-152, while making its way from Houston, TX to Tampa, FL, collided with submerged remains of a pipeline service platform that had collapsed during Hurricane Rita. Its cargo, 100,000 barrels of slurry oil, a by-product of petroleum refining, was released into the Gulf of Mexico. The oil had a very low API (4°) and sank to the seafloor.

The sunken oil was difficult to locate and monitor. Trawler vessels equipped with snare sentinels (e.g., chain drags and crab pots with absorbent material) and remotely operated vehicles (ROVs) were deployed to find the sunken oil. Very little (~5%) was collected by divers. Some of the oil remaining in the environment washed up on shorelines many months after the incident.

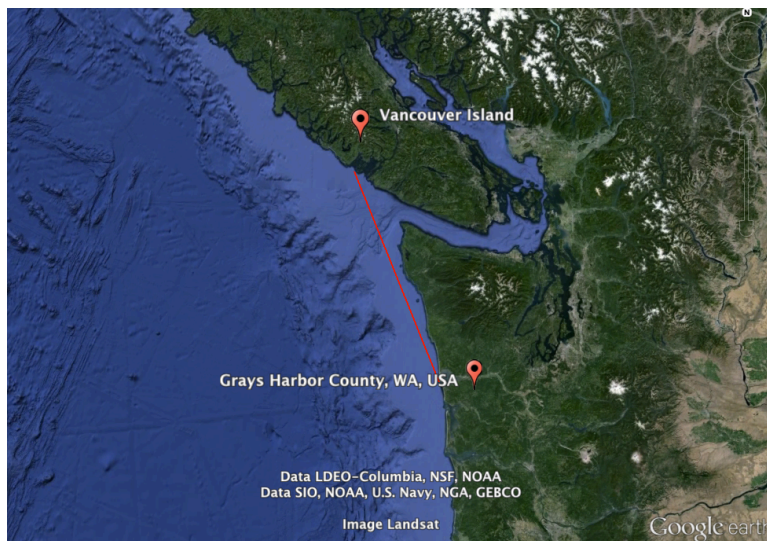


(epa.gov)

Nestucca Spill

A tug vessel lost its tow of the Nestucca barge in 1988 a few miles off Greys Harbor, WA. When the tug attempted to reestablish the connection, it collided with the bow of the barge. The collision ripped a hole in the barge causing 6,000 barrels of API 12 oil to spill along Washington's outer coast.

High seas and strong current precluded the use of containment booms, so no attempt was made for open water recovery. The spilled oil was over washed by waves and quickly formed tar balls that moved below the water surface and could not be tracked visually. Two weeks later, the oil unexpectedly came ashore in discontinuous patches along the coast of Vancouver Island, Canada, 175 kilometers north of the release site. It contaminated 150 kilometers of shoreline.



(Google Earth)

Kalamazoo River

In 2010, an Enbridge pipeline ruptured releasing > 1,000,000 barrels of dilbit (bitumen mixed with a diluted crude of lighter density) near Marshal, MI. The dilbit (~20 API) entered Talmadge Creek and flowed into the Kalamazoo River, which is a tributary of Lake Michigan. The oil became submerged in the tributary because, as the diluent evaporated, the remaining product became mixed with the high sediment load in the creek (due to recent flooding) and its density increased. The USEPA was in charge of the response to the spill and directed Enbridge to take removal actions. Unfortunately, due to the nature of the spill much of the oil could not be immediately recovered without causing significant adverse impacts to the creek and river. The sunken oil had to be carefully monitored and collected slowly over time. In 2013, the EPA ordered Enbridge to remove oil and oil-containing sediment along parts of the Kalamazoo River where significant accumulations were found.

The best way to identify the location of the sunken oil in these shallow waterways and determine its extent was using a field technique known as poling. Poling involves manually agitating soft sediment and river mud using a pole. When the sediment was agitated, the sunken oil rose to the surface in the form of oil sheen and globules. The resulting areas of recovery indicated where other sunken oil might reside and these locations were targeted for dredging.

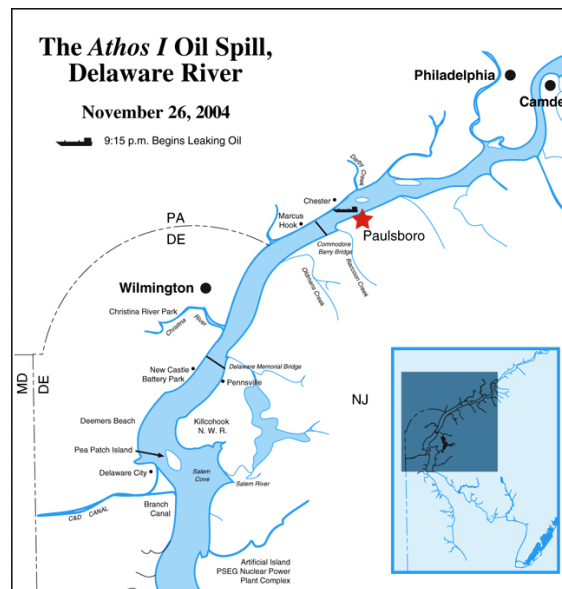


(epa.gov)

M/T Athos

On November 26, 2004, the M/T Athos I struck several submerged objects and released approximately 6,500 barrels of Bachaquero crude oil into the Delaware River, which is a major tidal estuary. The tanker's draft was 36 feet. It was traversing a channel depth thought to be 40 feet. At the time of the incident, the river was flooding with water current velocities around 1.5 kn. near the release site; divers spotted two large trenches filled with crude. The oil jetted out of the ship causing entrainment with clay and mud from the bottom, creating a cohesive mixture denser than the ambient seawater. The oil in the large trenches was vacuumed out. When samples of the oil were taken and placed in jars of cold, freshwater, the oil floated to the surface. A major concern for the Unified Command was that sufficient BSS applied to the oil in the trenches could cause erosion and allow it to move. Little, if any, real-time observations of waves, currents or bottom characteristics were available at the time of the incident. This scenario illustrated the

questions and problems modelers encounter when attempting to predict behavior of sunken oil during a response.



(epa.gov)

The sunken oil posed a major risk to a local nuclear power plant as it drew water from the river for cooling purposes. It cost millions of dollars a day to shut down the nuclear plant. If decision makers had known under what conditions and currents the sunken oil would resuspend or mobilize, then a more informed decision about closing the plant intakes could have been made.

Material Safety Data Sheet


PETRO-CANADA BITUMEN



1. Product and company identification

Product name	: PETRO-CANADA BITUMEN
Synonym	: MacKay River Bitumen, Dover Bitumen, Bitumen, Off-Spec Bitumen, Sales Oil
Code	: 90000124
Material uses	: Raw product for oil refineries to produce fuels and other petroleum based organic products.
Manufacturer	: PETRO-CANADA P.O. Box 2844 150 – 6th Avenue South-West Calgary, Alberta T2P 3E3
<u>In case of emergency</u>	: Petro-Canada: 403-296-3000 Canutec Transportation: 613-996-6666 Poison Control Centre: Consult local telephone directory for emergency number(s).

2. Hazards identification

Physical state	: Viscous liquid.
Odour	: Tarry odour. "Rotten egg" if H ₂ S present, but odour is an unreliable warning, since it may deaden the sense of smell.
WHMIS (Canada)	:  Class D-2B: Material causing other toxic effects (Toxic).
OSHA/HCS status	: This material is considered hazardous by the OSHA Hazard Communication Standard (29 CFR 1910.1200).
Emergency overview	: WARNING! CAUSES EYE AND SKIN IRRITATION. MAY CAUSE ALLERGIC SKIN REACTION. Irritating to eyes and skin. May cause sensitisation by skin contact. Do not breathe vapour or mist. Do not get on skin or clothing. Avoid contact with eyes. Wash thoroughly after handling.
Routes of entry	: Dermal contact. Eye contact. Inhalation. Ingestion.
<u>Potential acute health effects</u>	
<u>Inhalation</u>	: Inhalation of this product may cause respiratory tract irritation and Central Nervous System (CNS) Depression, symptoms of which may include; weakness, dizziness, slurred speech, drowsiness, unconsciousness and in cases of severe overexposure; coma and death. At higher concentrations (above 10 ppm), hydrogen sulphide is extremely toxic by inhalation, may cause respiratory-tract irritation and respiratory failure, coma and death. Pulmonary edema can occur up to 24 hours after hydrogen sulphide exposure. While hydrogen sulphide emits a strong odour of rotten eggs, detection by smell is not sufficient as a warning property for exposure to this substance, as it may deaden the sense of smell quickly.
<u>Ingestion</u>	: Ingestion may cause narcosis.
<u>Skin</u>	: Irritating to skin. May cause sensitisation by skin contact. Hot bitumen can burn skin.
<u>Eyes</u>	: Irritating to eyes. Hot bitumen can burn eyes.
<u>Potential chronic health effects</u>	
<u>Chronic effects</u>	: Once sensitized, a severe allergic reaction may occur when subsequently exposed to very low levels.
<u>Carcinogenicity</u>	: No known significant effects or critical hazards.
<u>Mutagenicity</u>	: No known significant effects or critical hazards.
<u>Teratogenicity</u>	: No known significant effects or critical hazards.
<u>Developmental effects</u>	: No known significant effects or critical hazards.

Date of issue : 5/28/2012.

Internet: www.petro-canada.ca/msds

Page: 1/7

Petro-Canada is a Suncor Energy business

™ Trademark of Suncor Energy Inc. Used under licence.

2. Hazards identification

- Fertility effects** : No known significant effects or critical hazards.
- Medical conditions aggravated by over-exposure** : Pre-existing skin disorders may be aggravated by over-exposure to this product. Repeated skin exposure can produce local skin destruction or dermatitis.

See toxicological information (Section 11)

3. Composition/information on ingredients

<u>Name</u>	<u>CAS number</u>	<u>%</u>
Bitumen	128683-24-9	100
Organo-sulphur compounds	7704-34-9	4 - 5

During storage or transit of hot bitumen, toxic hydrogen sulphide (7783-06-4) may be generated. Contains small amounts of polynuclear aromatic hydrocarbons (PNAs).

There are no additional ingredients present which, within the current knowledge of the supplier and in the concentrations applicable, are classified as hazardous to health or the environment and hence require reporting in this section.

4. First-aid measures

- Eye contact** : Check for and remove any contact lenses. Immediately flush eyes with plenty of water for at least 15 minutes, occasionally lifting the upper and lower eyelids. Get medical attention immediately.
- Skin contact** : In case of contact, immediately flush skin with plenty of water for at least 15 minutes while removing contaminated clothing and shoes. Wash skin thoroughly with soap and water or use recognised skin cleanser. Wash clothing before reuse. Clean shoes thoroughly before reuse. Get medical attention immediately.
- Inhalation** : Move exposed person to fresh air. If not breathing, if breathing is irregular or if respiratory arrest occurs, provide artificial respiration or oxygen by trained personnel. Loosen tight clothing such as a collar, tie, belt or waistband. Get medical attention immediately.
- Ingestion** : Wash out mouth with water. Do not induce vomiting unless directed to do so by medical personnel. Never give anything by mouth to an unconscious person. Get medical attention immediately.
- Protection of first-aiders** : No action shall be taken involving any personal risk or without suitable training. It may be dangerous to the person providing aid to give mouth-to-mouth resuscitation. Wash contaminated clothing thoroughly with water before removing it, or wear gloves.
- Notes to physician** : No specific treatment. Treat symptomatically. Contact poison treatment specialist immediately if large quantities have been ingested or inhaled.

5. Fire-fighting measures

- Flammability of the product** : May be combustible at high temperature.
- Extinguishing media**
- Suitable** : Use an extinguishing agent suitable for the surrounding fire.
- Not suitable** : None known.
- Special exposure hazards** : Promptly isolate the scene by removing all persons from the vicinity of the incident if there is a fire. No action shall be taken involving any personal risk or without suitable training.
- Products of combustion** : Carbon oxides (CO, CO₂), nitrogen oxides (NO_x), sulphur oxides (SO_x), hydrogen sulfide (H₂S), smoke and irritating vapours as products of incomplete combustion.
- Special protective equipment for fire-fighters** : Fire-fighters should wear appropriate protective equipment and self-contained breathing apparatus (SCBA) with a full face-piece operated in positive pressure mode.
- Special remarks on fire hazards** : Low fire hazard. This material must be heated before ignition will occur. Hydrogen sulphide may be released if the product is overheated.
- Special remarks on explosion hazards** : Do not pressurise, cut, weld, braze, solder, drill, grind or expose containers to heat or sources of ignition.

6. Accidental release measures

- Personal precautions** : No action shall be taken involving any personal risk or without suitable training. Evacuate surrounding areas. Keep unnecessary and unprotected personnel from entering. Do not touch or walk through spilled material. Avoid breathing vapour or mist. Provide adequate ventilation. Wear appropriate respirator when ventilation is inadequate. Put on appropriate personal protective equipment (see Section 8).
- Environmental precautions** : Avoid dispersal of spilled material and runoff and contact with soil, waterways, drains and sewers. Inform the relevant authorities if the product has caused environmental pollution (sewers, waterways, soil or air).

Methods for cleaning up

- Small spill** : Stop leak if without risk. Move containers from spill area. Dilute with water and mop up if water-soluble. Alternatively, if water-insoluble, absorb with an inert dry material and place in an appropriate waste disposal container. Dispose of via a licensed waste disposal contractor.
- Large spill** : Stop leak if without risk. Move containers from spill area. Approach the release from upwind. Prevent entry into sewers, water courses, basements or confined areas. Wash spillages into an effluent treatment plant or proceed as follows. Contain and collect spillage with non-combustible, absorbent material e.g. sand, earth, vermiculite or diatomaceous earth and place in container for disposal according to local regulations (see section 13). Dispose of via a licensed waste disposal contractor. Contaminated absorbent material may pose the same hazard as the spill product. Note: see section 1 for emergency contact information and section 13 for waste disposal.

7. Handling and storage

- Handling** : Put on appropriate personal protective equipment (see Section 8). Eating, drinking and smoking should be prohibited in areas where this material is handled, stored and processed. Workers should wash hands and face before eating, drinking and smoking. Remove contaminated clothing and protective equipment before entering eating areas. Persons with a history of skin sensitization problems should not be employed in any process in which this product is used. Do not get in eyes or on skin or clothing. Do not ingest. Avoid breathing vapour or mist. Keep in the original container or an approved alternative made from a compatible material, kept tightly closed when not in use. Empty containers retain product residue and can be hazardous. Do not reuse container.
- Storage** : Store in accordance with local regulations. Store in original container protected from direct sunlight in a dry, cool and well-ventilated area, away from incompatible materials (see section 10) and food and drink. Keep container tightly closed and sealed until ready for use. Containers that have been opened must be carefully resealed and kept upright to prevent leakage. Do not store in unlabelled containers. Use appropriate containment to avoid environmental contamination.

8. Exposure controls/personal protection

Ingredient	Exposure limits
Hydrogen sulphide	ACGIH TLV (United States). TWA: 1 ppm 8 hour(s). STEL: 5 ppm 15 minute(s).

Consult local authorities for acceptable exposure limits.

- Recommended monitoring procedures** : If this product contains ingredients with exposure limits, personal, workplace atmosphere or biological monitoring may be required to determine the effectiveness of the ventilation or other control measures and/or the necessity to use respiratory protective equipment.
- Engineering measures** : No special ventilation requirements. Good general ventilation should be sufficient to control worker exposure to airborne contaminants. If this product contains ingredients with exposure limits, use process enclosures, local exhaust ventilation or other engineering controls to keep worker exposure below any recommended or statutory limits.

8. Exposure controls/personal protection

Hygiene measures	: Wash hands, forearms and face thoroughly after handling chemical products, before eating, smoking and using the lavatory and at the end of the working period. Appropriate techniques should be used to remove potentially contaminated clothing. Contaminated work clothing should not be allowed out of the workplace. Wash contaminated clothing before reusing. Ensure that eyewash stations and safety showers are close to the workstation location.
Personal protection	
Respiratory	: Use a properly fitted, air-purifying or air-fed respirator complying with an approved standard if a risk assessment indicates this is necessary. Respirator selection must be based on known or anticipated exposure levels, the hazards of the product and the safe working limits of the selected respirator. Recommended: organic vapour cartridge or canister with a dust, fume or mist filter (R, or P series) may be permissible under certain circumstances where airborne concentrations are expected to exceed exposure limits. Protection provided by air-purifying respirators is limited.
Hands	: Chemical-resistant, impervious gloves complying with an approved standard should be worn at all times when handling chemical products if a risk assessment indicates this is necessary. Recommended: natural rubber (latex), Viton®.
Eyes	: Safety eyewear complying with an approved standard should be used when a risk assessment indicates this is necessary to avoid exposure to liquid splashes, mists or dusts.
Skin	: Personal protective equipment for the body should be selected based on the task being performed and the risks involved and should be approved by a specialist before handling this product.
Environmental exposure controls	: Emissions from ventilation or work process equipment should be checked to ensure they comply with the requirements of environmental protection legislation. In some cases, fume scrubbers, filters or engineering modifications to the process equipment will be necessary to reduce emissions to acceptable levels.

9. Physical and chemical properties

Physical state	: Viscous liquid.
Flash point	: Open cup: 182°C (359.6°F) [Cleveland.]
Auto-ignition temperature	: >245°C (>473°F)
Flammable limits	: Not available.
Colour	: Black.
Odour	: Tarry odour. "Rotten egg" if H ₂ S present, but odour is an unreliable warning, since it may deaden the sense of smell.
Odour threshold	: Not available.
pH	: Not available.
Boiling/condensation point	: 230°C (446°F)
Melting/freezing point	: Not available.
Relative density	: 1 to 1.1 (Water=1)
Vapour pressure	: Not available.
Vapour density	: Not available.
Volatility	: Not available.
Evaporation rate	: Not available.
Viscosity	: 29116 cSt @ 40°C (104°F)
Pour point	: 21°C (70°F)
Solubility	: Insoluble in water.

10 . Stability and reactivity

Chemical stability	: The product is stable.
Hazardous polymerisation	: Under normal conditions of storage and use, hazardous polymerisation will not occur.
Materials to avoid	: Reactive with oxidising agents.
Hazardous decomposition products	: May release COx, NOx, SOx, H ₂ S, smoke and irritating vapours when heated to decomposition.

11 . Toxicological information

Acute toxicity

Product/ingredient name	Result	Species	Dose	Exposure
Hydrogen sulphide	LC50 Inhalation Gas.	Rat	444 ppm	4 hours

Conclusion/Summary : Not available.

Chronic toxicity

Conclusion/Summary : Not available.

Irritation/Corrosion

Conclusion/Summary : Not available.

Sensitiser

Conclusion/Summary : Not available.

Carcinogenicity

Conclusion/Summary : Not available.

Mutagenicity

Conclusion/Summary : Not available.

Teratogenicity

Conclusion/Summary : Not available.

Reproductive toxicity

Conclusion/Summary : Not available.

12 . Ecological information

Environmental effects : No known significant effects or critical hazards.

Aquatic ecotoxicity

Conclusion/Summary : Not available.

Biodegradability

Conclusion/Summary : Not available.

13 . Disposal considerations

Waste disposal : The generation of waste should be avoided or minimised wherever possible. Significant quantities of waste product residues should not be disposed of via the foul sewer but processed in a suitable effluent treatment plant. Dispose of surplus and non-recyclable products via a licensed waste disposal contractor. Disposal of this product, solutions and any by-products should at all times comply with the requirements of environmental protection and waste disposal legislation and any regional local authority requirements. Waste packaging should be recycled. Incineration or landfill should only be considered when recycling is not feasible. This material and its container must be disposed of in a safe way. Care should be taken when handling emptied containers that have not been cleaned or rinsed out. Empty containers or liners may retain some product residues. Avoid dispersal of spilt material and runoff and contact with soil, waterways, drains and sewers.

Disposal should be in accordance with applicable regional, national and local laws and regulations.

13 . Disposal considerations

Refer to Section 7: HANDLING AND STORAGE and Section 8: EXPOSURE CONTROLS/PERSONAL PROTECTION for additional handling information and protection of employees.

14 . Transport information

Regulatory information	UN number	Proper shipping name	Classes	PG*	Label	Additional information
TDG Classification	Not regulated.	-	-	-		Special provisions For US Shipments Only: ELEVATED TEMPERATURE LIQUID, N.O.S., at or above 100°C and below its flash point, 9, UN3257, PGIII
DOT Classification	Not available.	Not available.	Not available.	-		-

PG* : Packing group

15 . Regulatory information

United States

HCS Classification : Irritating material
Sensitising material

Canada

WHMIS (Canada) : Class D-2B: Material causing other toxic effects (Toxic).

This product has been classified in accordance with the hazard criteria of the Controlled Products Regulations and the MSDS contains all the information required by the Controlled Products Regulations.

International regulations

Canada inventory : All components are listed or exempted.

United States inventory (TSCA 8b) : Not determined.

Europe inventory : Not determined.

16 . Other information

Label requirements : CAUSES EYE AND SKIN IRRITATION. MAY CAUSE ALLERGIC SKIN REACTION.

Hazardous Material Information System (U.S.A.) :

Health	*	2
Flammability		1
Physical hazards		0
Personal protection		H

National Fire Protection Association (U.S.A.) :



References : Available upon request.
™ Trademark of Suncor Energy Inc. Used under licence.

Date of printing : 5/28/2012.

Date of issue : 28 May 2012

Date of previous issue : 5/27/2009.

Date of issue : 5/28/2012.

Internet: www.petro-canada.ca/msds

Page: 6/7

Petro-Canada is a Suncor Energy business

™ Trademark of Suncor Energy Inc. Used under licence.

16 . Other information

Responsible name : Product Safety - DSR

Indicates information that has changed from previously issued version.

For Copy of (M)SDS : The Canadian Controlled Products Regulations (CPR) (Under the Hazardous Products Act, part of the WHMIS legislation) only apply to WHMIS Controlled (i.e., hazardous) products. Therefore, the CPR and the 3-year update rule specified therein do not apply to WHMIS Non-Controlled products. Although this is true, customarily Petro-Canada reviews and updates Non-Controlled product MSDS if a customer requests such an update. These Non-Controlled product updates are given a lower priority than Controlled products but are handled as soon as practicable. If you would like to verify if the MSDS you have is the most current, or you require any further information, please contact:

Internet: www.petro-canada.ca/msds

Western Canada, telephone: 403-296-7672; fax: 403-296-5147

For Product Safety Information: (905) 804-4752

Notice to reader

To the best of our knowledge, the information contained herein is accurate. However, neither the above-named supplier, nor any of its subsidiaries, assumes any liability whatsoever for the accuracy or completeness of the information contained herein.

Final determination of suitability of any material is the sole responsibility of the user. All materials may present unknown hazards and should be used with caution. Although certain hazards are described herein, we cannot guarantee that these are the only hazards that exist.

Appendix C: Density calculations for rock surrogate pretest

Bitumen specific gravity			1.01						
Rock specific gravity			2.6						
					Height (cm) =	Height (cm) =	Height (cm) =	Height (cm) =	Height (cm) =
					0.25	0.5	1	2	4
				Equivalent	Equivalent	Equivalent	Equivalent	Equivalent	Equivalent
	Bitumen	Bitumen	Bitumen	Rock	Rock	Rock	Rock	Rock	Rock
	Volume	Diameter	Weight	Volume	Dimensions	Dimensions	Dimensions	Dimensions	Dimensions
	(cc)	(cm)	(N)	(cc)	(cmxcmxcm)	(cmxcmxcm)	(cmxcmxcm)	(cmxcmxcm)	(cmxcmxcm)
	41	4.28	0.41	15.93	11.03	7.80	5.52	3.90	2.76
	131	6.30	1.30	50.89	19.72	13.94	9.86	6.97	4.93
	983	12.34	9.74	381.86	54.01	38.19	27.01	19.10	13.50

*Coral rock and density calculations provided by Dr. Thomas Ballestero

Appendix D: Annular flume background

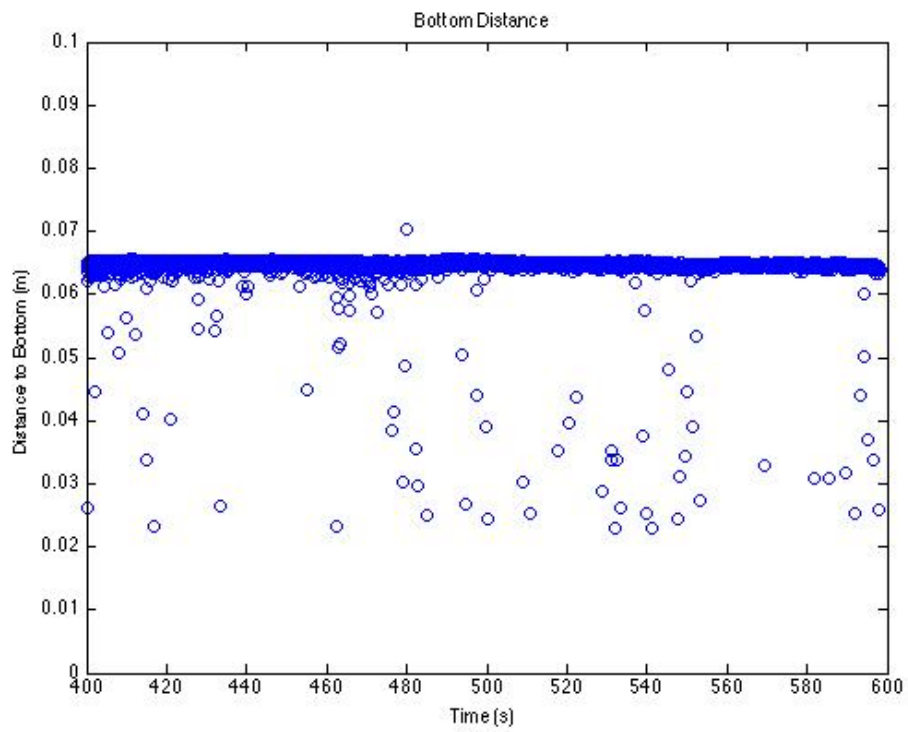
Battelle Memorial Institute (Duxbury, Ma) donated an annular flume to the University of New Hampshire (UNH) that is now operated by the Coastal Response Research Center (CRRC). Prior to being donated, the flume had been used to study the behavior of surface waves using a vane system to generate wind-driven waves.

In 2003, it was re-assembled in the Chase Ocean Engineering Laboratory. The goal was to establish a facility at UNH that could be used to investigate the weathering characteristics of oil spilled in water. Dr. M. Robinson Swift, a Professor of Mechanical and Ocean Engineering spearheaded the project. Initial objectives were to: set up the flume, test its wind- and wave-generating capabilities, choose suitable test oils, conduct water-contact experiments, and determine the feasibility of containment technology.

Dr. Swift's team developed and evaluated procedures for observing nonfloating oil behavior to enable future investigation of settling, transport, containment and recovery of nonfloating oils. This work represented UNH's first attempt in studying the nonfloating oil problem.

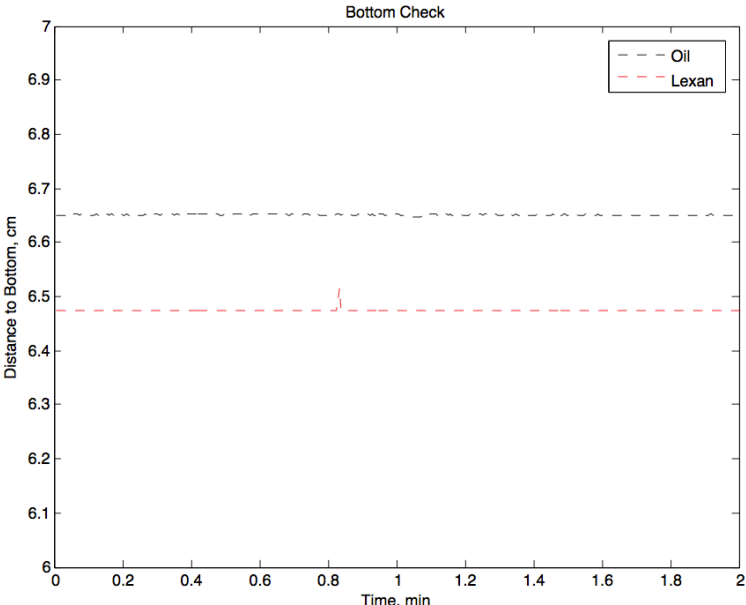
In 2012, the CRRC, a partnership with NOAA's Office of Response and Restoration (ORR), reassembled the flume in Gregg Hall. The Center understood the enormous potential of the circular flume to conduct research in initial oil-water contact processes, globule formation, settling, transport by currents, as well as containment technologies of oil below the surface.

Appendix E: Vectrino readout of ADV's elevation during experiments



*Solid line is lot of points on top of each other

Appendix F: Bottom check test

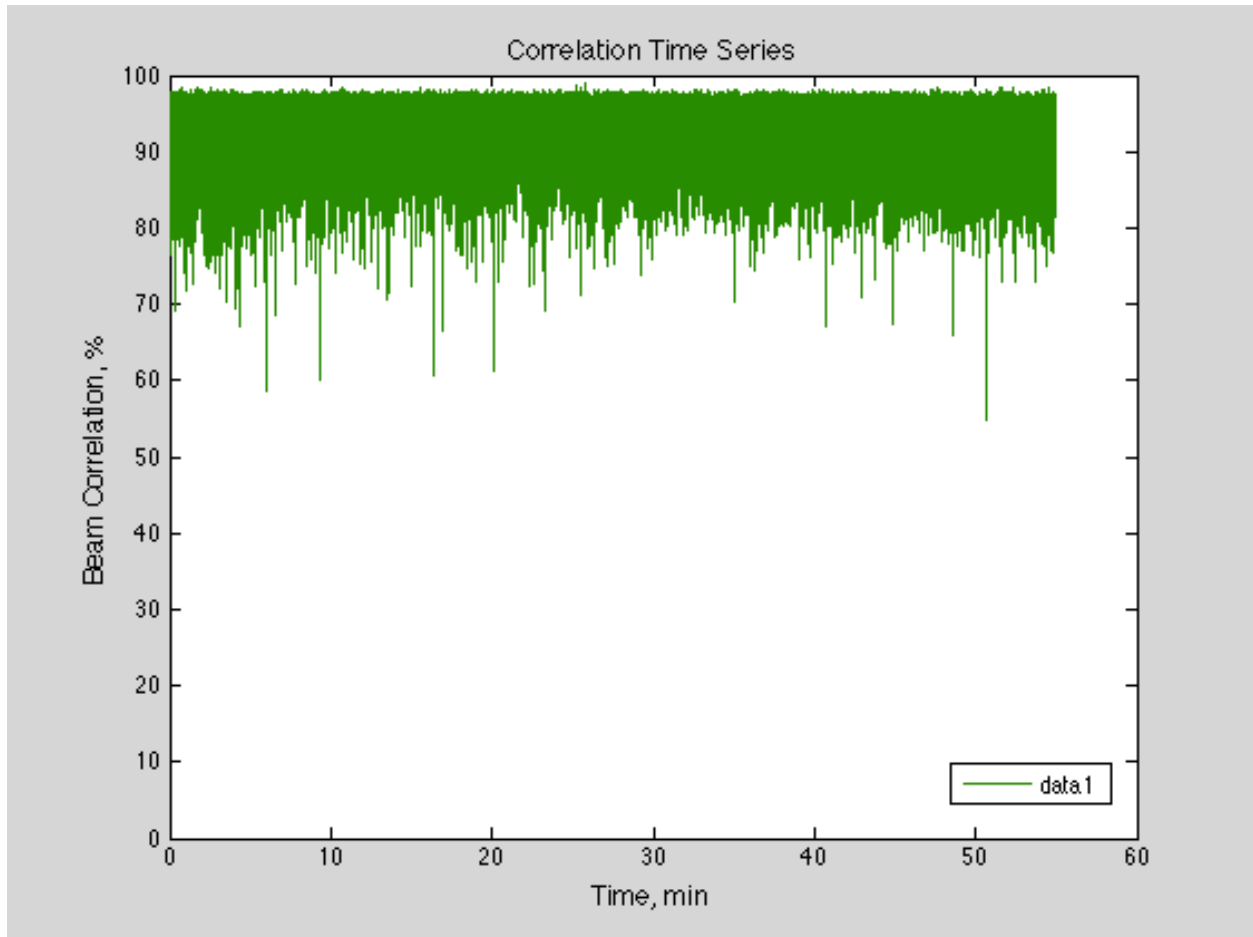


* Thickness of stranded oil (1.75mm - measured by digital caliper) and change in bottom distance (1.78mm - measured by ADV) were nearly identical indicating the ADV easily distinguishes between the two fluids (i.e., oil-water interface). Dashed lines are for oil (black) and Lexan (red) surfaces.

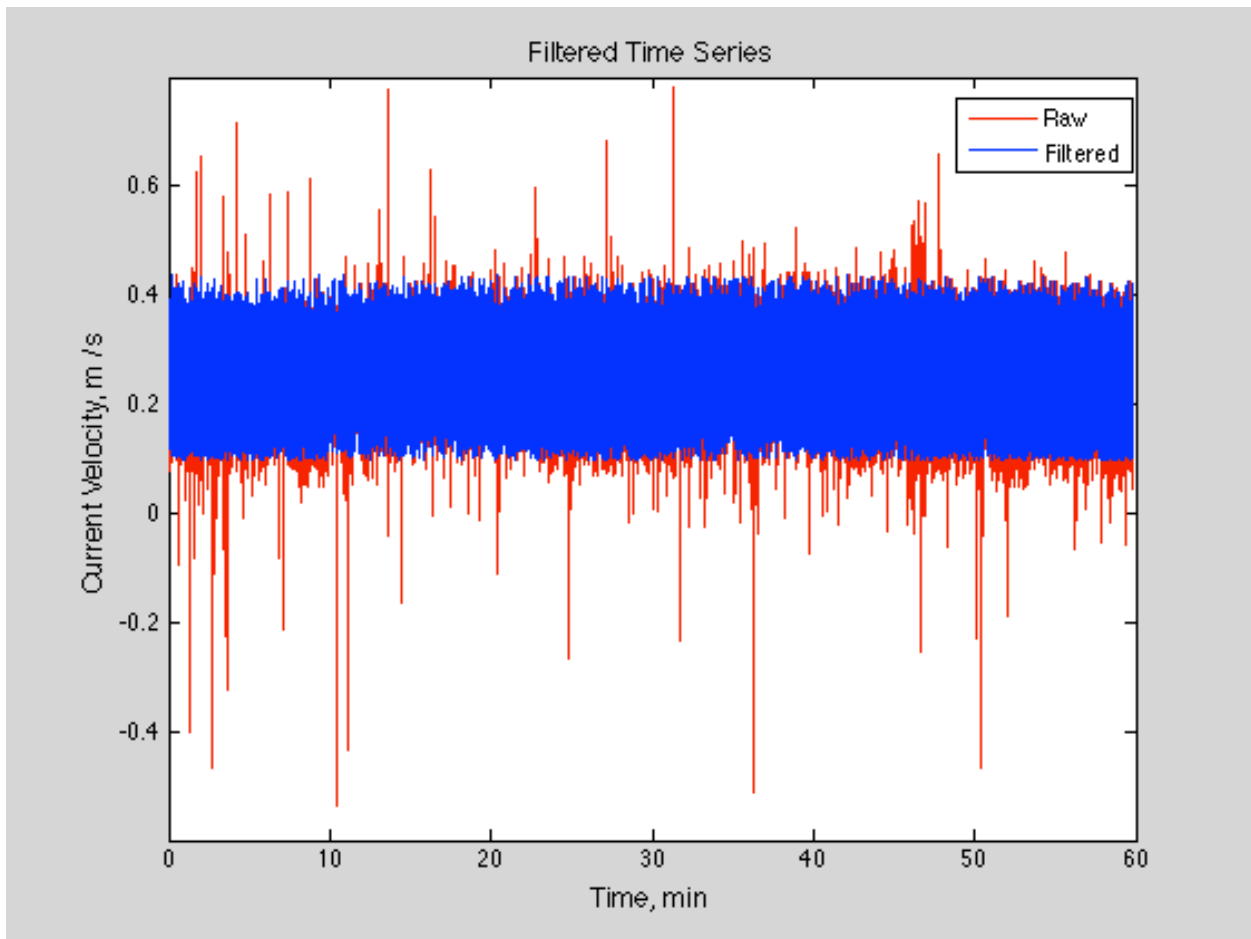
Appendix G: MATLAB data structure containing collected Vectrino data

Field	Value	Min	Max
Profiles_HostTime	<1x38063 doubl...>	1.3957e+09	1.3957e+09
Profiles_VelX	<38063x28 singl...>	<Too man...>	<Too many elem...>
Profiles_VelY	<38063x28 singl...>	<Too man...>	<Too many elem...>
Profiles_VelZ1	<38063x28 singl...>	<Too man...>	<Too many elem...>
Profiles_VelZ2	<38063x28 singl...>	<Too man...>	<Too many elem...>
Profiles_CorBeam1	<38063x28 singl...>	<Too man...>	<Too many elem...>
Profiles_CorBeam2	<38063x28 singl...>	<Too man...>	<Too many elem...>
Profiles_CorBeam3	<38063x28 singl...>	<Too man...>	<Too many elem...>
Profiles_CorBeam4	<38063x28 singl...>	<Too man...>	<Too many elem...>
Profiles_AmpBeam1	<38063x28 singl...>	<Too man...>	<Too many elem...>
Profiles_AmpBeam2	<38063x28 singl...>	<Too man...>	<Too many elem...>
Profiles_AmpBeam3	<38063x28 singl...>	<Too man...>	<Too many elem...>
Profiles_AmpBeam4	<38063x28 singl...>	<Too man...>	<Too many elem...>
Profiles_SNRBeam1	<38063x28 singl...>	<Too man...>	<Too many elem...>
Profiles_SNRBeam2	<38063x28 singl...>	<Too man...>	<Too many elem...>
Profiles_SNRBeam3	<38063x28 singl...>	<Too man...>	<Too many elem...>
Profiles_SNRBeam4	<38063x28 singl...>	<Too man...>	<Too many elem...>
Profiles_DataQualityBeam1	<38063x28 singl...>	<Too man...>	<Too many elem...>
Profiles_DataQualityBeam2	<38063x28 singl...>	<Too man...>	<Too many elem...>
Profiles_DataQualityBeam3	<38063x28 singl...>	<Too man...>	<Too many elem...>
Profiles_DataQualityBeam4	<38063x28 singl...>	<Too man...>	<Too many elem...>
Profiles_TimeStamp	<38063x1 single>	3.1965e+03	3.5951e+03
Profiles_Status	<38063x1 single>	4	36
Profiles_SpeedOfSound	<38063x1 single>	1.4964e+03	1.5007e+03
Profiles_Temperature	<38063x1 single>	24.9000	26.5400
Profiles_AveragedPingPairs	<38063x1 single>	61	101
Profiles_Range	<1x28 single>	0.0400	0.0679
Profiles_firstRecord	1.3957e+09	1.3957e+09	1.3957e+09
Profiles_startDate	'2014-03-24 12:...		
BottomCheck_HostTime	<1x4003 double>	0	1.3957e+09
BottomCheck_CenterBeamAmp	<4003x500 singl...>	<Too man...>	<Too many elem...>
BottomCheck_CenterBeamCurveFit	<4003x500 singl...>	<Too man...>	<Too many elem...>
BottomCheck_CenterBeamBottomPeak	<4003x500 singl...>	<Too man...>	<Too many elem...>
BottomCheck_TimeStamp	<4003x1 single>	0	3.5951e+03
BottomCheck_BottomDistance	<4003x1 single>	-0.0996	0.1303
BottomCheck_Status	<4003x1 single>	0	32
BottomCheck_Range	<1x500 single>	0.0200	0.5348
BottomCheck_firstRecord	1.3957e+09	1.3957e+09	1.3957e+09
BottomCheck_startDate	'2014-03-24 12:...		
Units	<1x1 struct>		
Comments	<1x1 struct>		

Appendix H: Sample correlation of ADV velocity measurements



Appendix I: 3-standard deviation filter applied to raw ADV data



```
Command Window
>> sum( (X_CLEANED{1}).Data_Raw )
ans =
    2.9815e+05
>> sum(isnan(X_CLEANED{1}).Data_Correlation_Filtered)
ans =
    85
>> sum(isnan(X_CLEANED{1}).Data_3_Sigma_Filtered)
ans =
    2209
fx
```

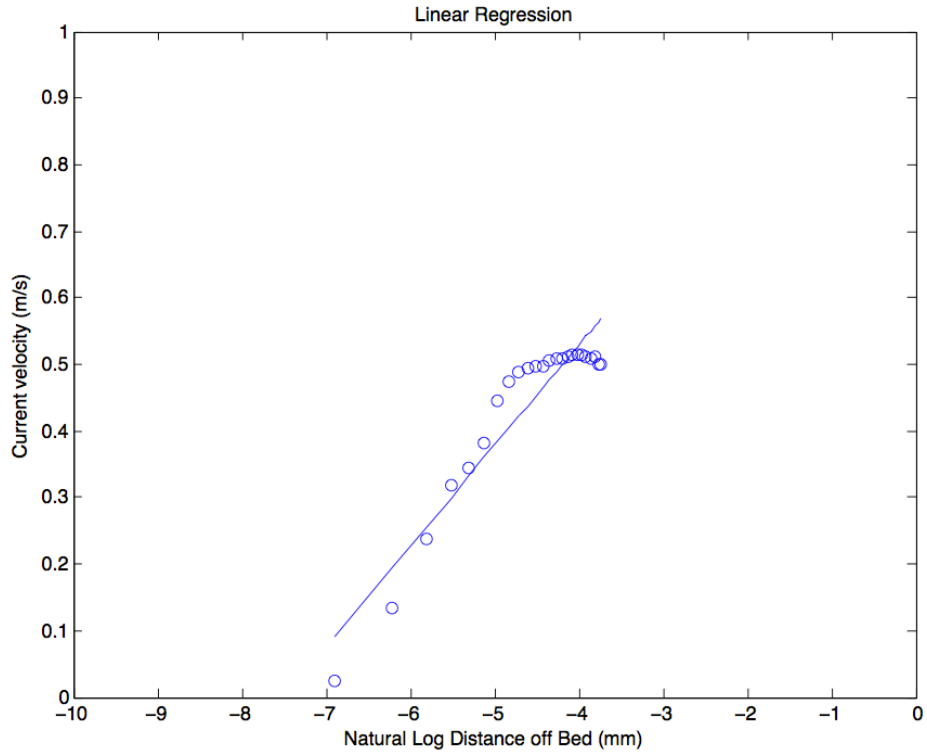
*Filter removed 2209 data points outside 3 standard deviations from the mean

Appendix J: LP BSS calculation code

```

1 -   clc
2 -   clear
3 -   format long
4
5 -   load('VectrinoData.308.13.Vectrino-II.00001.mat')
6
7 -   % declare constants
8 -   p=1000;
9 -   K=.4000;
10
11 -  % give start and stop row values for velocity average
12 -  row_start=1;
13 -  row_end=length(Data.Profiles_VelX)
14
15 -  % get median bottom distance (use median instead of mean!)
16 -  bottom_value=median(Data.BottomCheck_BottomDistance)
17
18 -  % assume the first measurement is the bottom distance - 4 cm
19 -  first_measurement = (bottom_value-.04)
20
21 -  % create a matrix of ranges, going from (bottom dist - 4cm) to 1
22 -  % NOTE: do not go to 0, as this will not be a valid value when I do the
23 -  % natural log!
24 -  z_range=flipr([1:round(first_measurement*1000)])/1000
25
26 -  % get the mean velocity values
27 -  mean_uX=mean(Data.Profiles_VelX(row_start:row_end,:));
28
29 -  % get the standard deviation of velocity values
30 -  std_uX=std(Data.Profiles_VelX(row_start:row_end,:));
31
32 -  % cut out the mean values; e.g. from (bottom dist - 4cm) to 1
33 -  mean_uX=mean_uX(1:length(z_range));
34
35 -  % plot profile
36 -  figure(1)
37 -  clf
38 -  plot(mean_uX,z_range*1000,'o')
39 -  xlabel('Current velocity (m/s)')
40 -  ylabel('Distance off Bed (mm)')
41 -  %%%
42
43 -  % calculate the natural log of the ranges
44 -  z_range_n1=log(z_range);
45
46 -  % linear regression of the natural log ranges and velocity
47 -  datafit_coeffs=polyfit(z_range_n1,mean_uX,1);
48
49 -  % this line is just so I can plot the line on the next graph
50 -  datafit_line=polyval(datafit_coeffs,z_range_n1);
51
52 -  % plot log fit
53 -  figure(2)
54 -  clf
55 -  plot(z_range_n1,mean_uX,'o')
56 -  hold on
57 -  plot(z_range_n1,datafit_line)
58 -  xlabel('Natural Log Distance off Bed')
59 -  ylabel('Current velocity (m/s)')
60
61
62 -  % calculate
63 -  m=datafit_coeffs(1)
64 -  b=datafit_coeffs(2)
65 -  z=exp(-b/m)
66 -  U=m*K
67 -  t=p*U^2
68

```



```

Command Window

bottom_value =
    0.0668

first_measurment =
    0.0268

z_range =
Columns 1 through 9
    0.0270    0.0260    0.0250    0.0240    0.0230    0.0220    0.0210    0.0200    0.0190
Columns 10 through 18
    0.0180    0.0170    0.0160    0.0150    0.0140    0.0130    0.0120    0.0110    0.0100
Columns 19 through 27
    0.0090    0.0080    0.0070    0.0060    0.0050    0.0040    0.0030    0.0020    0.0010

m =
    0.1976

b =
    1.3173

z =
    0.0013

U =
    0.0790

fx >>

```

Appendix K: TKE BSS calculation code

```

1 - clear
2 - clc
3
4 - CORRELATION_MINIMUM=80
5
6 - TIME_FLUC_START=1
7 - TIME_FLUC_STOP=1000
8
9 - TOP_PERCENT=1 % e.g. top 1%
10
11 - DEPTH_START=1
12 - DEPTH_STOP=3
13
14 %% I REFORMAT YOUR DATA TYPES INTO STRUCTURES, and REMANE v to X!!!
15 load matlab.mat
16 x=v; clear v;
17 X={};
18 for q=1:size(x,2)
19     X{q}=x(:,q);
20 end
21 Y={};
22 for q=1:size(y,2)
23     Y{q}=y(:,q);
24 end
25 Z={};
26 for q=1:size(z,2)
27     Z{q}=z(:,q);
28 end
29
30 % time vector had some random zero outs in it near
31 % the end....
32 t_sample_rate = t(2)-t(1);
33 t_new=[t(1):t_sample_rate:length(t)*t_sample_rate+t_sample_rate];
34
35
36 for i=['X' 'Y' 'Z']
37     eval(sprintf('v=%s;', i));
38
39     for n=DEPTH_START:DEPTH_STOP
40         %% correlation exclusion...
41         v_corr_cleaned{n}=v{n};
42         v_corr_cleaned{n}(find(c(:,n) < CORRELATION_MINIMUM))=NaN;
43
44         %% 3-sigma remove filter
45         v_std=std(v_corr_cleaned{n});
46         v_3sigma{n} = v_corr_cleaned{n};
47         v_3sigma{n}( find( v_corr_cleaned{n} >= 3*v_std + mean(v_corr_cleaned{n}) ) )=NaN;
48         v_3sigma{n}( find( v_corr_cleaned{n} <= mean(v_corr_cleaned{n}) - 3*v_std ) )=NaN;
49
50
51         %% calculate fluctuations...
52         [trsh window_start]=min(abs(TIME_FLUC_START-t_new));
53         [trsh window_end]=min(abs(TIME_FLUC_STOP-t_new));
54         mean_v=nanmean(v_3sigma{n}(window_start>window_end));
55         tmp=sort(abs(v_3sigma{n}(window_start>window_end)-mean_v),'descend');
56         fluctuation=nanmean(tmp(1:floor(TOP_PERCENT/100*size(tmp,1))));
57
58         V{n}=struct('Correlation_Filter_Value', CORRELATION_MINIMUM,...
59                 'Flucuation_Percent_Filter_Value', TOP_PERCENT,...
60                 'Time_Range_Values', [TIME_FLUC_START TIME_FLUC_STOP],...
61                 'Mean_Velocity_Over_Time_Range', mean_v,...
62                 'Fluctuation_Over_Time_Range', fluctuation,...
63                 'Data_Raw', v{n},...
64                 'Data_Correlation_Filtered',v_corr_cleaned{n},...
65                 'Data_3_Sigma_Filtered', v_3sigma{n},...
66                 'Time', t_new);
67
68         %% Plot time series
69         figure(n)
70         clf
71         plot(t_new,v{n})
72         hold on
73         plot(t_new,v_corr_cleaned{n},'y')
74         plot(t_new,v_3sigma{n},'r')
75     end
76
77     eval(sprintf('%s_CLEANED=V;', i));
78
79 end

```

```
Command Window
>> X_CLEANED{1}
ans =
    Correlation_Filter_Value: 80
    Flucuation_Percent_Filter_Value: 1
    Time_Range_Values: [1 1000]
    Mean_Velocity_Over_Time_Range: 0.2084
    Fluctuation_Over_Time_Range: 0.3570
    Data_Raw: [295752x1 single]
    Data_Correlation_Filtered: [295752x1 single]
    Data_3_Sigma_Filtered: [295752x1 single]
    Time: [1x295752 single]

>> Y_CLEANED{1}
ans =
    Correlation_Filter_Value: 80
    Flucuation_Percent_Filter_Value: 1
    Time_Range_Values: [1 1000]
    Mean_Velocity_Over_Time_Range: 0.0035
    Fluctuation_Over_Time_Range: 0.2354
    Data_Raw: [295752x1 single]
    Data_Correlation_Filtered: [295752x1 single]
    Data_3_Sigma_Filtered: [295752x1 single]
    Time: [1x295752 single]

>> Z_CLEANED{1}
ans =
    Correlation_Filter_Value: 80
    Flucuation_Percent_Filter_Value: 1
    Time_Range_Values: [1 1000]
    Mean_Velocity_Over_Time_Range: 0.0046
    Fluctuation_Over_Time_Range: 0.0685
    Data_Raw: [295752x1 single]
    Data_Correlation_Filtered: [295752x1 single]
    Data_3_Sigma_Filtered: [295752x1 single]
    Time: [1x295752 single]

>>
>>
>>
>>
>>
fx >>
```

Appendix L: Adhesion procedure (Jokuty, 2001)

Adhesion

This method requires the use of an analytical pan balance capable of weighing to 0.0001 g, and with provision for weighing from below the pan. Some type of draft shield will probably be required to obtain stable readings. Also required is a standard penetrometer needle as described in ASTM method D 5 - *Standard Test Method for Penetration of Bituminous Materials* (ASTM D 5), adapted for hanging below the balance.

- a) The oil sample is allowed to stand at room temperature for 30 minutes.
- b) The sample bottle is shaken for 30 minutes using the reciprocating shaker.
- c) The balance is prepared for measurement by hanging a penetrometer needle, for which the surface area of the stainless steel section has been calculated, from the balance hook and allowing the weight to stabilize. The weight of the clean needle is recorded.
- d) Approximately 80 mL of oil is poured into a 100-mL beaker. The beaker is elevated, using a lab jack, until the top of the stainless steel needle meets the top of the oil. Care must be taken to avoid having the oil

Properties of Crude Oils and Oil Products - 12/99

15

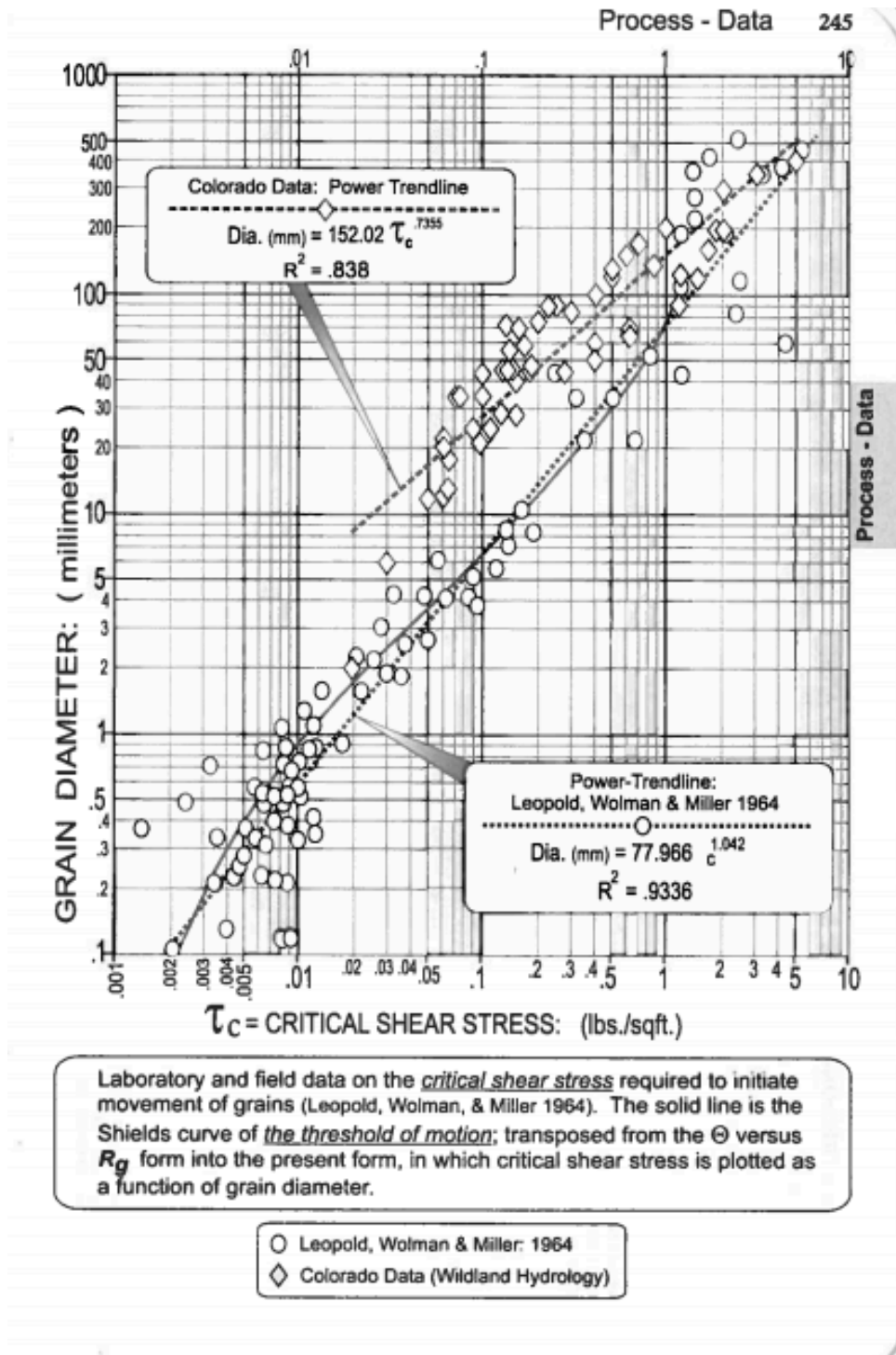
Appendix 1 - Methods

creep up onto the brass section of the needle, as the surface area calculation is based only on the stainless steel portion.

- e) The needle is left in the oil for 30 seconds, and then the beaker is lowered, allowing the needle to hang undisturbed.
- f) After 30 minutes, the weight of the needle plus oil is recorded.
- g) The needle is cleaned with dichloromethane and allowed to dry before the measurement is repeated. A minimum of four measurements are made for each oil. The same beaker of oil can be used for all measurements.
- h) The oil adhesion is calculated as the average weight of oil remaining on the needle divided by the needle's surface area.

Volatile Organic Compounds

Appendix M: Laboratory data on CSS estimates required to initiate movement of grains

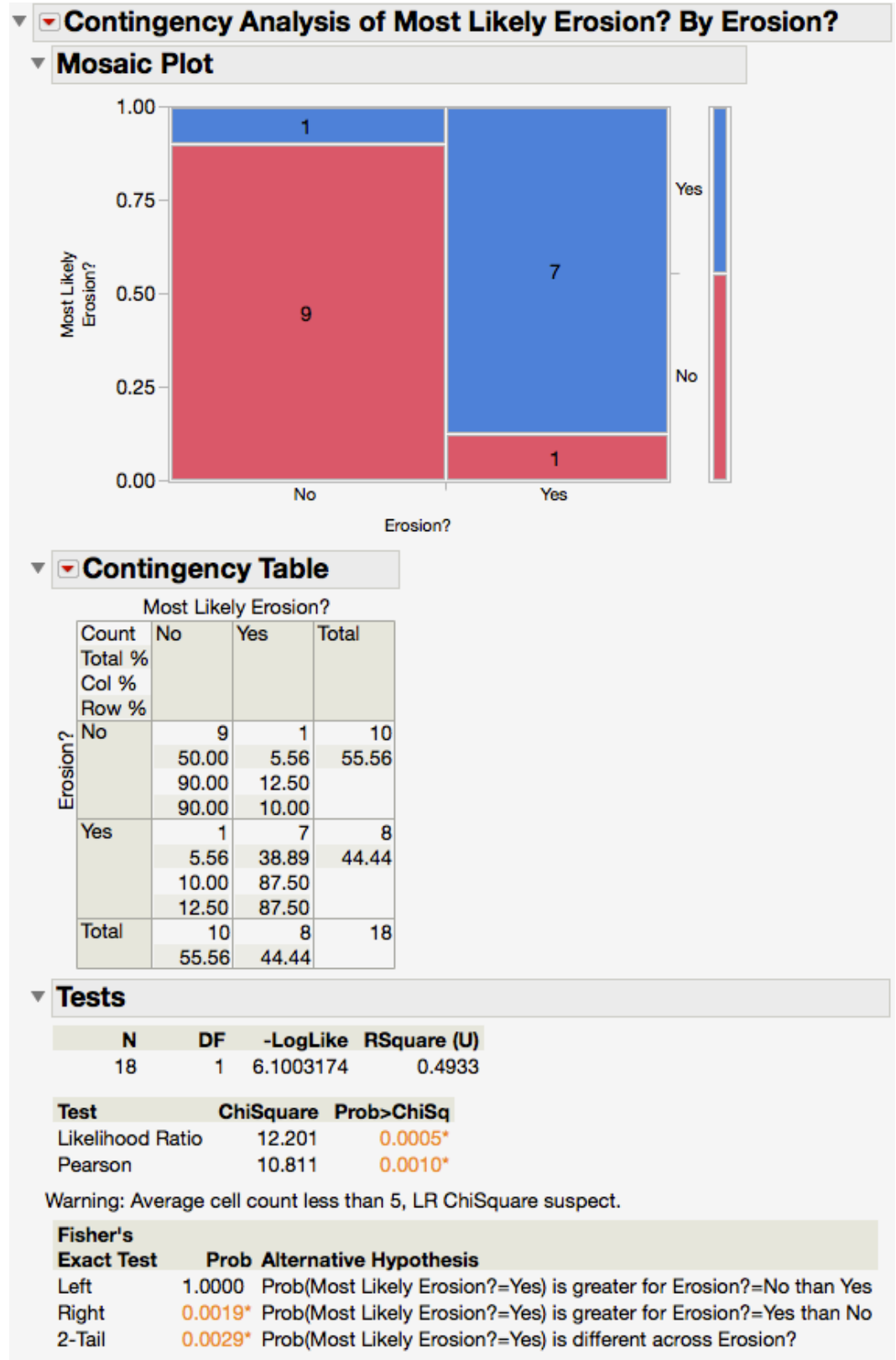


*CRRC flume generates maximum BSS of 18 Pa., or 0.4 lbs./sqft., which initiates movement of sedimentary rocks ~ 10cm in diameter. This was visually confirmed during surrogate testing using stones collected from Rye Beach, New Hampshire.

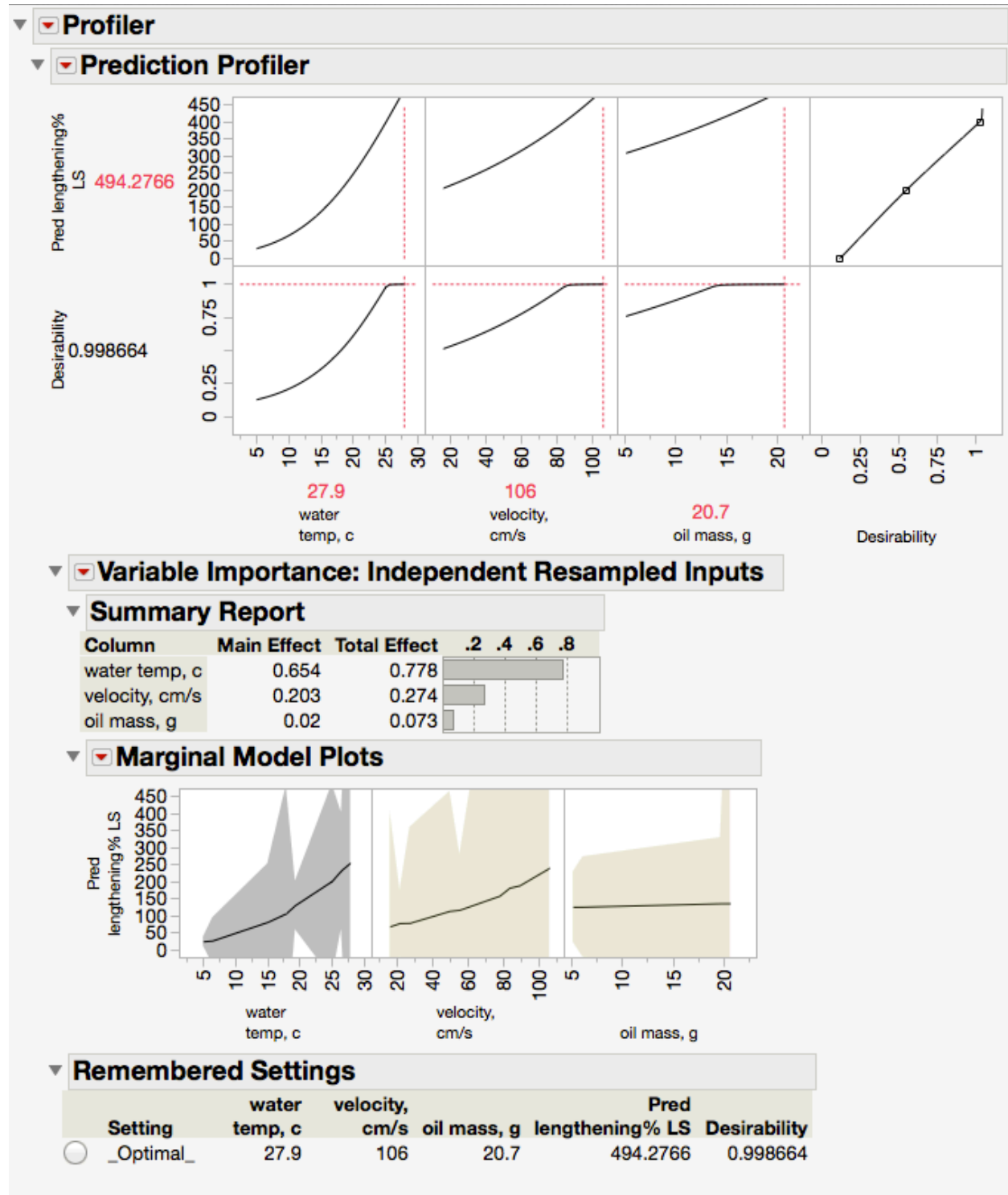
Appendix N: Parameter test of BSS values for LP and TKE in all experiments

Parameter	
Intercept	0
lp shear stress, pa	1
=	1
Value	0.3149646266
Std Error	0.2068311798
t Ratio	1.5228101823
Prob> t	0.1473247103
SS	17.300870457
Sum of Squares	17.300870457
Numerator DF	1
F Ratio	2.3189508513
Prob > F	0.1473247103

Appendix O: Contingency analysis



Appendix P: Least squared profiler model



Appendix Q: Eroded oil globule size

T=27.9C, V=24cm/s, M=20g					
Time	Size (cm)	Time	Size (cm)	Time	Size (cm)
5:07	0.1	22:45	0.1	32:15	.5
14:13	0.5	22:47	.1	32:20	.1
15:03	0.5	22:50	0.15	32:21	.1
15:03	0.25	22:53	.5 and .1	32:30	.25
15:43	0.2	23:35	0.6	32:48	.3
16:05	0.3	25:21	0.7	32:52	.1
16:30	0.2	25:35	0.6	36:21	.25
17:00	0.2	25:55	0.2	37:12	.2
17:15	0.2	26:28	0.3	37:50	.3
17:55	0.15	27:28	1	38:27	.1
18:10	0.1	28:38	0.15	40:30	.25
18:12	0.1	28:48	0.6	42:05	.2
18:25	0.25	29:17	0.2	42:20	.2
19:25	0.2	30:47	0.2	44:02	.3
20:10	0.3	30:50	0.3	46:40	.2
20:40	0.5	30:52	.1	49:15	.1
21:10	0.1	30:56	0.1	49:55	.2
21:15	0.2	31:15	0.2	50:15	.2
21:16	0.1	31:38	0.6	55:53	.3
21:18	0.1	31:50	.1 x 2	58:16	0.1
21:30	0.5	31:55	0.2	58:45	.8
21:55	0.5	31:00	0.2		
22:25	0.2	32:10	.3		

T=24.8C, V=53cm/s, M=6.6g	
Time	Size
36:50	0.1
38:01	0.3

T=26.7C, V=90cm/s, M=20.7	
Time	Size (cm)
1:39	0.6
47:27	0.2

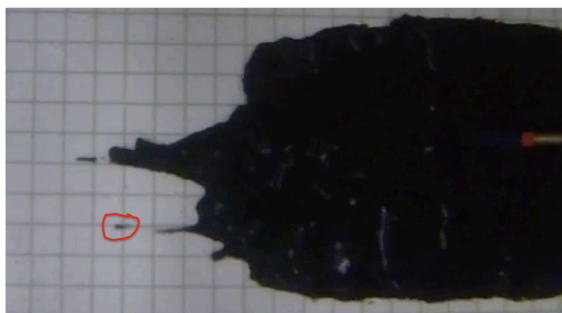
T=19.1C, V=57m/s, M=20.1g	
Time	Size (cm)
47:21	0.1

T=26.7C, V=86cm/s, M=5.9g	
Time	Size (cm)
7:33	0.1

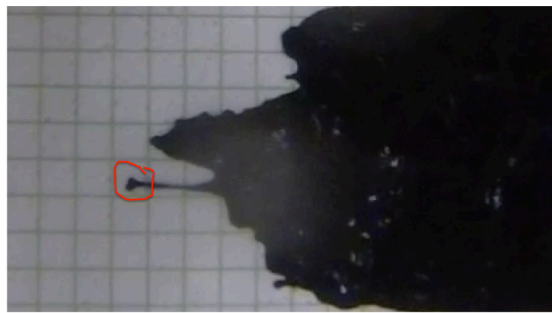
T=27C, V=16cm/s, M=5.1g	
Time	Size (cm)
37:06	0.3
37:40	0.2
41:35	0.2
41:55	0.5
46:58	0.2
47:35	0.1
47:50	0.2
49:32	0.1
49:43	0.1
50:43	0.1
53:05	0.8
55:25	0.2
55:50	0.8
59:59	0.2
1:00:40	0.8

T=20C, V=23cm/s, M=19.7g	
Time	Size (cm)
43:00	0.2
44:07	0.2
45:29	0.2
48:39	0.1
55:17	0.1
56:29	0.2
57:34	0.3
58:28	0.7
59:44	0.2
1:00:59	0.1

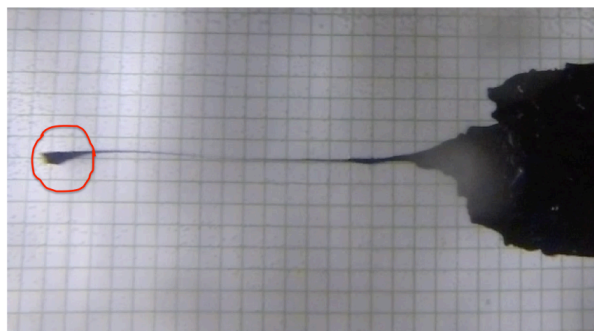
$x \leq 0.25$ cm



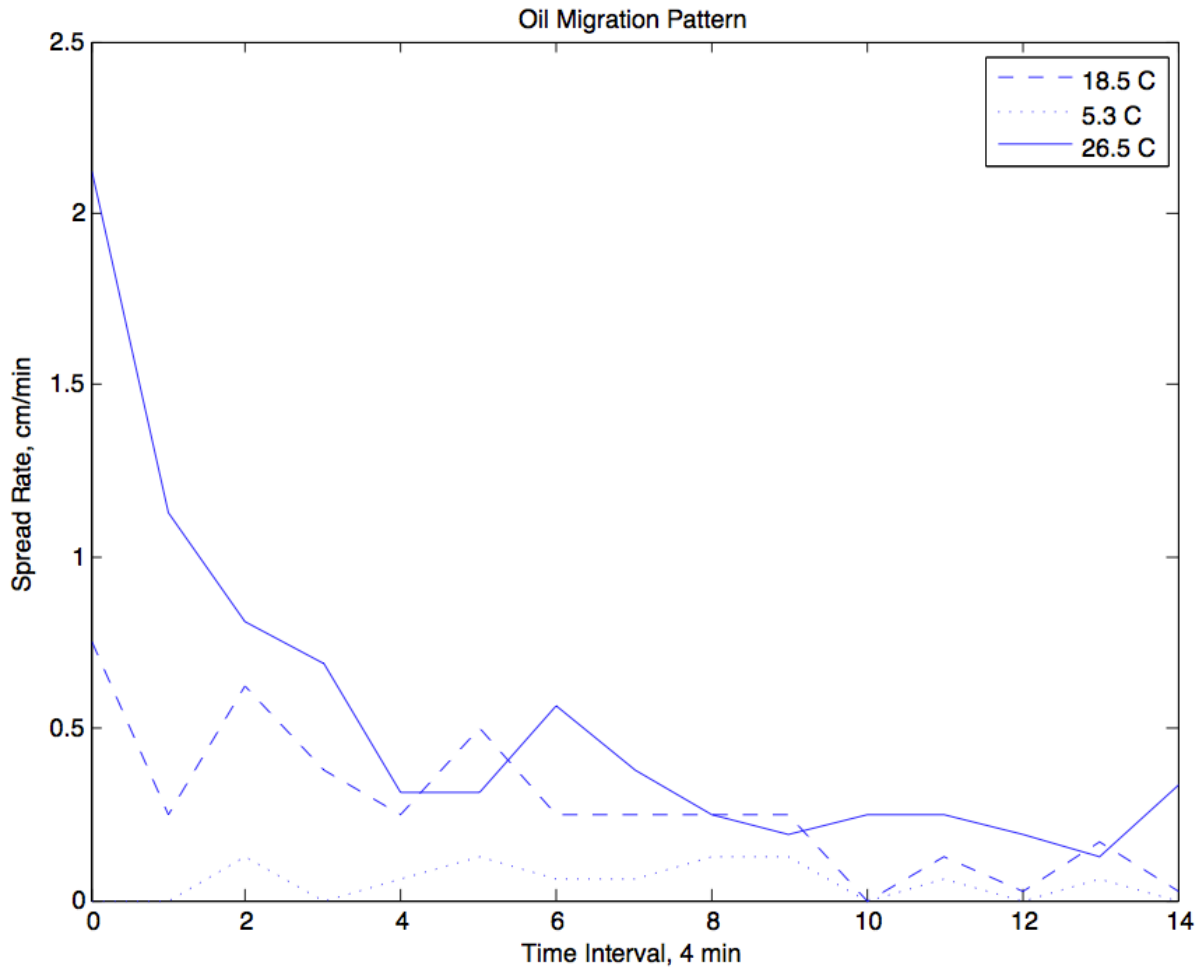
$0.25 \geq x \leq 0.75$ cm



$x \geq 1$ cm



Appendix R: Average oil migration patterns



*Oil migration becomes mass limited at ~30 min.

Appendix S: Instantaneous CSS

T=27C, V=16cm/s, M=5.1g		
Time	TKE	LP
37:06	2.8	1.4
37:40	3.1	1.0
41:35	2.7	0.6
41:55	2.7	1.3
46:58	2.7	1.0
47:35	3.0	1.4
47:50	3.2	0.8
49:32	2.6	0.7
49:43	3.1	0.7
50:43	3.0	0.7
53:05	3.8	1.0
55:25	3.3	1.0
55:50	2.4	0.9
59:59	1.7	0.9
1:00:40	2.0	0.6

T=20C, V=23cm/s, M=19.7g		
Time	TKE	LP
43:00	2.9	1.3
44:07	2.9	1.5
45:29	3.6	1.2
48:39	3.3	1.7

T=24.8C, V=53cm/s, M=6.6g		
Time	TKE	LP
36:50	4.1	4.7
38:01	3.8	5.4

T=26.7C, V=90cm/s, M=20.7		
Time	TKE	LP
1:39	8.7	14.3
47:27	5.8	12.7

T=19.1C, V=57m/s, M=20.1g		
Time	TKE	LP
47:21	4.5	4.9

T=26.7C, V=86cm/s, M=5.9g		
Time	TKE	LP
7:33	11.6	7.9

Appendix T: Parameter test of BSS values for LP and TKE in experiments with erosion

Parameter	
Intercept	0
tke css	1
=	1
Value	-0.262600856
Std Error	0.0533947485
t Ratio	-4.918102684
Prob> t	0.0026618788
SS	10.319048337
Sum of Squares	10.319048337
Numerator DF	1
F Ratio	24.18773401
Prob > F	0.0026618788

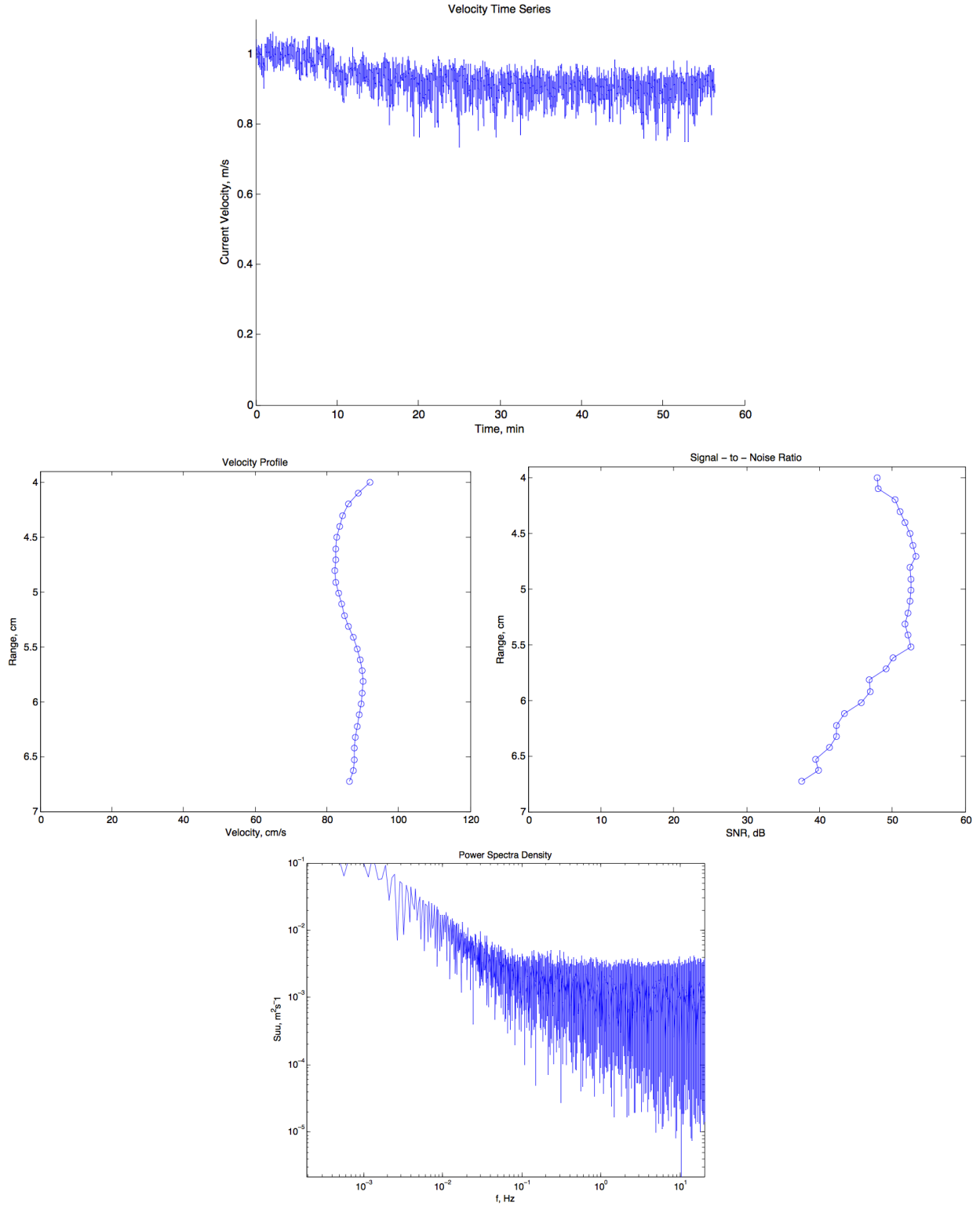
Appendix U: Supplemental data collected during replicate experiments

Temp, C	Velocity, cm/s	Mass, g	Erosion?	Lengthening %/hr	τ, Pa (TKE)	τ, Pa (LP)	Mean Globule Size (cm)
13.1	75	21.5	No	85	-	-	-
13.8	88	20.3	No	100	-	-	-
20.7	14	20	Yes	-	1.3	0.6	-
20.5	35	20	Yes	-	3.2	2.6	-
20.4	48	20	Yes	-	6.1	4.3	-
20.2	62	20	Yes	-	9.1	5.7	-
20.1	75	20	Yes	-	11.6	7.2	-
20.1	87	20	Yes	-	18.9	7.5	-
12	70	12	No	-	-	-	-
18	35	12	No	-	-	-	-

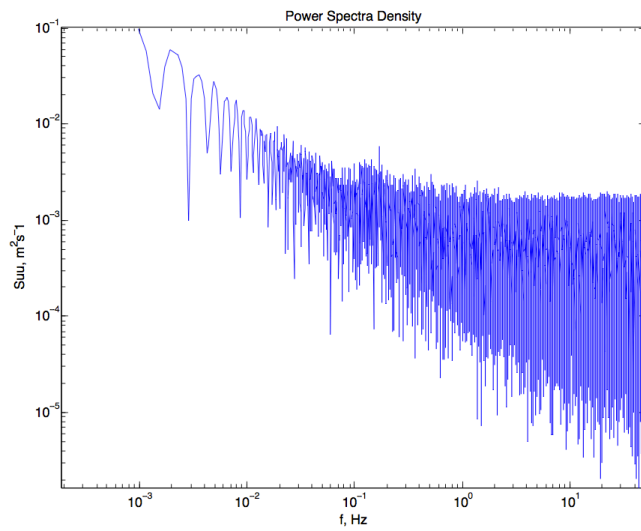
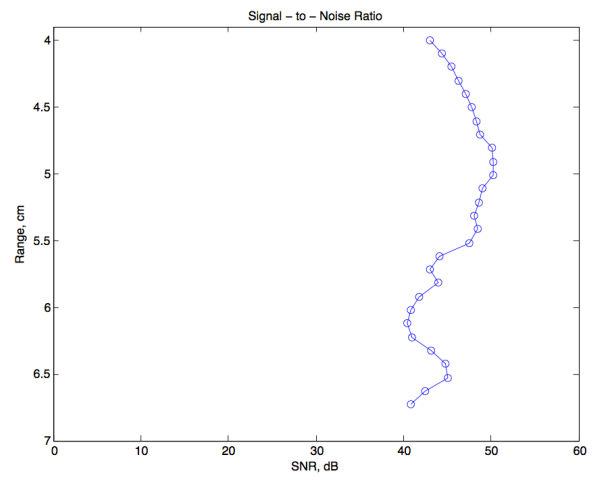
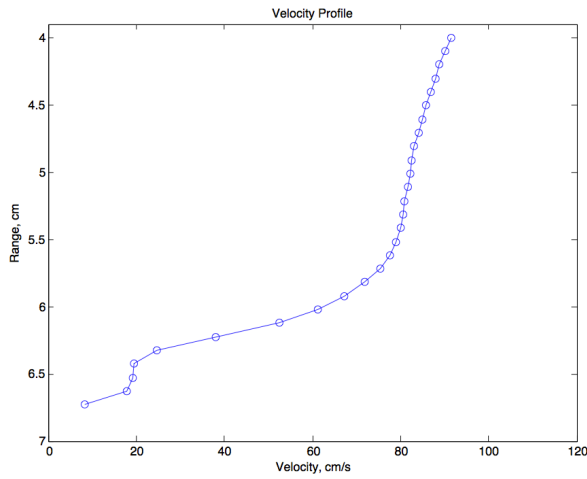
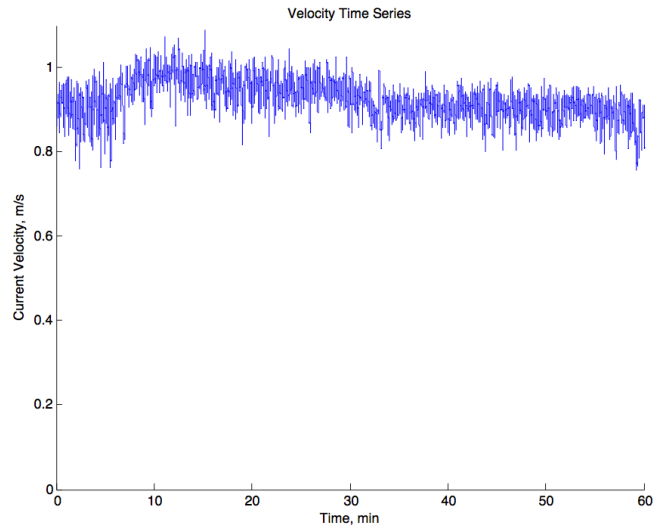
*(-) no measurements or calculations were made

Appendix V: ADV data of the experimental runs

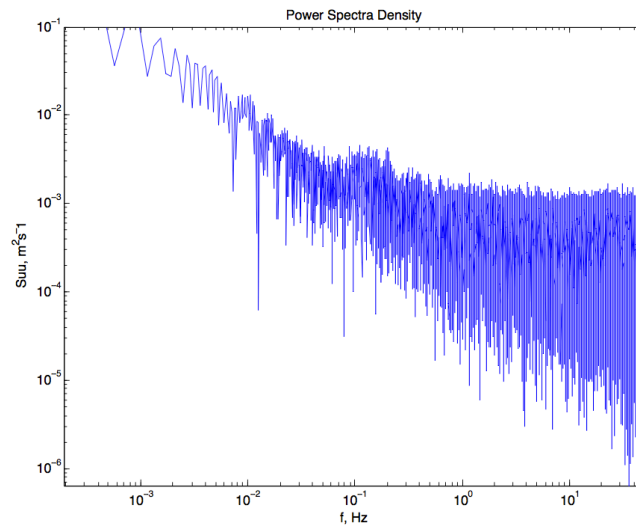
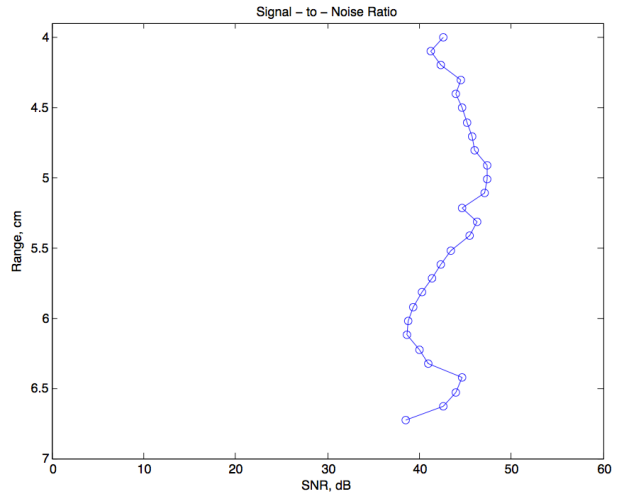
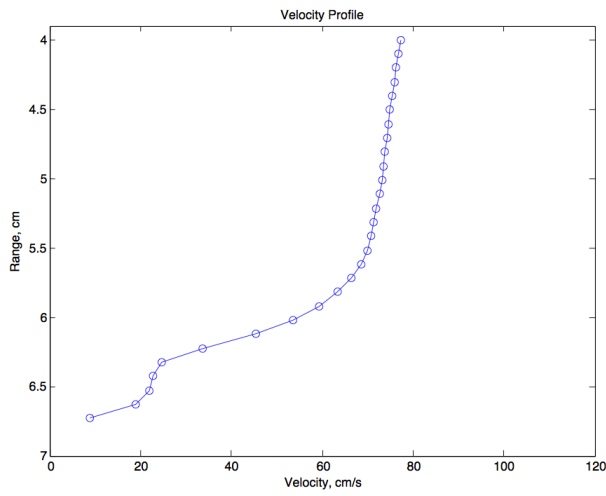
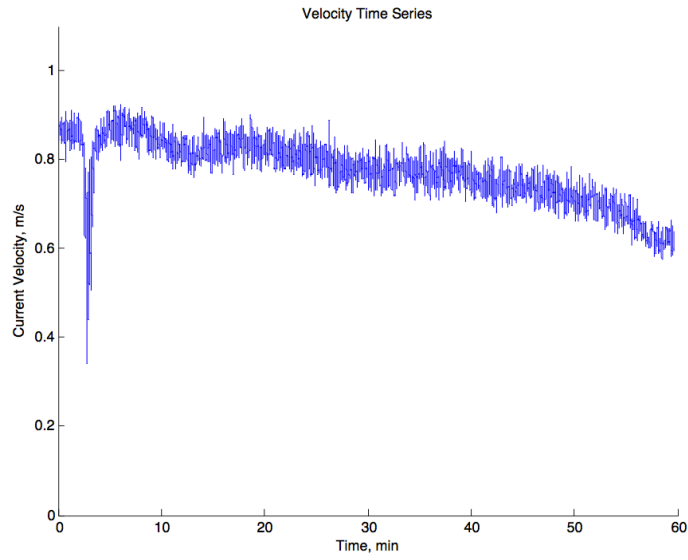
Yr.Day=14.041 x=91cm/s t=17.5C m=20.6g



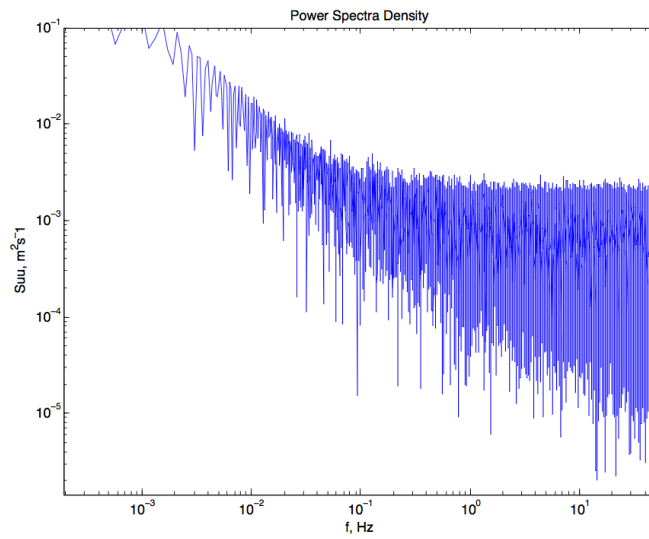
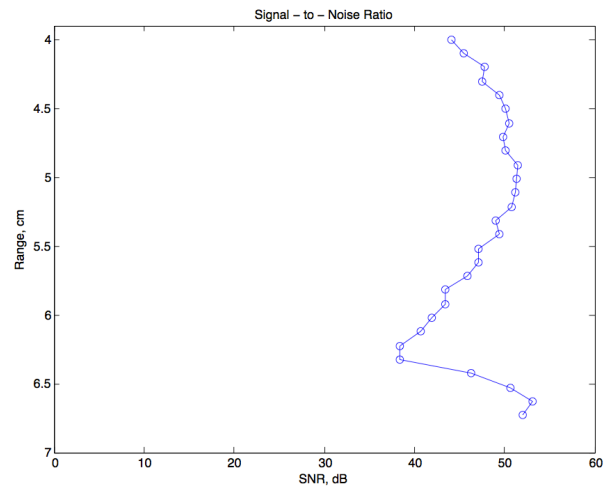
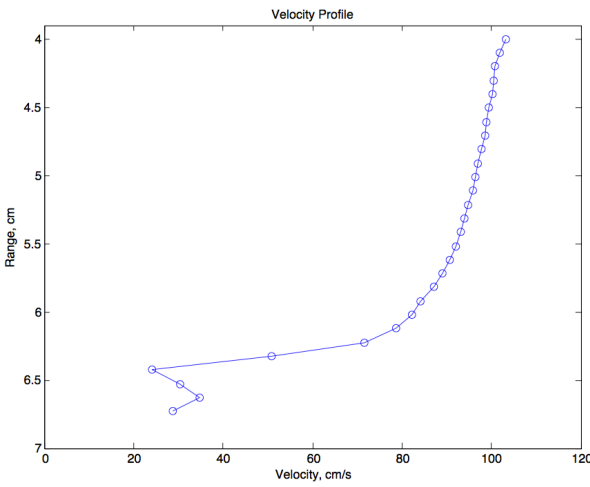
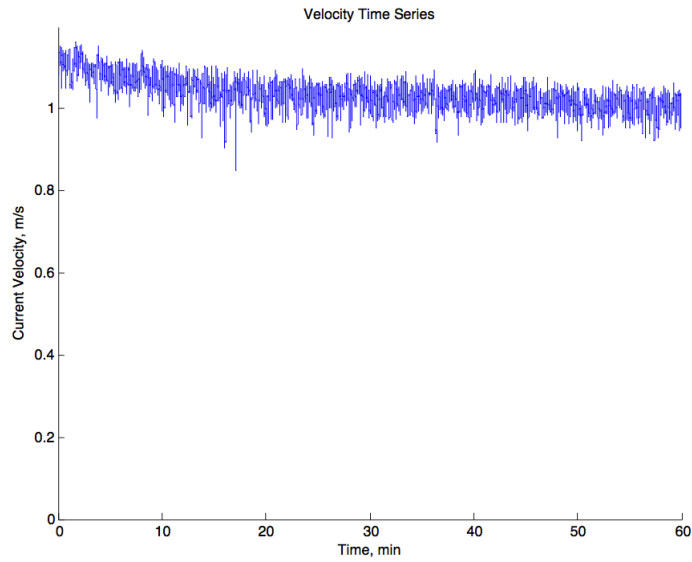
Yr.Day=14.041 x=88cm/s t=5.5C m=20g



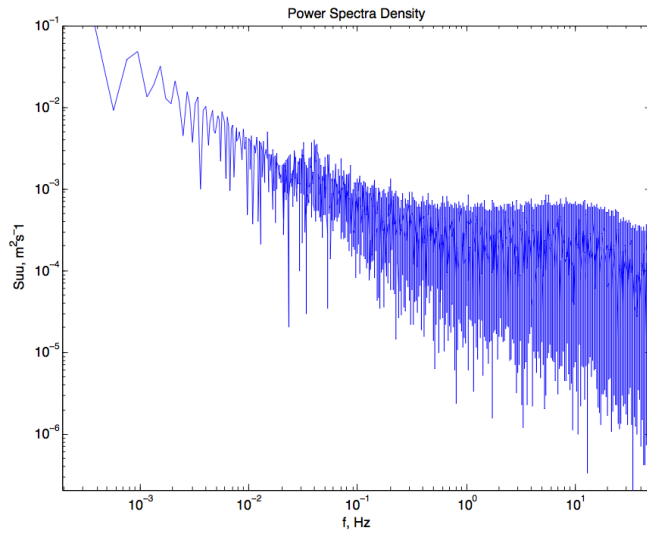
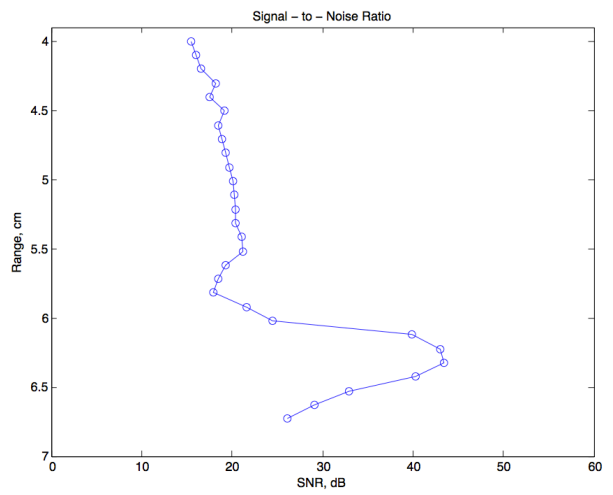
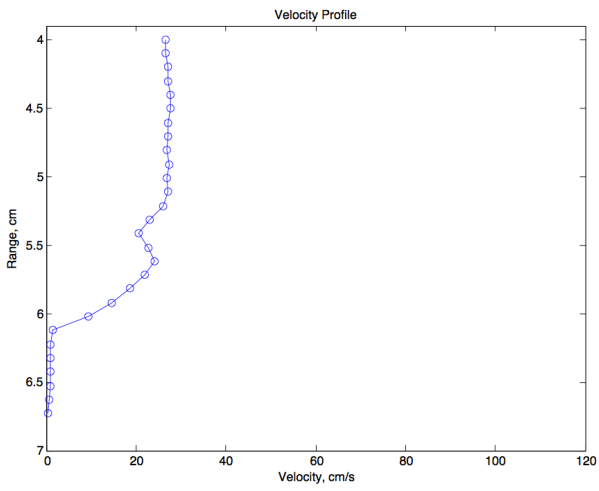
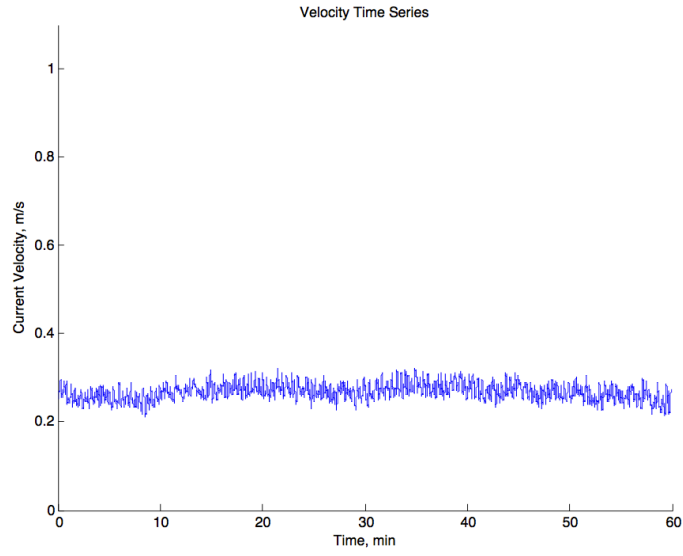
Yr.Day=14.041 x=78cm/s t=5.5C m=5.2g



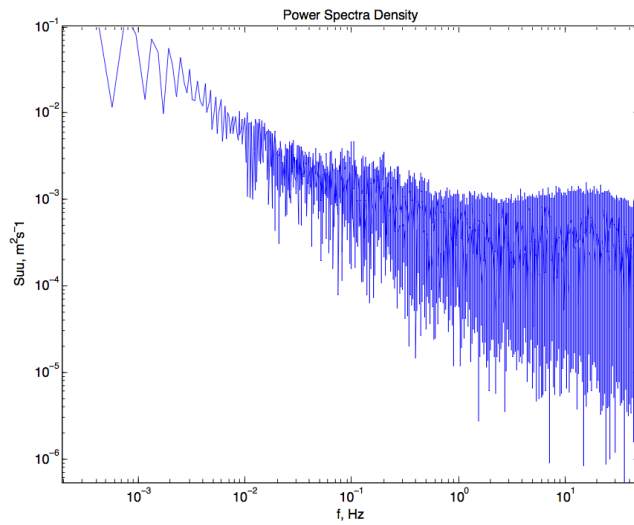
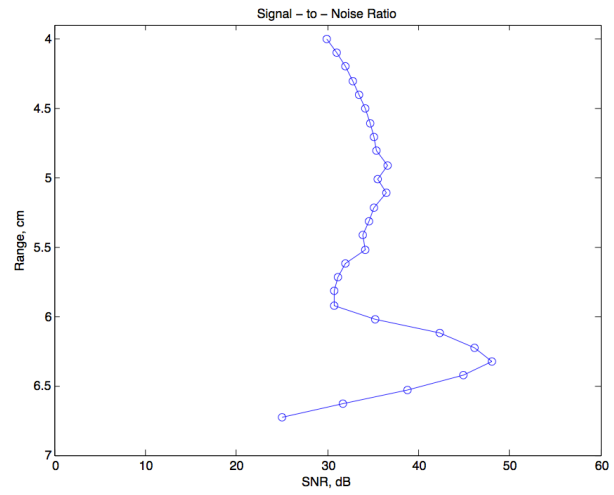
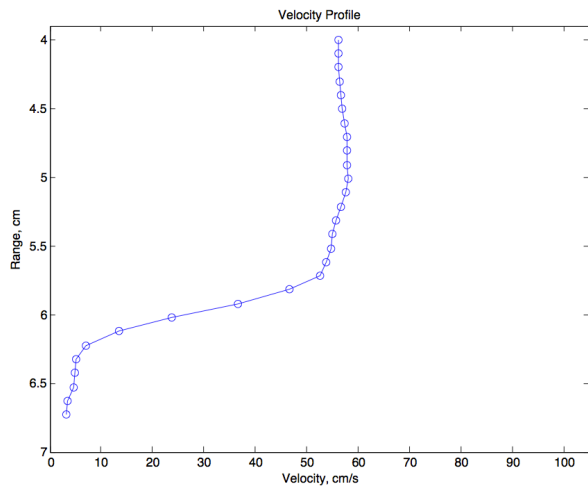
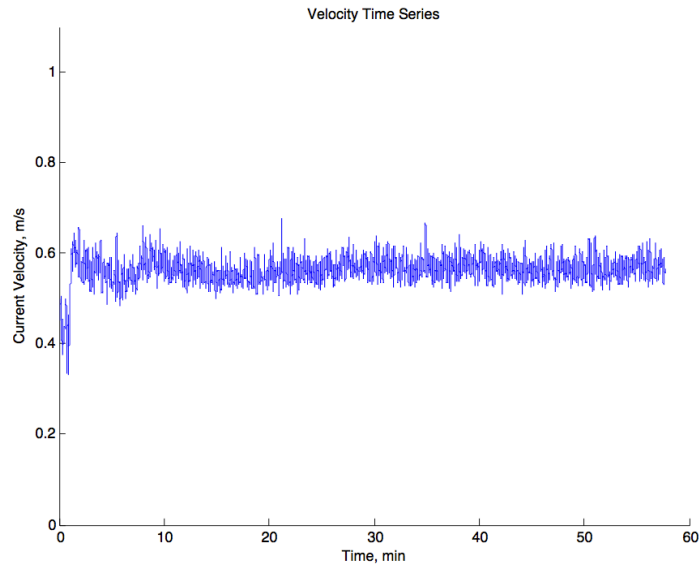
Yr.Day=14.042 x=106cm/s t=15C m=5.4g



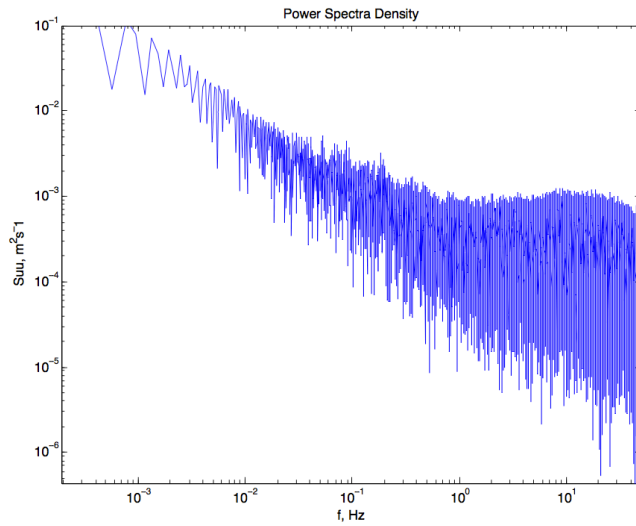
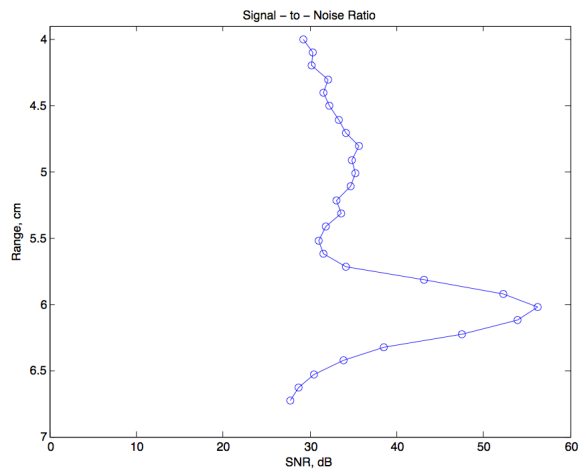
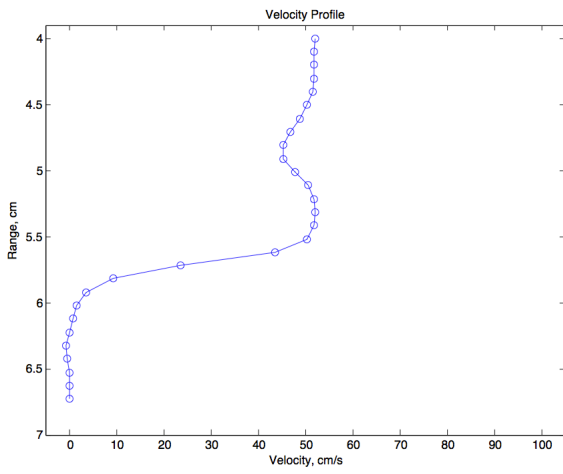
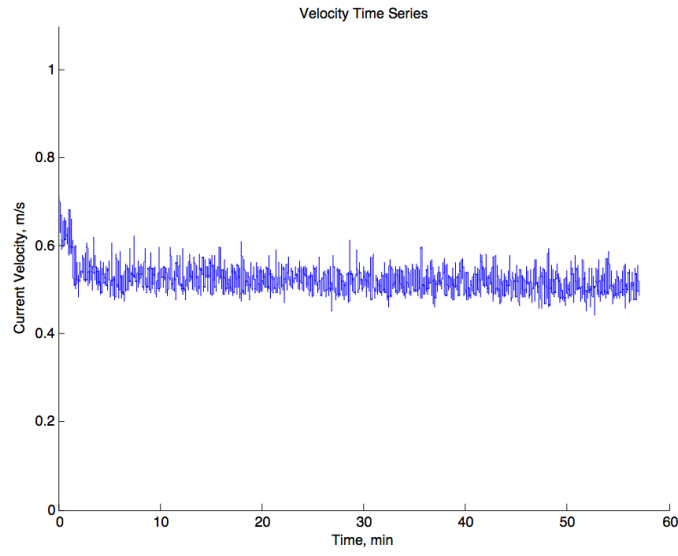
Yr.Day=14.042 x=26cm/s t=5C m=20.1g



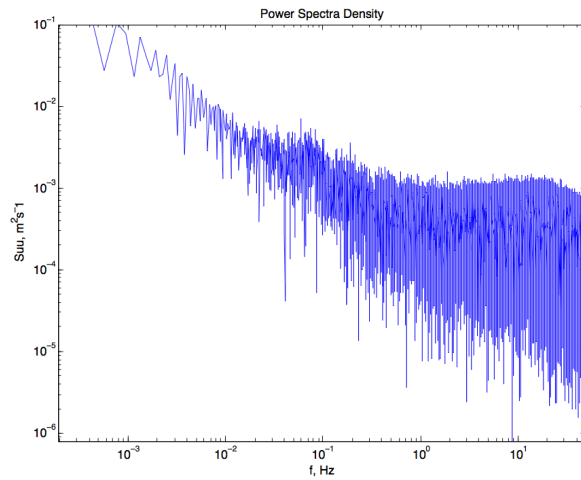
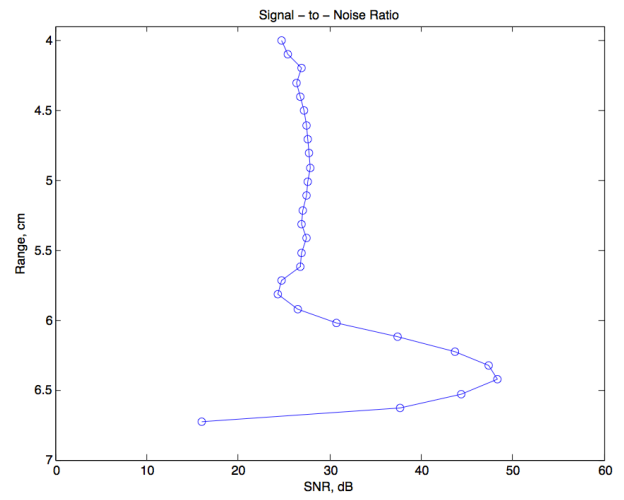
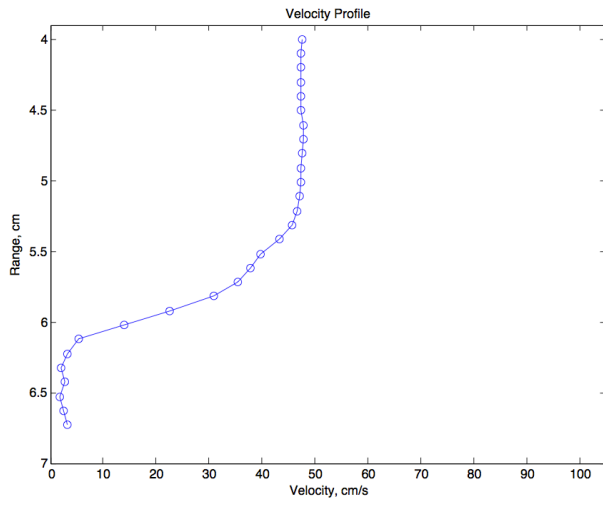
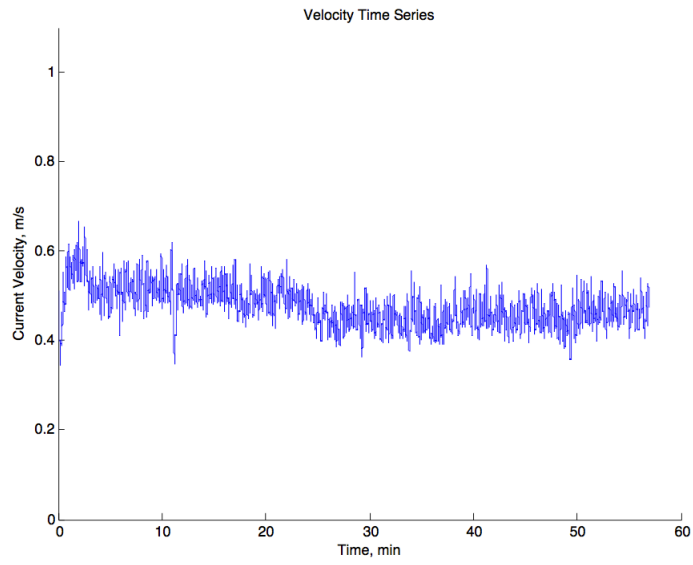
Yr.Day=14.048 x=55cm/s t=26.1C m=19.6g



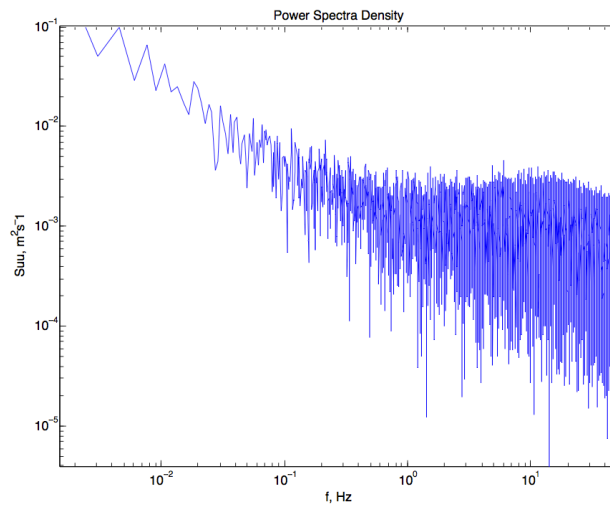
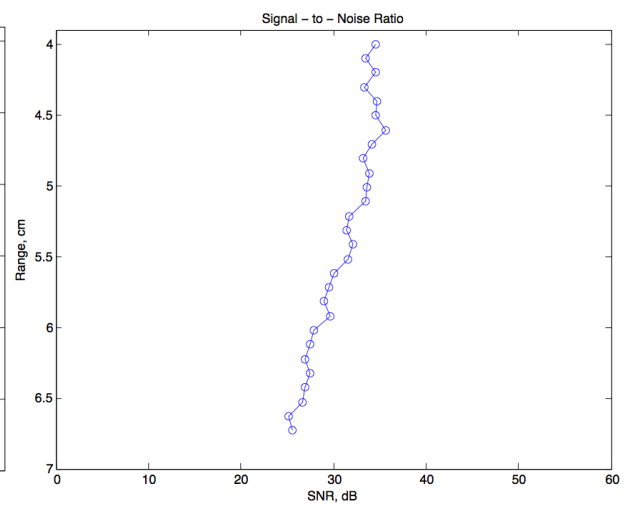
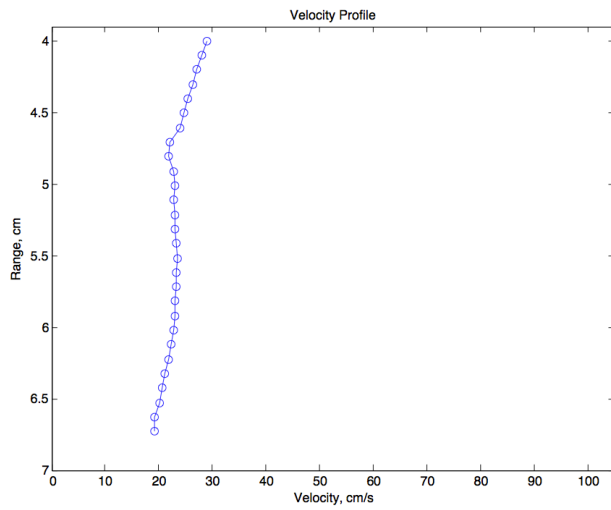
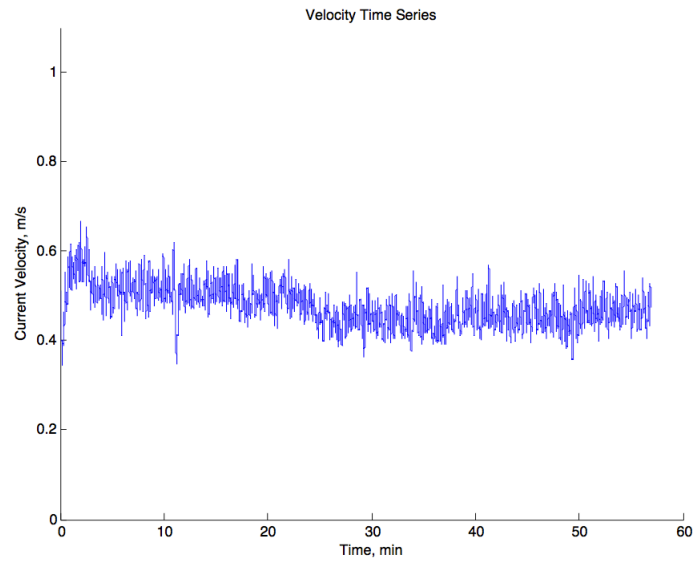
Yr.Day=14.056 x=53cm/s t=24.8C m=6.6g



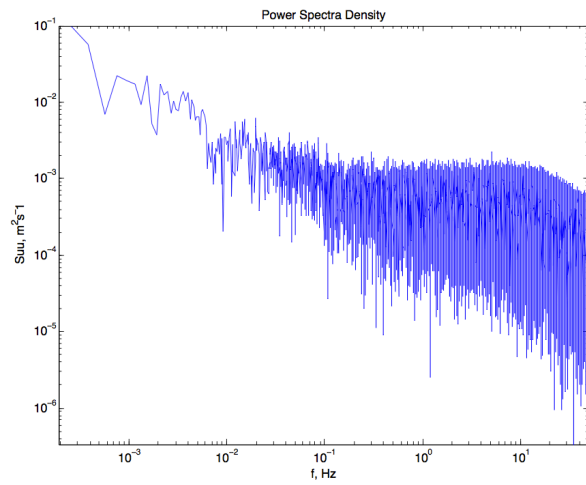
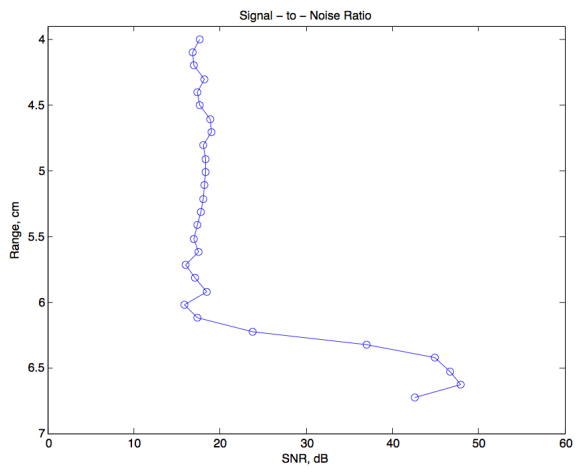
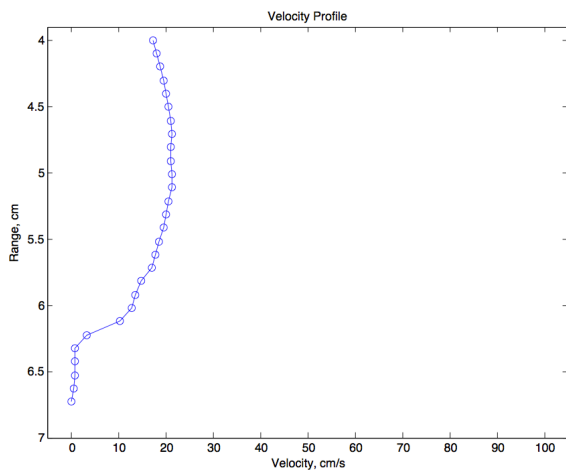
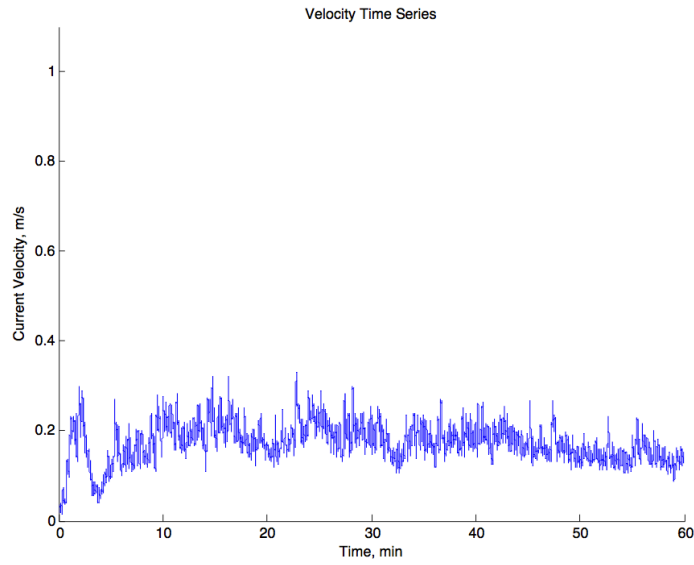
Yr.Day=14.056 x=51cm/s t=6.0C m=20.1g



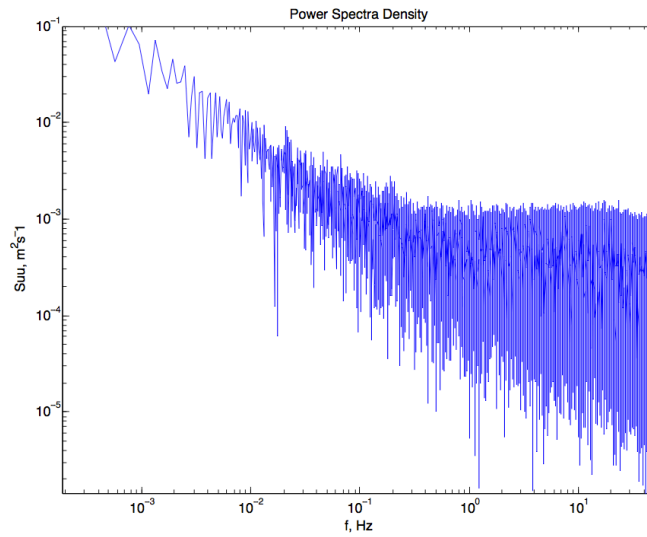
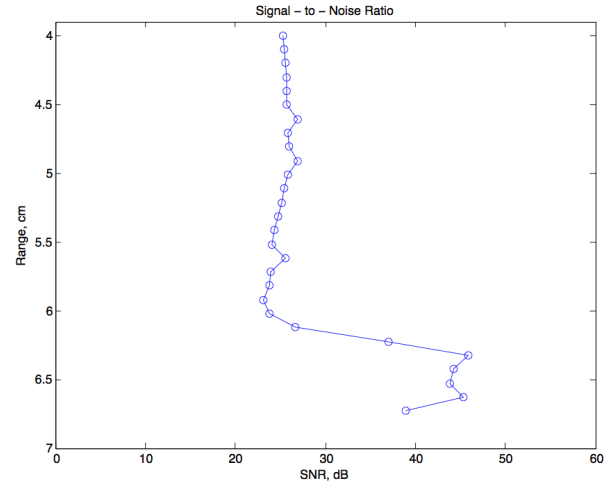
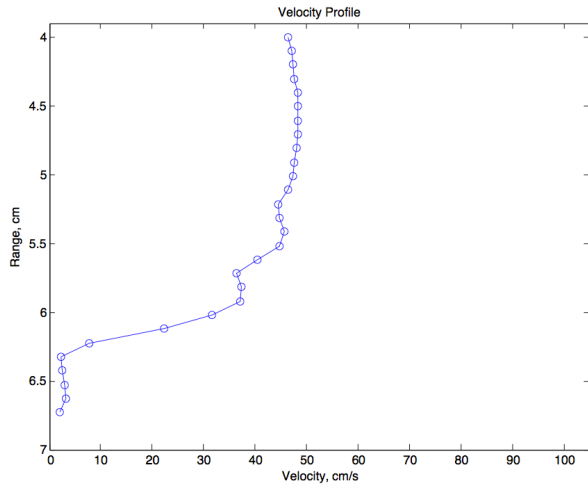
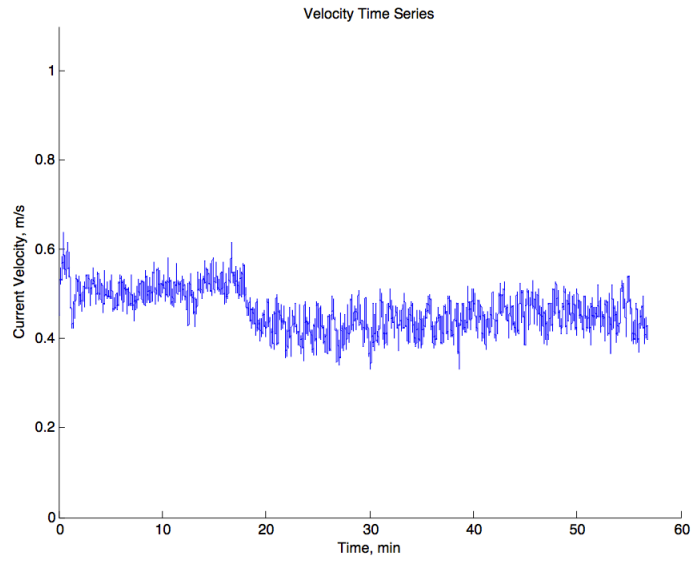
Yr.Day=14.057 x=24cm/s t=27.9C m=20g



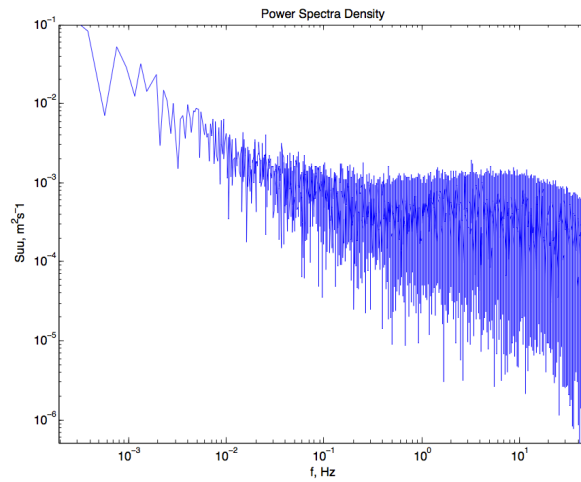
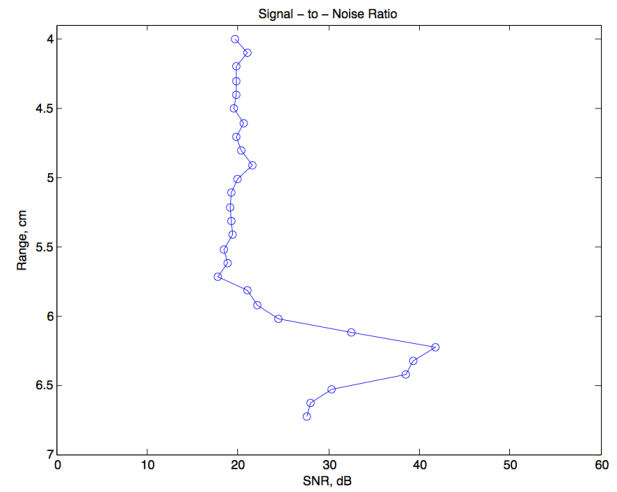
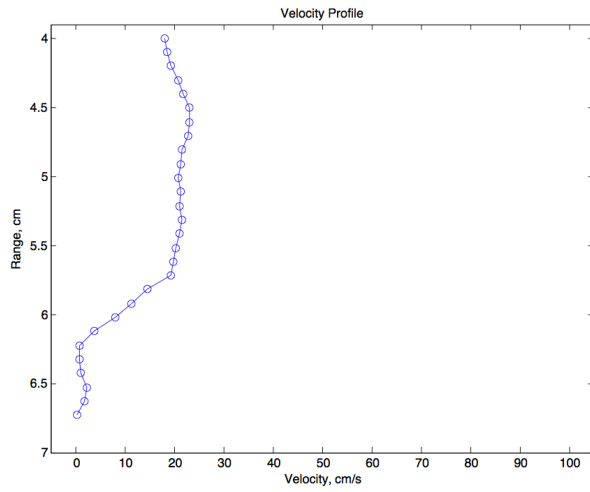
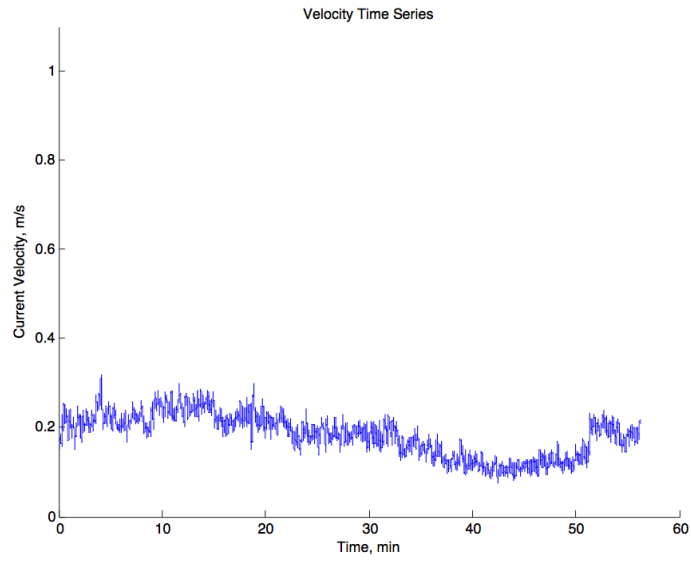
Yr.Day=14.057 x=16cm/s t=27C m=5.1g



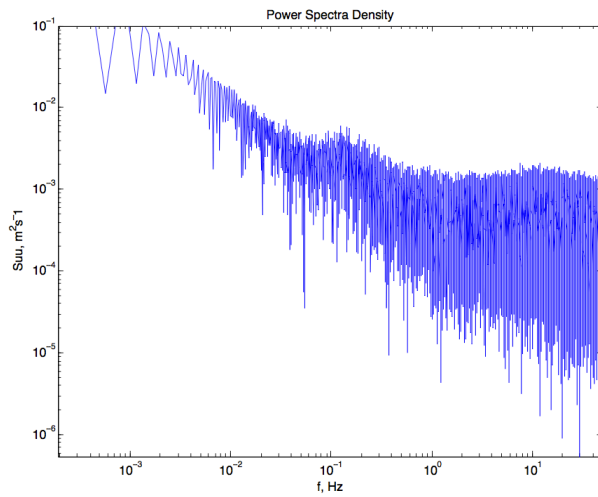
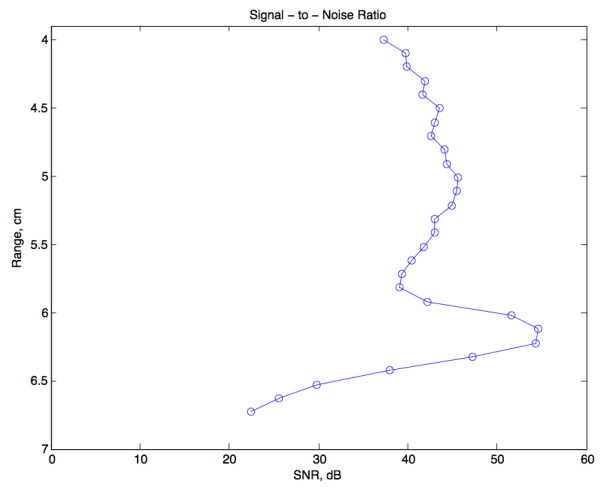
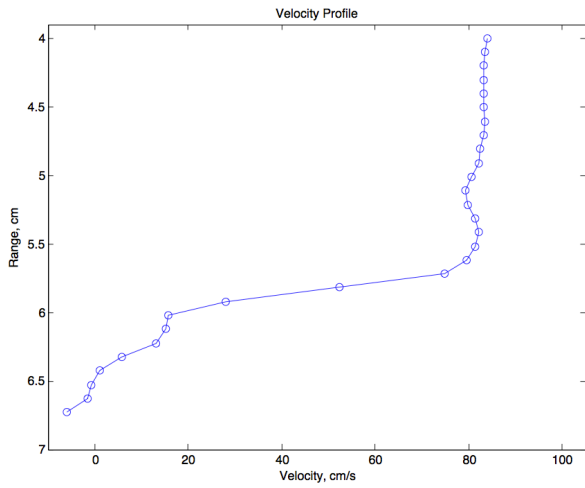
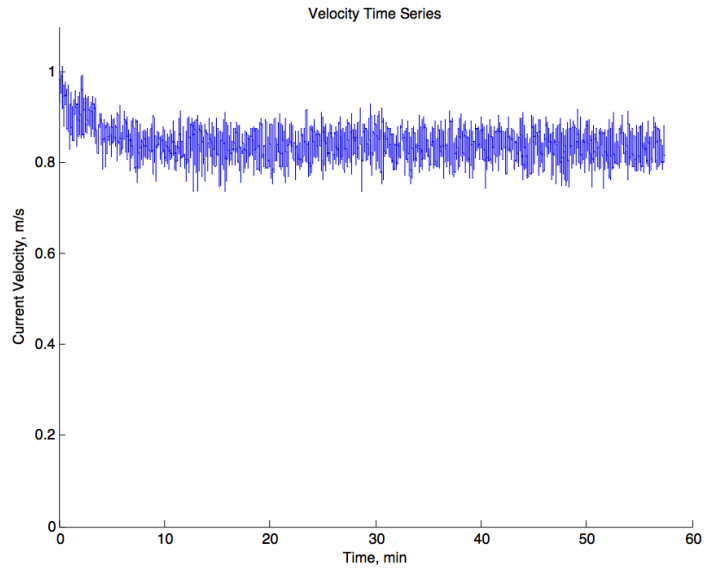
Yr.Day=14.058 x=52cm/s t=5.0C m=5.6g



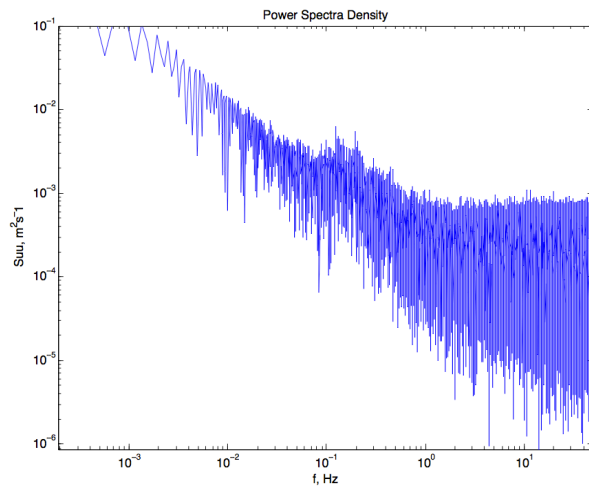
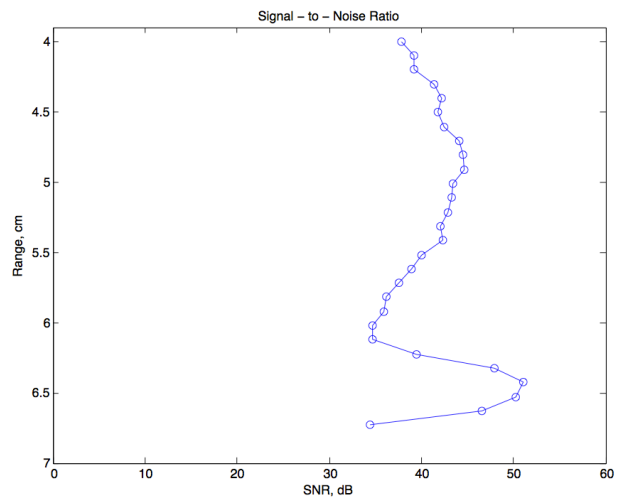
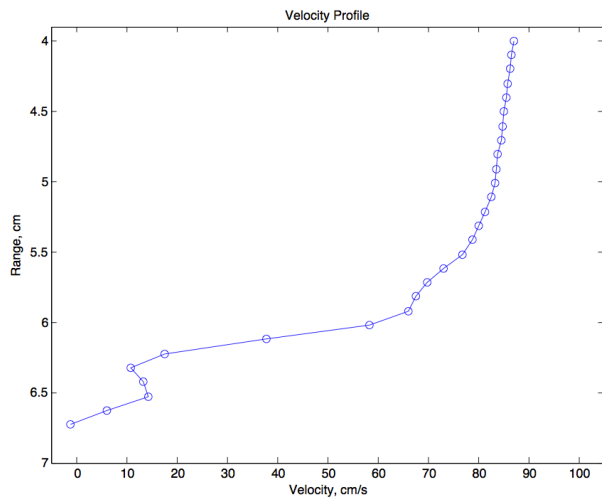
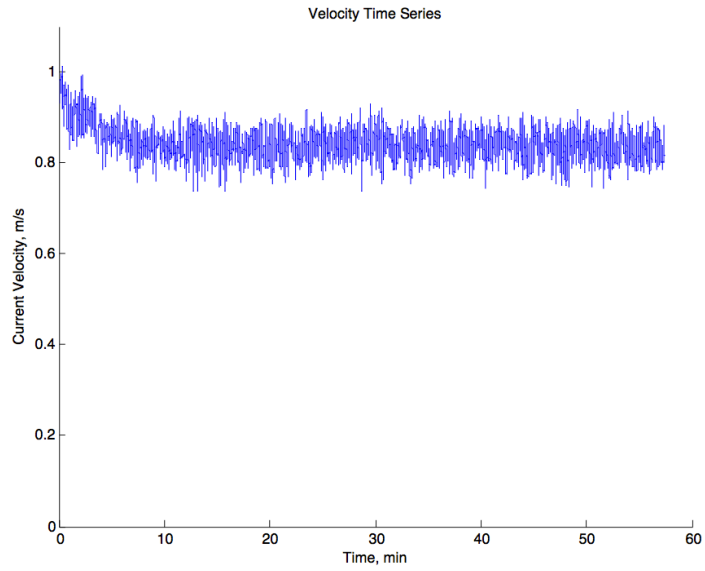
Yr.Day=14.062 x=25cm/s t=5C m=5.9g



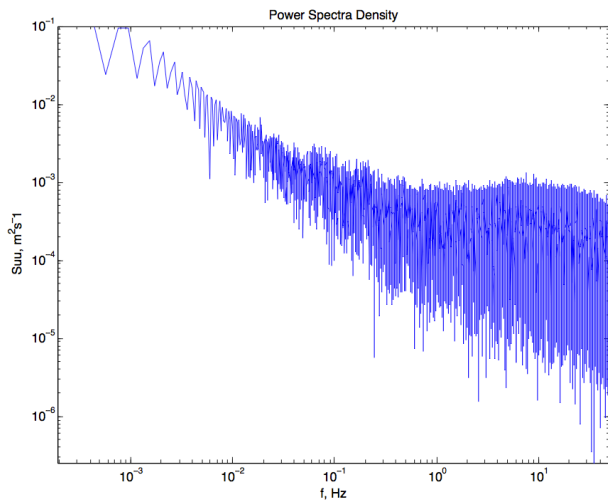
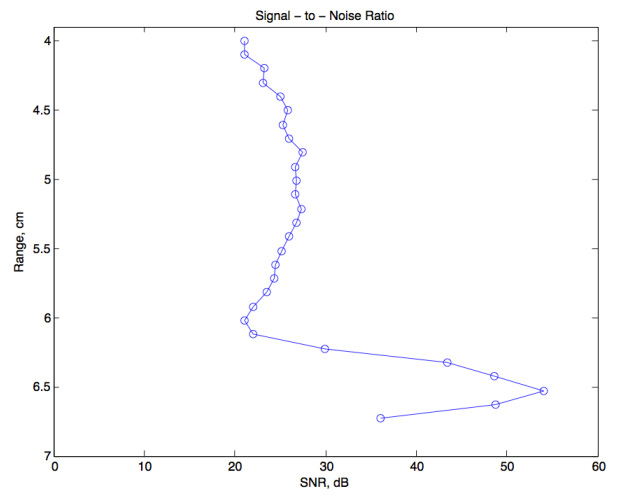
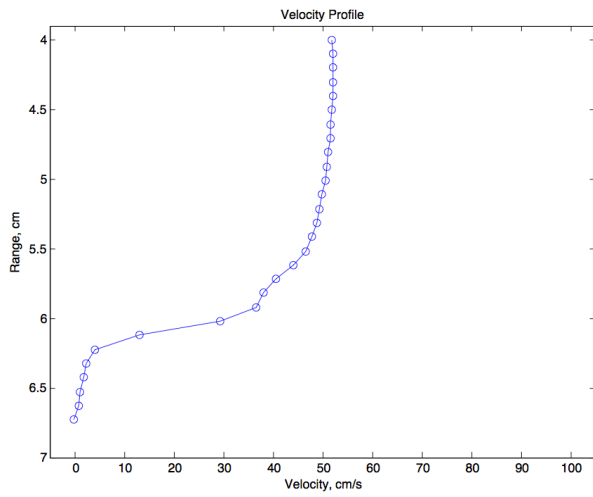
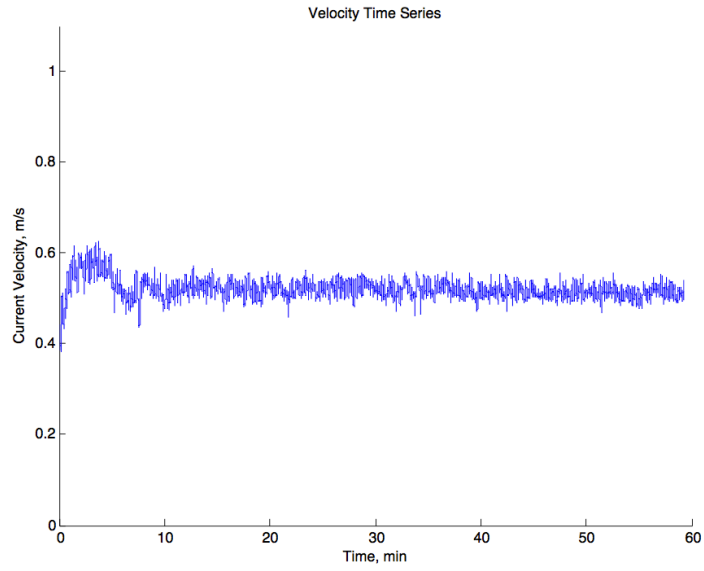
Yr.Day=14.062 x=86cm/s t=26.7C m=5.9g



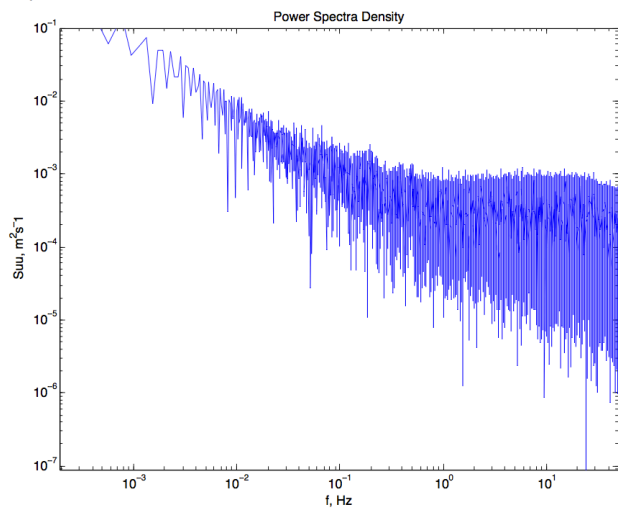
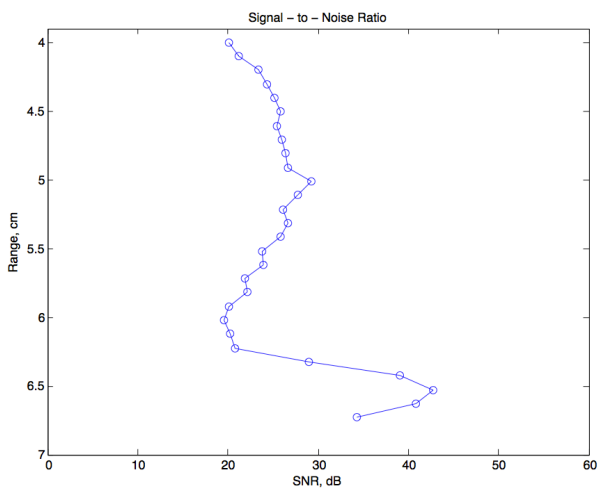
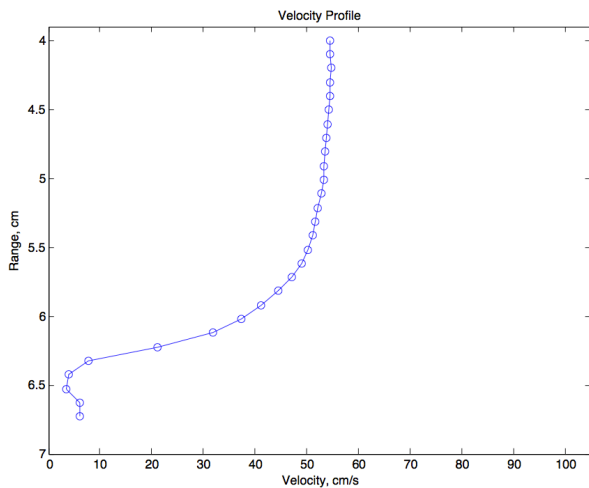
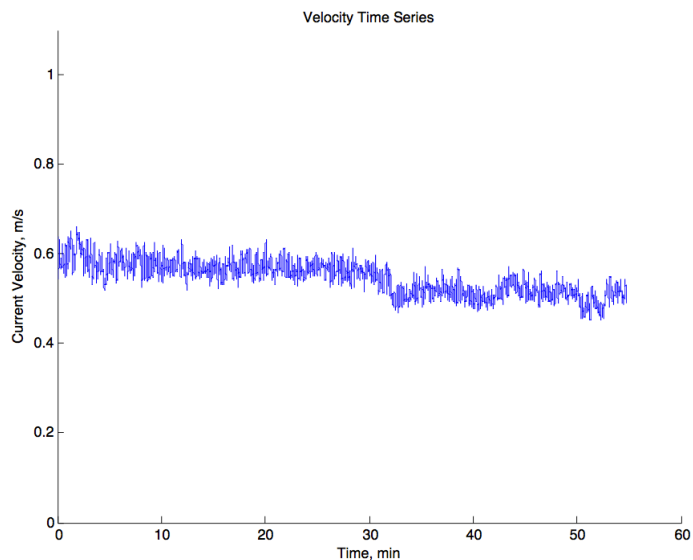
Yr.Day=14.064 x=90cm/s t=26.7C m=20.7g



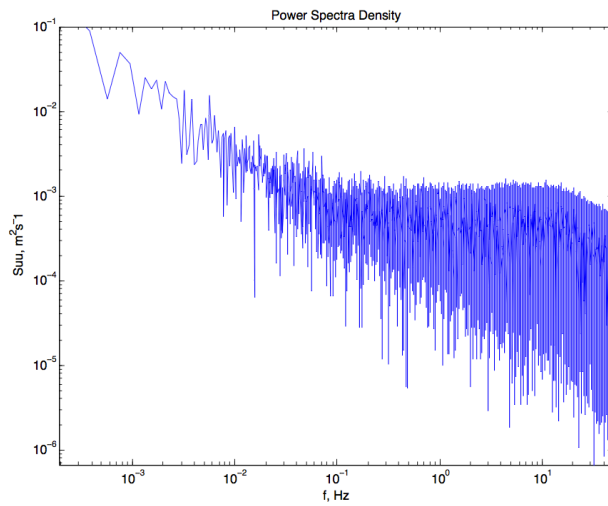
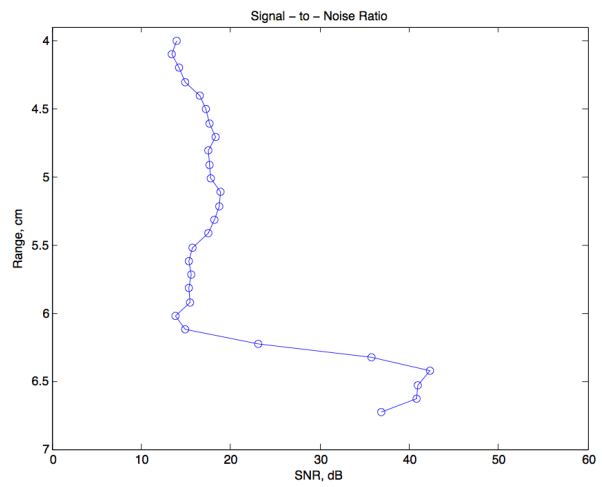
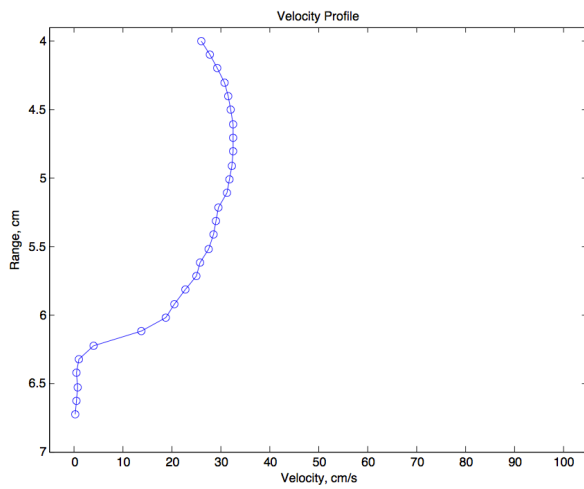
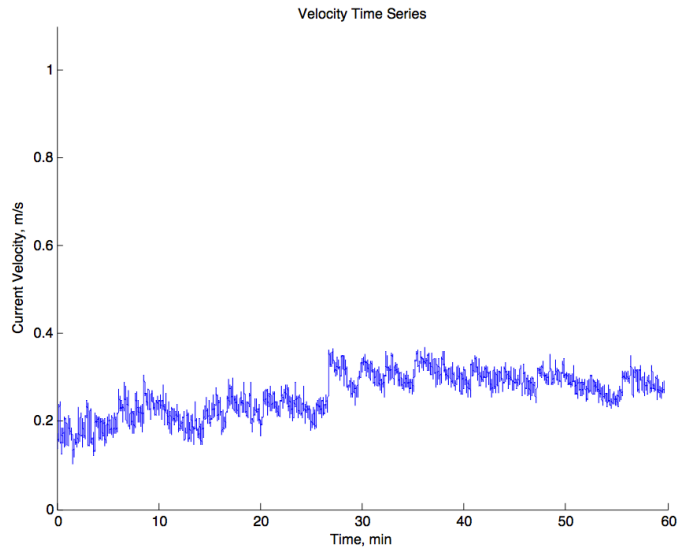
Yr.Day=14.066 x=53cm/s t=19.7C m=5.6g



Yr.Day=14.068 x=57cm/s t=19.1C m=20.1g



Yr.Day=14.072 x=24cm/s t=19.6C m=6g



Yr.Day=14.075 x=23cm/s t=20C m=19.7g

